

71-17,044

LAWSON, Michael Beau, 1944-
A STUDY OF THE STRUCTURE, SPECTRUM, AND
MAGNETIC SUSCEPTIBILITY OF BIS(INDAZOLE) COPPER
(II) CHLORIDE AND BIS(L-PHENYLALANINATO)
COPPER(II).

The University of Oklahoma, Ph.D., 1971
Chemistry, inorganic

University Microfilms, A XEROX Company, Ann Arbor, Michigan

THIS DISSERTATION HAS BEEN MICROFILMED EXACTLY AS RECEIVED

THE UNIVERSITY OF OKLAHOMA

GRADUATE COLLEGE

A STUDY OF THE STRUCTURE, SPECTRUM, AND
MAGNETIC SUSCEPTIBILITY OF BIS(INDAZOLE)
COPPER(II) CHLORIDE AND BIS(L-PHENYLALANINATO)
COPPER(II)

A DISSERTATION

SUBMITTED TO THE GRADUATE FACULTY

in partial fulfillment of the requirements for the

degree of

DOCTOR OF PHILOSOPHY

BY

MICHAEL BEAU LAWSON

Norman, Oklahoma

1971

A STUDY OF THE STRUCTURE, SPECTRUM AND MAGNETIC
SUSCEPTIBILITY OF BIS(INDAZOLE)COPPER(II)
CHLORIDE AND BIS(L-PHENYLALANINATO)
COPPER(II)

APPROVED BY

Norman Logel
James E. ...
J. Colberg
Bernard C. Nestor
William H. ...
Eric ...
Stanley C. ...

DISSERTATION COMMITTEE

PLEASE NOTE:

Some pages have small
and indistinct type.
Filmed as received.

University Microfilms

To Cheryl

ACKNOWLEDGEMENT

The author wishes to express his appreciation to Dr. Dick van der Helm, Dr. Norman Fogel, and Dr. Eric Enwall. All three offered valuable assistance and advice throughout the course of the research.

The author wishes to express his gratitude to Mrs. Nancy Heinicke and Mrs. Betty Rupp for their kind patience while typing the manuscript.

The author also expresses his thanks to Mr. David Hoover for his many drawings throughout the dissertation.

The author wishes to thank his wife for her patience and encouragement throughout the "graduate" years.

Finally, the author gives a vote of thanks to his mother for her encouragement. She always liked to quote the words of the hired-man. "Give it hell for thirty minutes."

TABLE OF CONTENTS

	Page
LIST OF TABLES	vii
LIST OF FIGURES	xi
 Chapter	
I. INTRODUCTION	1
II. EXPERIMENTAL TECHNIQUES	17
III. CRYSTAL AND MOLECULAR STRUCTURE OF BIS(L-PHENYLALANINATO)COPPER(II)	25
IV. CRYSTAL AND MOLECULAR STRUCTURE OF BIS(INDAZOLE)COPPER(II) CHLORIDE	81
V. THEORY OF CRYSTAL FIELD SPECTRA AND MAGNETIC SUSCEPTIBILITY	115
VI. CRYSTAL FIELD SPECTRA AND MAGNETIC SUSCEPTIBILITY OF FIVE COPPER(II) COMPLEXES ...	130
VII. SUMMARY AND CONCLUSIONS	159
 Appendix	
I. REFLECTIONS USED IN DETERMINATION OF LEAST- SQUARES CELL DIMENSIONS (BIS(L-PHENYL- ALANINATO)COPPER(II)	166

Appendix	Page
II. REFLECTIONS USED IN DETERMINATION OF LEAST-SQUARES CELL DIMENSIONS (BIS(INDAZOLE) COPPER(II) CHLORIDE	167
III. LIST OF OBSERVED AND CALCULATED STRUCTURE FACTORS FOR BIS(L-PHENYL-ALANINATO)COPPER(II)	169
IV. LIST OF OBSERVED AND CALCULATED STRUCTURE FACTORS FOR BIS(INDAZOLE)COPPER(II) CHLORIDE	172
V. SYMBOLISM USED FOR VARIOUS ORBITALS	174
VI. SIGN CHOICE FOR D _s AND D _t	176
VII. EVALUATION OF a ₂₂ ELEMENT OF THE SECULAR DETERMINANT	178
VIII. SELECTION RULES UNDER D _{4h} SYMMETRY	181
IX. SELECTION RULES UNDER D _{4h} ' SYMMETRY	182
X. MATHEMATICAL DEVELOPMENT OF MAGNETIC SUSCEPTIBILITY EQUATIONS	184
REFERENCES	188

LIST OF TABLES

Table	Page
1. Crystal Data for Bis(L-phenylalaninato) Copper(II)	26
2. Peak Heights of Hydrogen Atoms in Difference Fourier (Bis(L-phenylalaninato)Copper(II)).....	33
3. R Values for Bis(L-phenylalaninato)Copper(II)....	36
4a. Atomic Parameters of Bis(L-phenylalaninato) Copper(II)	37
4b. Anisotropic Temperature Values (Bis(L-phenylalaninato)Copper(II)	38
4c. Hydrogen Parameters of Bis(L-phenylalaninato)Copper(II)	39
5. Van der Waal's Contacts Less than 4.0 Å (Bis(L-phenylalaninato)Copper(II)).....	41
6. Bond Distances and Angles Around Copper (Bis(L-phenylalaninato)Copper(II)).....	46
7a. Least Squares Planes for Coordination Sphere (Bis(L-phenylalaninato)Copper(II))	50
7b. Least Squares Planes for Coordination Sphere (Bis(L-phenylalaninato)Copper(II))	51
7c. Least Squares Planes for Coordination Sphere (Bis(L-phenylalaninato)Copper(II))	52
8. Least Squares Planes for Chelate Rings (Bis(L-phenylalaninato)Copper(II))	56
9. Chelate Angles Compared to Average Values (Bis(L-phenylalaninato)Copper(II))	57

Table	Page
10. Comparison of Bond Angles and Lengths of Bis(L-phenylalaninato)Copper(II) With Those of Histidine Hydrochloride Monohydrate and Other Copper Complexes of Amino Acids and Peptides	59
11. Least Square Planes for Carboxylic Groups	61
12. Conformational Angles for L-phenylalanine.....	62
13. Intramolecular Bond Angles and Distances (Bis(L-phenylalaninato)Copper(II)).....	65
14. Angles Between Principal Axes of Thermal Ellipsoids and the Mean Planes of the Rings (Bis(L-phenylalaninato)Copper(II)).....	72
15. Least Squares Planes for Aromatic Rings (Bis(L-phenylalaninato)Copper(II))	76
16. Principal Axes and Direction Cosines with Respect to the Cell Edges of the Anisotropic Ellipsoids (Bis(L-phenylalaninato)Copper(II)) ...	77
17. Crystal Data of Bis(indazole)Copper(II) Chloride	82
18. Peak Heights of Hydrogen Atoms in Difference Fourier (Bis(indazole)Copper(II) Chloride)	86
19. R Values for Bis(indazole)Copper(II) Chloride ...	88
20. Final Atomic Positions (Bis(indazole)Copper(II) Chloride	89
21. Anisotropic Thermal Parameters (Bis(indazole) Copper(II) Chloride	90
22. Comparison of "Data" Intensities With "Twin" Intensities	92
23. Van der Waal's Contacts Less than 4.0 Å (Bis(indazole)Copper(II) Chloride)	94
24. Dihedral Angles Between Coordination Planes Bis(indazole)Copper(II) Chloride	99
25. Comparison of Copper-Chlorine Bond Lengths for Various Structures having Octahedral Coordination	100

Table	Page
26. Intramolecular Bond Angles and Distances for Indazole Compared to Selected Average Values	102
27. Least Squares Planes for Indazole	107
28. Angles Between Principal Axes of Thermal Ellipsoids and the Mean Plane of the Indazole Molecule	109
29. Lengths and Direction Cosines with Respect to Unit Axes of the Principal Axes of the Thermal Ellipsoids (Bis(indazole)Copper(II) Chloride	110
30. Effect of Octahedral Operator on "d" Orbitals ...	117
31. Effect of Tetragonal Operator on "d" Orbitals ...	118
32. Wave Functions Used for Perturbation Calculations	119
33. Results of Applying Spin-Orbit Operator	120
34. Selection Rules Under D_{4h} Symmetry	124
35. Selection Rules Under D_{4h} Symmetry	125
36. Ligand Distances and Magnetic Moments for Three D_{4h} Copper(II) Complexes	131
37. Energy Level Ordering for Selected Copper(II) Complexes Having D_{4h} Symmetry	134
38. Calculated and Observed Transitions for (Bis(indazole)Copper(II) Chloride	136
39. Comparison of Six Ways of Ordering Orbitals in Bis(indazole)Copper(II) Chloride	139
40. Experimental Susceptibility of Bis(indazole) Copper(II) Chloride	141
41. Copper to Ligand Bond Distances (Bis(L-alaninato)Copper(II) and Bis(L-phenylalaninato)Copper(II)	149

Table	Page
42. Ordering of "d" Orbitals for Bis(L-alaninato) Copper(II)	152
43. Magnetic Susceptibility of Bis(L-phenyl-alaninato)Copper(II)	153

LIST OF FIGURES

Figure	Page
1. Schematic of Magnetic Balance	21
2. $m \cdot \chi_g$ vs d for Determination of Diamagnetism of Sample Bucket	23
3. Projection onto "ac" Plane (Bis(L-phenylalaninato) copper(II))	45
4. Coordination Sphere of Copper Ion (Bis(L-phenyl- alaninato)copper(II))	47
5. Configuration of Chelate Rings (Bis(L-phenyl- alaninato)copper(II))	55
6. Labeling of Conformational Angles	62
7. Bond Distances in L-phenylalanine for Molecule A .	67
8. Bond Distances in L-phenylalanine for Molecule B .	68
9. Angles in L-phenylalanine for Molecule A	69
10. Angles in L-phenylalanine for Molecule B	70
11. Stereoscopic Drawing of Bis(L-phenylalaninato) copper(II))	74
12. Orientation of "Twinned" Reciprocal Lattices	92
13. Bond Distances and Angles for Square Plane in Bis(indazole)copper(II) Chloride	96
14. Stereoscopic Drawing of Bis(indazole)copper(II) Chloride	97
15. Coordination Around Copper Ion (Bis(indazole) copper(II) Chloride).....	98

Figure	Page
16. Bond Lengths for Indazole Molecule	104
17. Bond Angles for Indazole Molecules.....	105
18. Projection of Bis(indazole)copper(II) Chloride Down "a" Axis.....	112
19. Effect of Various Perturbations on "d" Orbitals.....	116
20. Secular Determinant From First Order Perturbation Theory.....	121
21. Orientation of Cartesian Coordinates for D_{4h} Symmetry.....	123
22. Orientation of Cartesian Coordinates for D_{4h}' Symmetry	125
23. Spectrum of Bis(indazole)copper(II) Chloride.....	137
24. T vs $1/(\chi_m^{\text{CORR}})_1$ for Bis(indazole)copper(II) Chloride.....	143
25. $(\chi_m^{\text{CORR}})_1$ vs $[1/(T-\theta)]$ for Bis(indazole) copper(II) Chloride.....	144
26. $(\chi_m^{\text{CORR}})_1$ vs T for Bis(indazole)copper(II) Chloride.....	146
27. Spectrum of Bis(L-phenylalaninato)copper(II).....	148
28. T vs $1/(\chi_m^{\text{CORR}})_1$ for Bis(L-phenylalaninato) copper(II).....	154
29. $(\chi_m^{\text{CORR}})_1$ vs $1/(T-\theta)$ for Bis(L-phenylalaninato) copper(II).....	156

Figure	Page
30. $(\chi_m^{\text{corr}})_2$ vs T for Bis(L-phenylalaninato) copper(II).....	158
31. Compounds Conducive to Corrosion Control.....	163
32. Mode of Bonding Proposed by Cotton.....	164

A STUDY OF THE STRUCTURE, SPECTRUM AND MAGNETIC
SUSCEPTIBILITY OF BIS(INDAZOLE)COPPER(II)
CHLORIDE AND BIS(L-PHENYLALANINATO)
COPPER(II)

CHAPTER I

Introduction

"As a result of the distorted octahedral or square coordination of Cu(II), a detailed interpretation of its electronic absorption spectrum is somewhat complicated.... There is still some uncertainty as to whether all of the bands are really under the envelope of the absorption observed in the visible (1)."

This dissertation has as one of its primary concerns the elucidation of the electronic transitions of the "d" orbitals of copper (II) when subjected to tetragonally distorted octahedral force fields. The mode of attack was first to determine the structure of two copper(II) complexes by means of x-ray analysis. The magnetic susceptibility of the two complexes was then determined and an attempt was made to calculate the susceptibility using wave functions based upon empirical parameters obtained from the visible spectrum. The parameters, and hence the susceptibility, depend upon correctly assigning the electronic transitions.

"A second point involves formation of the substrate-enzyme complex. Since ceruloplasmin will not attack monoamines or monophenols, one might consider that the points of attachment would be at the ring substituents, such as the two amino groups in p-phenylenediamine. However, it has also been found that compounds of the type which are fully substituted (e.g., N,N,N',N'-tetramethyl-p-phenylenediamine) are readily oxidized by ceruloplasmin. Therefore, it is suggested that enzyme binding may not be through the amine or phenolic groups, but instead directly to the ring, or more specifically, to the pi electrons of the ring (2)."

The bis(L-phenylalaninato)copper(II) complex is one in a series of copper(II) - chelate complexes that has been studied at the University of Oklahoma to examine a possible interaction between the aromatic residue of the amino acid and the copper. It has been shown in the Cu(II) chelate of glycyl-L-leucyl-L-tyrosine (3) and in the Cu(II) - tyrosine (4) complex that the ring occupies the sixth coordination site of the octahedron. It was decided that it would be interesting to see if the same thing occurred in the phenylalanine complex which is lacking in an electron - donating substituent.

"The reaction between benzotriazole-type compounds and the surface of metallic copper, or more correctly, the oxide-covered surface of the metal yields insufficient material for a detailed study of the chemistry of the process and to obtain some understanding of these reactions it is necessary to investigate the compounds formed in reaction between copper ions in solution and these organic compounds (5)."

Certain organic compounds, viz. benzotriazole and indazole, among others have been used to preserve the bright surface condition

present on copper base alloys immediately after fabrication. The mechanism of the interaction is not well understood. It is hoped that the x-ray analysis of the bis(indazole)copper(II) chloride complex yields insight into the nature of the bonding mechanism occurring at the metal surface.

From the preceding paragraphs one can see that there is justification for the study of copper(II) and its interaction with indazole and L-phenylalanine.

Polder (6) was one of the first to consider the effects of a tetragonally distorted, electric potential on the d orbitals of Cu(II). He shows how the five degenerate orbitals in the free ion are split until all degeneracy is removed when subjected to the influence of a tetragonally perturbed cubic field if one also includes the effect of spin-orbit coupling. In order to obtain information about the relative positions of the perturbed levels he used a model composed of six electric dipoles oriented with their negative sides toward the copper ion to obtain an expression for the electric potential. Using this potential function, and first order perturbation theory he was able to arrive at an expression for the parallel and perpendicular component of the magnetic susceptibility. He could account for the observed anisotropies of $\text{CuSO}_4 \cdot 5\text{H}_2\text{O}$ and $\text{K}_2\text{Cu}(\text{SO}_4)_2 \cdot 6\text{H}_2\text{O}$ with Curie constants of 0.56 and 0.40 respectively in the direction of the tetragonal axis and in a direction at right angles with this axis.

The problem of the spectral behavior becomes apparent when one considers the work of Yama, et al. (7). They examine the dichroism of planar cupric complexes of the type, $\text{Cu}(\text{chelate})_2$. Explicitly the spectral curve for bis(dimethylethylenediamine) copper(II) perchlorate

is given and the comment is made that there is only one transition apparent as opposed to the three predicted on the basis of tetragonal distortion. The statement is also made that the absorption spectra exhibited by planar complexes of copper(II) can be explained neither by the crystal field theory nor by simple application of the molecular orbital treatment.

Some very fine work was done by Belford, Calvin, and Belford on the solution spectra of copper(II) chelates (8). They reach the opposite conclusion to that of Yama, et al.. They examined the visible and near infrared spectra of bis(acetylacetonato)copper(II) and its 3-ethyl variant in solvents of increasing basicity. They were able to analyze the resulting spectra in terms of Gaussian curves and show that there were three transitions in the region of contention. They were also able to demonstrate that the transitions could be explained using either the ionic(crystal field) model or molecular orbital theory. The really pleasing aspect of their work was their ability to correlate the shift of the orbitals having a "z" component with the augmented potential upon going to a more basic solvent. One can have little doubt that they were approaching the problem correctly.

Holmes & McClure (9) examined the spectrum of $\text{CuSO}_4 \cdot 5\text{H}_2\text{O}$. The x-ray structure had been reported as having four water molecules arranged in an approximate square with two polar sulfate oxygens at slightly greater distances from the Cu(II). This gave the tetragonal environment desired to see the three transitions. Realizing this they measured the polarized spectrum and analyzed the resulting curve on the basis of three Gaussian curves with maxima located at 10,500, 13,000,

and $14,500 \text{ cm}^{-1}$. They unfortunately admit that there are inconsistencies in the spectral data. Of the four polarized spectral curves presented only three are independent, and the fourth should be derivable on the basis of the other three. The fourth cannot be derived satisfactorily and is attributed to uncertainties in the base line of zero absorption.

As time progressed the theory governing the electronic deportment became more abstruse and is expressed in all its mathematical complexity in a paper by Liehr (10). He gives the detailed theory of the splitting of the d orbitals for the d^9 case when the orbitals are subjected to tetragonal and spin-orbital coupling perturbations.

A hint of things to come is given in a paper by Graddon (11). The absorption spectrum of cupric ethylacetoacetate was measured by him in a variety of solvents in the visible and near ultraviolet range. He analyzes the visible region in terms of two Gaussian curves as opposed to the three that Belford, Calvin, and Belford choose to use. A third transition occurring in the uv region is ascribed to the third crystal field transition under the influence of tetragonal distortion. The ordering of the orbitals is given as $d_{x^2-y^2} > d_{xy} > d_z^2 > d_{xz}, d_{yz}$.

In order to check how some of the predictions of crystal field theory correlate with experiment, Pappalardo (12) studied the absorption of copper(II) in different crystal coordinations. Among other spectra he reports those of crystals of $\text{CuSiF}_6 \cdot 6\text{H}_2\text{O}$ and trigonal crystals of $\text{ZnSiF}_6 \cdot 6\text{H}_2\text{O}$ doped with Cu. In such crystals the crystal field around copper is predominantly cubic with a weak trigonal perturbation of the cubic field. The spectrum of the $\text{CuSiF}_6 \cdot 6\text{H}_2\text{O}$ complex shows a transition at $12,500 \text{ cm}^{-1}$ and one at $10,860 \text{ cm}^{-1}$ at 78° K . The doped crystal con-

sisted of an asymmetric band with a peak situated at $11,760 \text{ cm}^{-1}$. Using the spin-orbit coupling as a further perturbation, Pappalardo uses the results of Liehr to deduce a value of -1120 cm^{-1} for Dq , the octahedral splitting parameter for the doped crystal. He comments that this is in good agreement with the Dq values in other divalent ions of the iron group as evidence for the validity of the crystal field approach.

One very significant paper appeared shortly after Pappalardo's work. It initiated a controversy that resounded through the literature from its date of publication to the present. Ferguson (13) studied the polarized spectrum of bis(acetylacetonato)copper(II) and reported the startling conclusion that the ground state of copper(II) was not the orbital directed to the ligands, but rather arose from one of the d orbitals having a "z" component. He attributed this unusual effect to π overlap. He observes four transitions in the visible and near uv region occurring at $14,500$, $15,600$, $18,000$, and $26,000 \text{ cm}^{-1}$, and using D_{2h} symmetry which he knew to be approximately correct from the x-ray structure he gives symmetry arguments based upon vibronic selection rules for his assignments. It should be noted that Ferguson reports a shoulder on the $18,000 \text{ cm}^{-1}$ transition. This will become significant later in the story. He further states that the most disturbing feature of the analysis is the complete failure of the simple crystal field model. He emphasizes that a large number of copper complexes have been investigated by him and in every case where the polarized spectrum has been analyzed the most energetic orbital appears to be the one directed to the ligands in the plane!

An immediate rebuttal was given by Piper and Belford (14)

about the ground state of bis(acetylacetonato)copper(II). It is shown that the x-ray structure that Ferguson based his polarization directions on was not correct. Ferguson had available to him the crystal structure as based on two dimensional projection techniques. L. F. Dahl made available to Piper and Belford the refinement of the structure based on three dimensional x-ray data, and it is noted that the inclination of the molecular plane in the unit cell is considerably different from the one used by Ferguson. In spite of this, they arrive at approximately the same polarizations that Ferguson did. They do point out the fallacy in Ferguson's analysis however. "The complete model should include all ungerade stretching and bending vibrations: B_{2u}, B_{3u}, B_{1u}, and A_u. Some previous analyses, without explanation, omitted any mention of A_u." With the inclusion of this vibration mode all polarizations are vibronically active under D_{2h} symmetry. They point out that since the crystal spectra offer no firm basis for assignments, other evidence must be used to make the assignments. A resort is made to the crystal field model and the analysis of the electron spin resonance spectra of certain copper(II) compounds wherein extensive delocalization of pi electrons occurs. It is known, e.g., that in the copper phthalocyanine complex the spectrum cannot be interpreted in terms of the type of ground state that Ferguson proposes.

They also comment on the band at 26,000 cm⁻¹. It is suggested that this is possibly a spin-forbidden pi - pi* or n - pi* transition in the ligand. This is based on conclusions from other spectra studied by the authors.

One further comment about the article of Piper and Belford

is notable. They examine the interpretation of the spectra using various symmetries. They point out that if one uses D_{4h} symmetry and only considers the three transitions below $19,000 \text{ cm}^{-1}$ the correct number of transitions are present. However on an incorrect analysis of the vibronic selection rules they conclude that D_{4h} symmetry is quite probably insufficient to explain the spectrum. This point will be considered in more detail later.

In order to keep the chronology correct a digression from the acetylacetate controversy will be made. Shortly after the work of Piper and Belford a paper appeared by Gerritsen and Starr (15) comparing optical data with e.s.r. spectra for Cu(II) in a TiO_2 matrix. The copper is surrounded by a nearly cubic field with a small tetragonal component to a first approximation. When the effects of spin-orbit coupling are included with the other perturbations, they show how the d orbitals split into five levels. They place one of the transitions in the infrared and make the comment that detection of the transition will be prevented due to lattice absorption. The three transitions that they do observe are assigned to the three other levels. When this is done they report a value for Dq which they say is rather surprising (1510 cm^{-1}) in light of previously reported values. The rather high value comes about because they assign the transition that characterizes $10 Dq$ as being the most energetic one, contrary to the usual way in which this transition is assigned. "These data would indicate that the E_4 and E_5 levels (E_1 indicates energy level order with E_5 being the most energetic level)--which coincide in this approximation but will be separated due to spin orbit coupling by just the spin orbit constant itself--have an energy

lower than E_3 . This does not seem to agree well with a point charge model in which one assumes elongation along the z-axis." By taking the average of the two other transitions they are able to make a comparison with the predicted spectra based on e.s.r. measurements. Once again it is seen that something is amiss in the interpretation of the copper(II) spectrum.

A study of the magnetic and spectral properties of chlorocuprates was made by Hatfield and Piper (16). For the CsCuCl_3 complex they report two transitions at 11,800 and 11,000 cm^{-1} which they assign as the most energetic transitions under tetragonal splitting. For CuCl_2 they observe a transition at 12,200 cm^{-1} which is assigned as the most energetic transition.

One article that has special relevance to the research comprising this dissertation was written by Dijkgraaf (17). He reports the absorption spectra of some copper complexes of α -amino acids, including the polarized spectrum of bis(alaninato)copper(II) polarized parallel and perpendicular to the crystallographic b-axis with the incident light beam perpendicular to the 100 face. He further reports that the absorption spectrum of the copper complex of L-phenylalanine has also been measured and it is of the same type as the L-alanine copper spectrum.

Now, if the environment around the copper in the L-alanine complex is similar to that in the L-phenylalanine complex it is logical that the polarized spectrum of bis(L-phenylalaninato)copper(II) might resemble that of the alanine complex very closely.

Dijkgraaf reports two absorption bands in the polarized spectrum at 16,120 cm^{-1} and 17,230 cm^{-1} . However, upon close examina-

tion of his spectral curves one catches a hint of a third transition present in the $15,300 \text{ cm}^{-1}$ region of the spectrum with the light polarized parallel to the b-axis. He uses C_2 symmetry to tentatively assign the transition at $16,120 \text{ cm}^{-1}$ to the ${}^2A \rightarrow {}^2A$ exchange and the peak at $17,230 \text{ cm}^{-1}$ as being the ${}^2A \rightarrow {}^2B$ transition.

Dijkgraaf continued studying copper(II) spectra and his results are presented in two more papers (18, 19). In the first paper he reinterprets the spectrum of bis(L-alaninato)copper(II) in terms of the crystal field theory of Davydov (20) and describes how the single peak of the solution spectrum of the complex will split into two transitions when the complex is present in the crystalline form. The same type of interpretation is made for the copper(II) complex of DL-aminobutyric acid.

The second paper by Dijkgraaf adds to the controversy about the copper acetylacetonate complex. He reexamines the polarized spectrum of the complex and contrary to the work of Ferguson he reports four transitions being present located at $15,600$, $16,100$, $18,000$, and about $18,500 \text{ cm}^{-1}$. He once again invokes the theory of molecular excitons to explain the transitions. He comments, "The theory gives the right number of the bands observed and the predicted directions of the transition moments agree with the observed data. The magnitude of the energy split is difficult to predict, but the order of magnitude comes up to expectation."

The approach of Dijkgraaf to explain the spectrum of the acetylacetonate complex has been questioned seriously. Belford and Belford comment (21), "However, a more serious objection is that the

previously published crystal spectra at 30° K, (22), which show better resolution than the previous spectra of Ferguson (13) and the later spectra of Dijkgraaf (19) taken at higher temperatures, clearly show that there are two components in the vicinity of 15,000 cm^{-1} , each of which appears in both parallel and perpendicular polarizations (14,500 and 16,300 cm^{-1}). Therefore, they cannot be Davydov - split (\parallel & \perp) components of the same transition, as suggested by Dijkgraaf."

Further reinforcement of the incorrectness of the application of Davydov splitting has been given by Ferguson (23).

Allen (24) has attempted an analysis of bis(acetylacetonato)copper(II) complex using C_{2h} symmetry. Based upon the polarizations of Belford and Piper he presents an argument for the assignment of the three transitions that he states is consistent with other copper(II) assignments. The $xy \rightarrow z^2$ transition is assigned as occurring at 14,500 cm^{-1} , the $xy \rightarrow xz$ at 15,600 cm^{-1} , and the $xy \rightarrow x^2 - y^2$ at 18,000 cm^{-1} . The assignments are based on the idea that the $xy \rightarrow xz$ transition has just the opposite types of vibronically allowed transitions as the other two transitions, and the observed polarizations for the $xy \rightarrow xz$ transition are different from the observed polarizations of the other two transitions.

Cotton (25) examined the bis(2,2,6,6-tetramethyl-3,5-heptanedionato)copper(II) complex ($\text{Cu}(\text{DPM})_2$) in an attempt to understand the electronic properties of the bis(acetylacetonato)copper(II) complex. The electronic structure should not differ a great deal from the acetate complex. Using MO calculations with the restriction that the coefficients of the d orbitals in the MO eigenvectors remain consistent with the

magnitude indicated for them by e.s.r. data, he demonstrated that the d_{xy} orbital lies some $18,000 \text{ cm}^{-1}$ higher than the other four d orbitals. The other four lie within a few thousand wavenumbers of one another. With these MO calculations as a basis he suggests that the absorption spectrum of bis(acetylacetonato)copper(II) includes all four 'd-d' transitions in the $15,000\text{-}20,000 \text{ cm}^{-1}$ region. The polarized spectrum he reports for $\text{Cu}(\text{DPM})_2$ lends credibility to his MO conclusions. There are four transitions observed at ca. 20,000, 18,200, 16,400, and $15,600 \text{ cm}^{-1}$.

A very fine contribution to the bis(acetylacetonato)copper(II) spectral problem has been made by Belford and Carmichael (26). They study the polarized spectrum of bis(3-phenyl-2,4-pentanedionato)copper(II) complex which differs from the acetylacetonate complex only by the replacement of the hydrogen atom on the 3-carbon atom by a phenyl group. The bonding of the two complexes should be very similar, the alteration being in the packing. Spectra were taken at various temperatures with the electric intensity vector parallel to the b crystallographic axis, perpendicular to the b-axis incident on the (001) face, and perpendicular to the b-axis incident on the (100) face. It is shown that all bands are polarized in the molecular y direction much more than in the x or z directions. Actually, of the four bands present the one occurring at $19,000 \text{ cm}^{-1}$ shows no polarization in the z direction. The other bands occur at 20,600, 16,900, and $15,400 \text{ cm}^{-1}$. An attempt is made to analyze the spectrum in terms of D_{2h} pseudosymmetry and it is concluded that it is not possible to use polarizations to make assignments based upon vibronic symmetries. However, using arguments based upon the tempera-

ture dependence of the intensities they are able to infer that two lowest-energy transitions involve the z^2 and x^2-y^2 orbitals, whereas the next two bands involve the xz and yz orbitals (the x^2-y^2 or xy orbital can be the ground state orbital depending upon orientation of axes, cf. p.124). An argument is also made that the intensity of the d transitions is borrowed from a charge transfer transition from a nonbonding oxygen orbital to an antibonding copper orbital. This is really a reiteration of the argument made by Ferguson that there is some type of interaction between the metal orbitals and the ligand orbitals other than straight forward σ bonding.

Some of the most comprehensive work done on the study of copper(II) spectra appears in a series of papers by Billing, et al.. The first of these (27) describes the polarized spectra and e.s.r. spectra of six tetraamminecopper(II) complexes. A total of eight different tetraamminecopper(II) complexes are studied and a systematic attempt is made to order the energy levels on the criteria of the x-ray structure and the above measurements. All of the complexes contain the square coplanar $\text{Cu}(\text{NH}_3)_4^+$ cation. It is demonstrated that the energy of the $d_{x^2-y^2} \rightarrow d_z^2$ transition can be used as a measure of the relative tetragonal distortion. This transition is correlated with the in-plane copper-nitrogen bond lengths. The complexes $\text{Cu}(\text{NH}_3)_4(\text{NO}_2)_2$ and $\text{Cu}(\text{NH}_3)_4(\text{SCN})_2$ have been given the one electron sequence $d_{x^2-y^2} > d_z^2 > d_{xy} > d_{xz}, d_{yz}$. Both complexes are octahedral with tetragonal distortion. For the purely square-planer complex $\text{Na}_4\text{Cu}(\text{NH}_3)_4(\text{Cu}(\text{S}_2\text{O}_3)_2)$ the sequence may be $d_{x^2-y^2} > d_z^2 > d_{xz}, d_{yz} > d_{xy}$.

The monoethylenediaminecopper(II) dichloride complex was in-

investigated by Billing, et al. shortly thereafter (28). Using D_2 symmetry a successful analysis was made of the polarized spectrum of the complex. An argument was made against other possible symmetries on the basis of the observed gyromagnetic ratio and those expected on the basis of these different symmetries. Essentially four transitions were observed in the visible region and the most probable sequence of one electron energy levels was given as $d_{x^2-y^2} > d_{xy} > d_{xz} > d_{yz}$.

All three transitions are shown (29) to be present under D_{4h} symmetry in single crystals of meta-zeunerite $(Cu(UO_2)_2(AsO_4)_2 \cdot 8H_2O)$. The three transitions occur at 15,000, 13,000, and 12,000 cm^{-1} , and the sequence of orbitals is convincingly established as $d_{x^2-y^2} > d_{xy} > d_z^2$, d_{xz} , d_{yz} on the basis of vibronic selection rules. A correlation is then made between the $d_{x^2-y^2} \rightarrow d_z^2$ transition and the amount of tetragonal distortion as given by x-ray analysis for various copper(II)-oxygen complexes. With increasing axial bond length the transition, as expected, becomes more energetic.

The polarized single-crystal spectra and e.s.r. spectra of six bis(ethylenediamine)copper(II) compounds have also been studied by Billing and co-workers (30). Three transitions are reported with the $d_{x^2-y^2} \rightarrow d_{xz}, d_{yz}$ occurring in the 18,400 to 19,000 cm^{-1} region, the $d_{x^2-y^2} \rightarrow d_{xy}$ transition occurring in the 15,200 to 19,000 cm^{-1} region, and the $d_{x^2-y^2} \rightarrow d_z^2$ transition being in the 15,200 to 18,000 cm^{-1} region. The symmetry used was D_{2h} although the statement is made that D_{4h} symmetry cannot be ruled out on the basis of the polarized spectra. There is uncertainty as to the exact location of the $d_{x^2-y^2} \rightarrow d_{xy}$ transition as it is masked by the other transitions.

Electronic and e.s.r. studies have been made on the two complexes dihydrogenethylenediaminetetraacetatoaquocopper(II) and bis(diethylenetriamine)copper(II) bromide monohydrate (31). The polarization data yields the orbital sequence as $d_{xy} > d_z^2 > d_{xz} > d_{x^2-y^2} > d_{yz}$ for the $\text{CuH}_2\text{edta}(\text{H}_2\text{O})$ complex and $d_{x^2-y^2} > d_z^2 > d_{xy} > d_{xz} > d_{yz}$ for the bromide complex. Different orientations of the axes were chosen in the two crystals due to the molecular orientation of the complex in the crystal habit. The four transitions are all observed in the visible region. The electronic consequence of having a d_{xy} ground state is discussed. Little effect is noticed on the e.s.r. spectra, but there are radical effects in the intensities of the polarizations.

The final paper in the series by Billing, et al. is concerned with the electronic energy levels of the cis-distorted octahedral complex nitrobis(2,2'-bipyridyl)copper(II) nitrate (32). The polarized single-crystal spectra are reported. There are three transitions apparent at ca. 15,000, 14,600, and 9,500 cm^{-1} . It is suggested that there is probably another band under the vibronic envelope at 14,600 cm^{-1} and this would account for the fourth transition under the C_{2v} symmetry the authors choose to work with. The one electron sequence is assigned as $d_z^2 > d_{xy} > d_{x^2-y^2} > d_{xz}$ with the d_{yz} orbital comparable in energy with the $d_{x^2-y^2}$ & d_{xz} orbitals. The axes were chosen such that the x and y axes split the ligand-metal-ligand angle, and such that there is axial compression. This explains the d_z^2 ground state.

One final paper deserves consideration. A very interesting approach to the study of copper(II) spectra has been given by Smith (33). He uses an empirical theory which takes into account σ and π bonding and

electrostatic effects. The theory applies to the spectra of tetragonal and trigonal bipyramidal chloro-complexes. Covalence effects are discussed in terms of the angular overlap model of Jorgensen, et al. The destabilization of the metal orbitals due to impingement of ligand orbitals is expressed as being proportional to the square of the relevant overlap integral. This overlap integral is then defined by a radial and angular part. The angular part can be evaluated for the d orbitals, whereas the radial part is left as a single parameter to be fitted from the transition energies. This way of attacking the assignment of the transitions shows much promise.

One can see that many formidable and elegant attempts have been made to describe the ordering of the levels in copper(II) complexes where tetragonal distortion occurs. The molecular orbital formalism has been pitted against the theory of molecular excitons. Both approaches have been protested and supplanted with crystal field theory by certain individuals. Still controversy is manifest and there is disagreement as to the number, location, and ordering of the "d" orbitals.

Certain patterns are emerging as more information about various complexes becomes available. These patterns will be discussed in more detail as the work comprising this dissertation is examined.

CHAPTER II

EXPERIMENTAL TECHNIQUES

Preparation of Compounds. The bis(indazole)copper(II) chloride complex was prepared in the following manner: diaquocopper(II) chloride was dissolved in isopropyl alcohol (0.7180 g in 100 ml), while in a separate container 0.1559 g of indazole ($C_7N_2H_6$) were dissolved in 10 ml of isopropyl alcohol. The indazole solution was stirred constantly as 31.3 ml of the copper(II) chloride solution were added dropwise. This yielded an indazole to copper(II) stoichiometric ratio of 2:1. Precipitation occurred almost immediately upon addition of the copper(II) chloride solution, indicating that the complex that was formed was highly insoluble in isopropyl alcohol. The precipitate was microcrystalline and could not be used for either x-ray work or the spectral studies.

It was necessary to recrystallize the precipitate in a suitable solvent. Dimethylformamide was decided upon after testing several solvents, and a vapor diffusion method was used to obtain the crystals. A small vial of the complex dissolved in DMF (0.1 g complex: 2 ml of DMF) was placed inside a larger vial containing isopropyl alcohol. The larger vial was then sealed and the system was allowed to equilibrate at room temperature. It took approximately two days for the light-green crystals to form. The crystals were quite small and all the cry-

stals examined under the polarizing microscope were, in fact, not single, but rather double crystals that resembled two swords crossed and joined at the hilt. It was necessary to cut off one end of the single blades for x-ray intensities and spectral studies. Some of the crystals were taken and ground into a fine powder for magnetic susceptibility measurements.

The bis(L-phenylalaninato)copper(II) complex was prepared in the following manner: a small vial containing a saturated solution of L-phenylalanine in water was placed inside a larger vial that had been previously filled 3/4 full with distilled water. This caused the smaller vial to be flooded with the distilled water. An eyedropper was then used to layer a saturated solution of copper(II) acetate into the bottom of the larger vial. The two original solutions then diffused together and blue crystals formed at the lip of the smaller vial in approximately three days at room temperature (94).

It was possible to find an x-ray data crystal using the above method although the majority of crystals had a very large mosaic. One of the single crystals was used for spectral studies, and several of the crystals were ground to a fine powder for the magnetic susceptibility work.

The pH of the solution from which the crystals were grown was 5 - 6.

Several other methods of crystallization were attempted one of which deserves mention. Scientific American (34) describes a method wherein a silica-gel plug is placed in the bottom of a "U" tube and the species are allowed to diffuse together through the silica gel. It took approximately two weeks to grow crystals by this method, but

when they formed they were quite large and well developed. The crystals grown this way still had a high mosaic. This looks like one of the most promising ways to grow crystals that has been encountered which can be used for systems of future interest.

Experimental Measurements. The x-ray intensities for both structures were taken on a G. E. - X. R. D. - 5 diffractometer using the $\theta - 2\theta$ scan method with Ni - filtered, Cu - $K\alpha$ radiation. The diffraction unit was equipped with an SPG Single Crystal Orienter, a scintillation counter, and pulse height analyzer.

Single crystals were used for the x-ray intensity data.

The density of both crystals was measured by the flotation method using a Westphal balance. The liquids used for the bis(indazole) copper(II) chloride complex were diodomethane and carbon tetrachloride. The two liquids used for the bis(L-phenylalaninato)copper(II) were carbon tetrachloride and hexane. The density of the indazole complex was measured at 24°C and L-phenylalanine complex at 25°C.

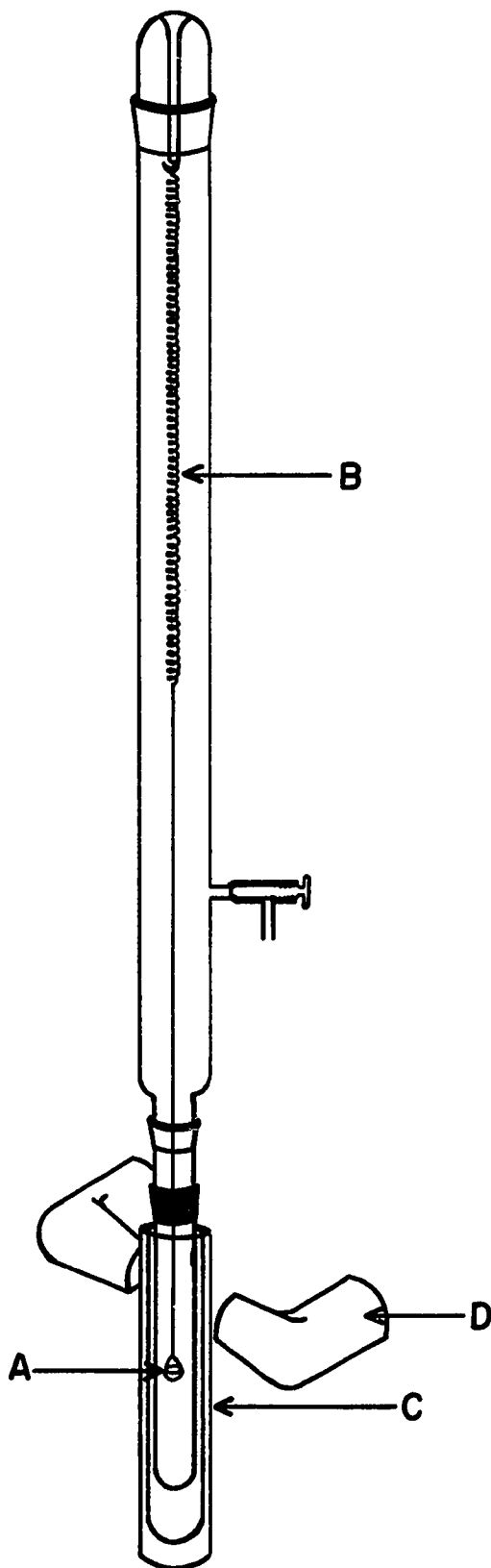
The spectra were run on a Beckman DK-1 recording spectrophotometer. The method employed was rather unique in the way in which single crystals were used to obtain the spectra. The manner in which this was accomplished was to mount a thin crystal on an aluminum strip and then place the strip in a specially designed holder that had been machined to fit in the cuvette holder of the spectrophotometer. The crystal was placed over a small hole that had been drilled in the aluminum strip and held in place by placing a small amount of Ambroid styrene plastic cement on each end of the crystal. The cement did not in any way obscure the hole in the strip. Another strip with a small

hole drilled in it (0.015 in. diameter) was placed in the reference beam of the spectrophotometer. The indazole crystal was placed over a 0.015 in. diameter hole, whereas the L-phenylalanine crystal was placed over a 0.033 in. diameter hole. All spectra were measured at room temperature. No attempt was made to obtain the extinction coefficients of the complexes, and therefore the spectra are simply wavelength vs. relative absorbance. The peak positions of the spectra as reported are only good to $\pm 10 \text{ m}\mu$.

Figure 1 shows the Faraday balance used in the determination of magnetic susceptibilities of the two complexes. The powdered sample is contained in the small quartz bucket (A) which is attached to a quartz spring (B) via a hook. This quartz spring is in turn attached to the top of the cylindrical vacuum chamber by means of another hook. The vacuum chamber is sectioned for easy access to the spring and sample. The bottom section is encased by a Dewar flask (C) such that the temperature can be controlled, and such that susceptibility can be measured as a function of temperature. In order to measure the susceptibility of the sample the double pole magnet (D) is passed upwards at a very slow speed and the deflection of the bucket is measured with a cathetometer. The magnet can be moved up or down with a reversing switch that operates a lift to which the base of the magnet is attached. The speed of the motor that runs the lift can be varied.

It was necessary to determine the quartz spring constant as given by equation (1), where χ_g is the gram susceptibility, m is the

Figure 1. Schematic of Magnetic Balance



$$(1) \quad \chi_g = kd/m$$

mass, and d is the total up and down deflection as measured by the cathetometer.

The measured deflection is the resultant of the paramagnetic contribution from the complex and a diamagnetic contribution due to the bucket. To determine the diamagnetic contribution a plot of $m \cdot \chi_g$ vs. d was made (Figure 2) using the complex HgCo(SCN)_4 as a standard. This plot will give an intercept that is the diamagnetic contribution. This diamagnetic deflection will have to be added to the measured deflection in susceptibility determinations to get the correct total deflection. The data were fit using a least-squares program written by Tucker (65). The resulting equation is:

$$m\chi_g = 3.685 \times 10^{-6}(d + 0.0022)$$

where 0.0022 cm is the deflection of the bucket, and it is seen that the spring constant is:

$$k = 3.685 \times 10^{-6}$$

The calibration was done at 0°C. The gram susceptibility of the HgCo(SCN)_4 is 17.44×10^{-6} cgs units at this temperature (35).

The molar susceptibility is that which is usually reported.

$$\chi_M = \chi_g M$$

where M is the molecular weight. χ_M was determined as a function of temperature for both complexes. Four temperatures were used for the determination: room temperature, a water-ice mixture, a dry ice-acetone bath, and a liquid nitrogen bath. The temperature of each bath was measured in two ways. A multiple junction thermocouple was prepared (copper-constantan) and calibrated against an NBS certified platinum

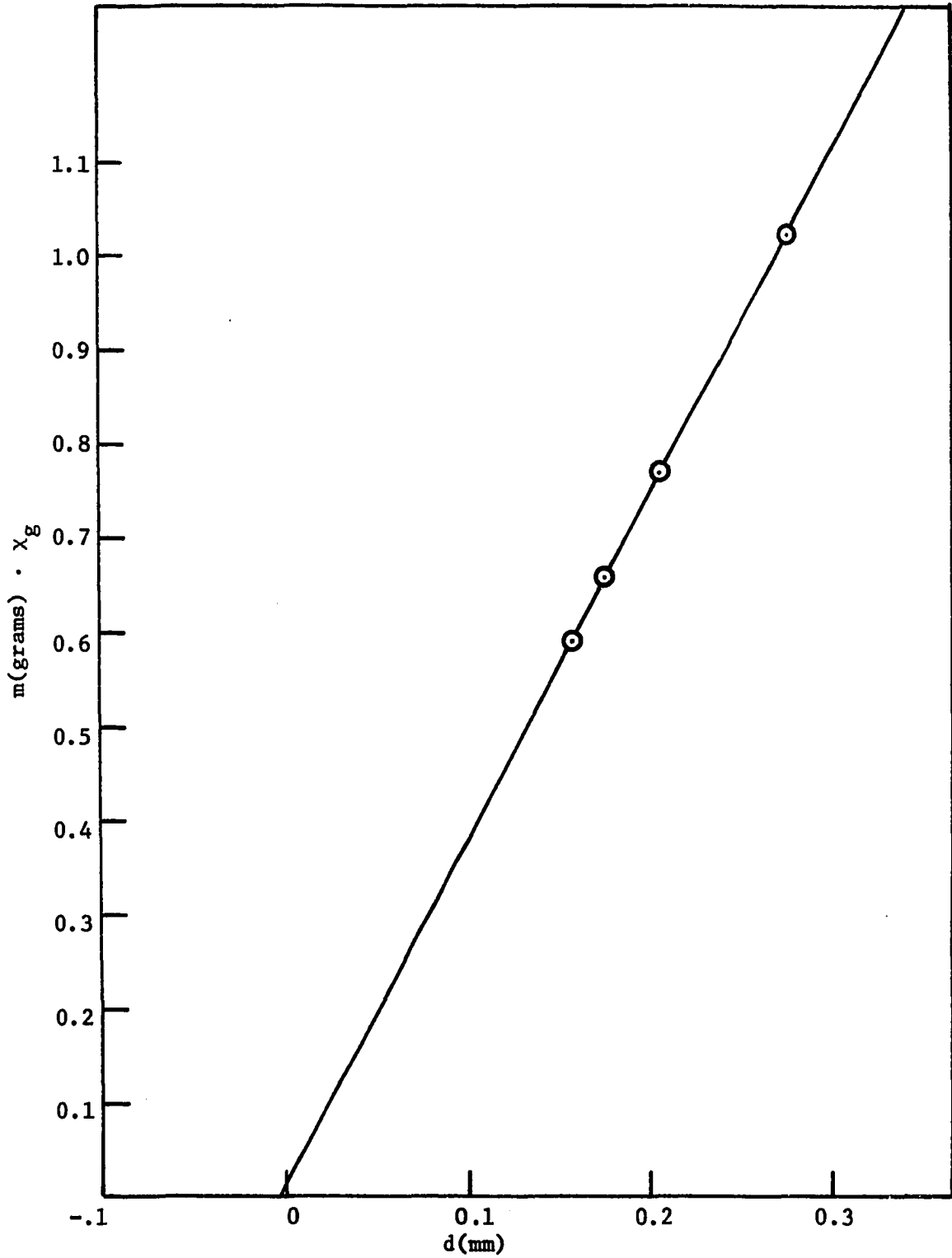


Figure 2. $m \cdot \chi_g$ vs. d for Determination of
Diamagnetism of Sample Bucket

resistance thermometer. This thermocouple was inserted in the Dewar that surrounds the sample chamber and was used to monitor the temperature. The temperature readings from this calibrated thermocouple were not used in the χ_M vs. $1/T$ graphs because the thermocouple was not linear over the temperature range investigated. It did allow one to determine when the system was approaching thermal equilibrium. The temperature of the bath in the Dewar was measured with the platinum resistance thermometer immediately after the deflection readings were taken. This temperature was used in the susceptibility determinations.

The vacuum chamber was evacuated and allowed to come to thermal equilibrium before deflection readings were recorded. The thermal equilibration took from six to twelve hours.

CHAPTER III

CRYSTAL AND MOLECULAR STRUCTURE OF

BIS(L-PHENYLALANINATO)COPPER(II)

Solution and Refinement of Structure. The light-blue crystals of the copper(II)-L-phenylalanine complex are monoclinic with systematic extinctions occurring for the $0k0$ planes when k is odd. This indicates that the space group is $P2_1$ since the L-phenylalanine molecule prohibits a centrosymmetric space group. The least-squares (36) cell dimensions from 43 reflections (Appendix I) measured at 22°C indicated that there are two copper atoms per unit cell, each being coordinated with two L-phenylalanine molecules. The pertinent space group information is presented in Table 1.

A small crystal (0.36 X 0.10 X 0.02 mm) was used as the data crystal due to the high mosaic of all crystals examined. The data crystal had a mosaic of 1° . The reason for this high mosaic became apparent when the structure was solved and is discussed later.

The crystal was mounted with b^* parallel to the polar axis, and a theta-two theta scan technique with a take-off angle of 3° was used to collect the intensities. All reflections within a 2θ value of 140° were measured with Cu-K α radiation. Of the 1745 reflections within this 2θ limit, 1702 were observed. Lorentz, polarization, and absorption

Table 1

Crystal Data for Bis(L-phenylalaninato)Copper(II)

Space Group	P_{2_1}
No. of Molecules	2
Molecular Formula	$\text{Cu}(\text{C}_9\text{H}_{10}\text{O}_2\text{N})_2$
Formula Weight	391.90
Cell Dimensions	
a	$= 16.710(0.014)$
b	$= 5.217(0.009)$
c	$= 9.509(0.007)$
β	$= 98.40(0.06)$
Density	
obs.	$= 1.575 \text{ g/cc}$
calc.	$= 1.587 \text{ g/cc}$
Vol.	$= 820.14$
F(000)	$= 406$
Reciprocal cell dimensions	
a^*	$= 0.06049(0.00005)$
b^*	$= 0.1917(0.0004)$
c^*	$= 0.1063(0.0001)$
β^*	$= 81.60(0.07)$
Vol. [*]	$= 0.001219$

corrections ($\mu = 21.50 \text{ cm}^{-1}$) were applied to the data.

A three dimensional numerical integration was made to correct the intensities for absorption. The intensity of a diffracted beam is

given by the expression

$$I = I_0 \int e^{-\mu t} dV$$

where μ is the linear absorption coefficient of the crystal, t is the total path length traversed by the beam, dV is the diffracting element of volume, and I_0 is the intensity of the diffracted beam without absorption. The evaluation of this integral was done by using a computer program written by Dr. Philip Shapiro. The program does a three dimensional numerical integration using the method of Gauss (37).

Lorentz and polarization corrections were made on the intensities by multiplying them by the factor

$$L. P. = \frac{2 \sin 2\theta}{1 + \cos^2 2\theta}$$

A sharpened Patterson synthesis was calculated. The map was sharpened by multiplying $|F|^2$ by the function (38)

$$M(s) = \left(\frac{\sum z_i}{\sum f_i} \right)^2$$

$\sum z_i$ = Sum of the atomic numbers

$\sum f_i$ = Sum of the scattering factors at $\sin \theta/\lambda$ of the amplitude which is modified.

All unobserved reflections were omitted from the Patterson function.

One-fourth of the unit cell was calculated with sections perpendicular to the b axis having points fixed approximately 0.2 \AA apart in (u,v,w) . Since the equivalent positions for the $P2_1$ space group are

x,y,z

and

$-x, y + \frac{1}{2}, -z$

the copper-copper vector will be located at $2x, \frac{1}{2}, 2z$. The Harker section at $y = \frac{1}{2}$ was examined for this heavy-heavy atom vector, and the x and z coordinates for copper were determined. Following the usual convention for this space group the y coordinate was fixed at $\frac{1}{2}$.

The usual way to solve a Patterson map is to first assume that one of the heavy atoms is located at the origin. One then looks for a heavy-light atom vector in the Patterson and assumes that this vector represents a light atom position having (x,y,z) coordinates in real space obtained by displacing the Patterson vector (u,v,w) such that its new origin is the heavy atom position in real space. One then derives the vector defined by these (x,y,z) coordinates and the second heavy atom position in real space and returns to the Patterson to see if such a vector can be found. If this new vector is found it is considered proof that the (x,y,z) coordinates derived above actually constitute an atomic position.

For the L-phenylalanine complex any vector examined in the Patterson map with coordinates (u,v,w) will also have coordinates $(-u,-v,-w)$, $(u,-v,w)$, and $(-u,v,-w)$ due to the centrosymmetric nature of the Patterson, i.e., the Patterson symmetry is $P2/m$. This means that all four equivalent positions will have to be checked to see if any of them meets the criterion for being an atomic position.

Since the Patterson is centrosymmetric two of the equivalent positions should check, viz. the mirror images should each be a possible solution of the Patterson. This ambiguity can be removed for the phenylalanine complex because it is known that the L form is the one present.

Unfortunately when the previously described method was applied to the Patterson it could not be solved. This interesting deviation occurred because of the positions of the two heavy atoms in the unit cell. The Harker plane at $y = \frac{1}{2}$ gave the copper coordinates as $(\frac{1}{2}, \frac{1}{4}, \frac{1}{4})$ and $(\frac{1}{2}, 3/4, 3/4)$. In order to demonstrate the difficulty assume a heavy-light atom vector is present in the Patterson at (u, v, w) . One now adds the real coordinates $(\frac{1}{2}, \frac{1}{4}, \frac{1}{4})$ to the vector and then subtracts this position $(u + \frac{1}{2}, v + \frac{1}{4}, w + \frac{1}{4})$ from the position of the second heavy atom to obtain the vector $(-u, \frac{1}{2} - v, \frac{1}{2} - w)$. As was explained this must be done for all four equivalent positions yielding the table

$$(-u, \frac{1}{2} - v, \frac{1}{2} - w), (u, \frac{1}{2} + v, \frac{1}{2} + w)$$

$$(-u, \frac{1}{2} + v, \frac{1}{2} - w), (u, \frac{1}{2} - v, \frac{1}{2} + w)$$

When this table is examined one immediately sees the problem, namely that the four vectors are related by the symmetry of the Patterson. This means that all four peaks will necessarily check in the Patterson, and hence none of them can be eliminated.

Another method was employed to solve the Patterson. One way of looking at a Patterson is to regard it as a combination of N images of the original crystal structure, each offset by the amount required to bring one of the atoms to the origin (39). The peak heights of course will be the product of the respective atoms defining the vector, but this makes no difference as to the visualization of the location of the peaks in a Patterson synthesis. If one knows approximately what the structure looks like then it may be possible to sort one of the images of the structure from the Patterson. Assuming the copper atom at the origin, the image of the two L-phenylalanine molecules was

sought. The image, of course, was composed of the copper-light atom vectors. Once the relative position of a light atom with respect to the copper atom was established its position in real space could be determined by simply adding the Patterson (u,v,w) coordinates to the known copper atom coordinates. The problem resolved itself to building a model that yielded either an unreasonable structure or one that was compatible with the two L-phenylalanine molecules. Although this was not a very elegant way to solve the structure it proved effective in this instance.

To check the trial coordinates an initial structure factor calculation was done. The atomic scattering factors used were taken from the International Tables for X-ray Crystallography (40). The scattering power curves for Cu^{2+} , N° , and C° were taken directly from the tables. The curve for oxygen was derived by taking an average of 0^{-1} and 0° curves. The scattering factors that were used later in the refinement for hydrogen were those of Stewart, Davidson, and Simpson (41). A modification of ORFLS, a FORTRAN structure factor and least-squares program written by Busing, Martin, and Levy (42), was used for the structure factor calculation. This same program was used for the remainder of the refinement. The program performs successive cycles of refinement using the entire matrix of the normal equations. The program minimizes the quantity

$$\sum_r w(F_{\text{or}} - KF_c)^2$$

where w is the weight given to each reflection. The program was re-dimensioned to refine 386 parameters. This initial structure factor calculation gave an R value of 0.35.

$$R = \frac{\sum ||F_o| - |F_c||}{\sum |F_o|}$$

This was a reasonable residual; therefore, it was decided to cycle the least-squares program twice. The R dropped to 0.13 and served as an indication that most of the structure was correct. It was noticed, however, that two of the carbon atoms had excessively large temperature factors. Therefore a difference Fourier was run using Ahmed's Fourier program (NRC-8) (43). All reflections were included in the structure factors used to calculate this difference Fourier since it can be shown (39) that the most significant reflections for solution of the phase problem are the unobserved reflections. The coordinates for the two atoms with the high temperature factors were not included in the structure factors. The difference Fourier was calculated on the absolute scale. The difference map indicated the positions of the two other atoms. Upon addition of these positions to the rest of the atoms, and after two more cycles of the least-squares program the R value dropped to 0.087. At this time all temperature factors were still isotropic.

The copper atom was made anisotropic at this stage of refinement. After two cycles of the least-squares program the R index was lowered to 0.074.

Another difference Fourier was calculated just as previously described in order to locate the hydrogen atoms. The hydrogen positions program was written in this laboratory by C. E. Tatsch. With the aid of this program it was possible to locate positive peaks in the difference Fourier that could be considered hydrogen atoms for all of the calculated positions. There was some question about the hydrogens attached to the

nitrogen atoms, but there was positive electron density in their vicinity. Several other of the possible hydrogen peaks were moot but here again there was positive electron density close to the calculated positions. It was decided to use the calculated hydrogen coordinates in subsequent refinement because of the uncertainty in locating the centers of the electron density for the hydrogen atoms. An average value of the electron density for hydrogen atoms was $0.33 \text{ e}/\text{\AA}^3$. Table 2 gives the densities for the various hydrogen peaks.

While the difference Fourier was being studied, all of the atoms already being refined were made anisotropic. This further lowered the R value to 0.058 after two more cycles of the least-squares program.

Upon addition of the hydrogen atoms the R value dropped to 0.055. Up to this stage of refinement only the reflections that had been observed had been refined. The value assigned to the unobserved reflections was simply an average value obtained by estimating that the largest reflection that could not be seen would be four counts on the diffractometer. Statistically an average value for these unobserved reflections would be two counts. This is the value used for the unobserved reflections.

A test was incorporated in the least-squares program to deal with the unobserved reflections. If the value calculated for the unobserved reflections was equal to or greater than twice the value that had been used for the unobserved reflection then the reflection was used in subsequent refinement. Eight of the unobserved reflections were included in the refinement as a result of this test.

It is possible to use many different weighting schemes when

TABLE 2

Peak Heights of Hydrogen Atoms in Difference Fourier

Atom	$e/\text{\AA}^3$	Atom	$e/\text{\AA}^3$
H(C ₂ A)	0.40	H(C ₂ B)	0.40
H ₁ (NA)	0.30	H ₁ (NB)	0.40
H ₂ (NA)	0.30	H ₂ (NB)	0.10
H ₁ (C ₃ A)	0.16	H ₁ (C ₃ B)	0.40
H ₂ (C ₃ A)	0.31	H ₂ (C ₃ B)	0.40
H(C ₅ A)	0.30	H(C ₅ B)	0.30
H(C ₆ A)	0.22	H(C ₆ B)	0.35
H(C ₇ A)	0.55	H(C ₇ B)	0.40
H(C ₈ A)	0.30	H(C ₈ B)	0.40
H(C ₉ A)	0.25	H(C ₉ B)	0.30

one refines a crystal structure (38). Properly the correct weight to use is given by (39)

$$\sqrt{W} = 1/\sigma_{F_0}$$

where σ is the standard deviation in the F_0 . However one can take the weight of any F_0 as being proportional to $1/|\Delta F|^2$ as a reasonable approximation. This is certainly better than using unit weights. In order to get a proper estimation of $|\Delta F|^2$ one can use a virial expansion of the form (44):

$$|\Delta F|^2 = A + B|F_0| + C|F_0|^2 + D|F_0|^3$$

This is the weighting scheme that was instigated at this time and used for the rest of the refinement. In order to obtain the coefficients in this virial expansion the output of an error analysis (45) program was taken and a polynomial regression performed (46) using F_0 as the independent variable and $|\Delta F|^2$ as the dependent variable.

The coefficients obtained using the above procedure are listed below.

$$A = 4.671$$

$$B = -0.1596$$

$$C = 0.0049022$$

$$D = -0.00002675$$

Anomalous dispersion corrections were made for the copper atom. Anomalous dispersion arises when the wavelength of the incident beam is approximately the same energy as an absorption edge of an atom in the crystal. The effect is produced by the interaction of the incident beam with the inner electrons of the anomalous dispersing atom (38). When the effect occurs the atomic scattering factor is written as

$$f = f_0 + \Delta f' + i\Delta f''$$

where f_0 is the scattering power without anomalous dispersion, and $\Delta f'$ and $\Delta f''$ are the real and imaginary parts due to anomalous dispersion. Using Cu-K α radiation the real and imaginary corrections for the copper atom are -2.1 and 0.7 respectively (40). Any correction for the other atoms in the unit cell was negligible. In this structure factor program the anomalous dispersion corrections are applied to the calculated structure factors.

Upon inclusion of anomalous dispersion and the virial weighting scheme the residual index fell to 0.044 after only one cycle. New hydrogen positions were calculated after every cycle for the rest of the refinement. After three more cycles of the structure factor-least-squares program the R fell to 0.041, and the errors in the positional parameters divided by the shifts in the parameters all fell below 0.22. The same ratio for all thermal parameters fell below 0.28. Refinement was considered complete. Table 3 lists the pertinent R values where the weighted R'' is defined as

$$R'' = \frac{\sum_i w_i (|F_{oi}| - |F_{ci}|)^2}{\sum_i w_i |F_{oi}|^2}$$

The coordinates of the atoms along with the standard deviations are shown in Tables 4a and 4c. The anisotropic temperature factors and their estimated standard deviations are shown in Table 4b.

A difference Fourier was run to check the correctness of the final structure and to gain some idea of the residual error. The program included all reflections in the summation. The original program was called FORDAP and was written by A. Zalkin at the University

TABLE 3

R Values for Bis(L-phenylalaninato)copper(II)

R factor Including Unobserved Reflection	
For Which $F(\text{calc}) > 2F(\text{unobs})$	0.041

R factor omitting Unobserved Reflections	0.040
--	-------

Weighted R'' Factor Including Reflections	
For which $F(\text{calc}) > 2F(\text{unobs})$	0.043

Weighted R'' Factor Omitting Unobserved Reflections	0.043
---	-------

of California, Berkeley (Unpublished). The program used is a modification of the version from the University of Canterbury. The major peaks in the difference Fourier occurred around the copper atom position. Four positive peaks occurred around the copper atom ranging from $0.302 e/\text{\AA}^3$ to $0.458 e/\text{\AA}^3$. These peaks are arranged at the approximate corners of a square with the copper atom at the center. Two negative peaks of $-0.797 e/\text{\AA}^3$ and $-0.420 e/\text{\AA}^3$ are arranged on either side of the center of the above mentioned square such that a line joining them is perpendicular to the square and passes through the copper atom. Apparently conventional anisotropy is not able to adequately describe the thermal motion. In the derivation of the expression for anisotropic thermal motion the assumption is made that the force on an atom is proportional

TABLE 4a

Atomic Parameters of Bis(L-phenylalaninato)copper(II)

Atom	X	Y	Z
Cu	0.4907(0.0001)	0.2500	0.2504(0.0001)
O ₁ A	0.4704(0.0002)	0.4555(0.0008)	0.0780(0.0003)
O ₂ A	0.4028(0.0002)	0.4482(0.0009)	-0.1423(0.0003)
C ₁ A	0.4164(0.0003)	0.3657(0.0012)	-0.0197(0.0004)
C ₂ A	0.3630(0.0003)	0.1520(0.0011)	0.0248(0.0004)
N(A)	0.4065(0.0002)	0.0154(0.0009)	0.1498(0.0004)
C ₃ A	0.2868(0.0003)	0.2856(0.0013)	0.0602(0.0005)
C ₄ A	0.2151(0.0003)	0.1160(0.0012)	0.0772(0.0005)
C ₅ A	0.1919(0.0003)	-0.0885(0.0014)	-0.0111(0.0007)
C ₆ A	0.1213(0.0003)	-0.2265(0.0018)	-0.0023(0.0007)
C ₇ A	0.0721(0.0004)	-0.1538(0.0017)	0.0944(0.0008)
C ₈ A	0.0939(0.0003)	0.0501(0.0019)	0.1817(0.0007)
C ₉ A	0.1654(0.0003)	0.1841(0.0015)	0.1750(0.0006)
O ₁ B	0.5173(0.0002)	0.0395(0.0008)	0.4214(0.0003)
O ₂ B	0.6057(0.0002)	0.0190(0.0009)	0.6206(0.0003)
C ₁ B	0.5831(0.0003)	0.1069(0.0011)	0.5015(0.0004)
C ₂ B	0.6363(0.0002)	0.2972(0.0010)	0.4321(0.0004)
N(B)	0.5804(0.0002)	0.4711(0.0009)	0.3428(0.0004)
C ₃ B	0.7019(0.0003)	0.4274(0.0012)	0.5363(0.0005)
C ₄ B	0.7744(0.0003)	0.4989(0.0012)	0.4669(0.0005)
C ₅ B	0.7728(0.0004)	0.7120(0.0015)	0.3809(0.0007)
C ₆ B	0.8398(0.0005)	0.7780(0.0022)	0.3166(0.0008)
C ₇ B	0.9076(0.0004)	0.6251(0.0024)	0.3384(0.0008)
C ₈ B	0.9099(0.0004)	0.4136(0.0024)	0.4219(0.0008)
C ₉ B	0.8431(0.0003)	0.3483(0.0016)	0.4861(0.0006)

TABLE 4b

Anisotropic Temperature Values * X10⁴

* $\exp(-[h^2b_{11}+k^2b_{22}+l^2b_{33}+2hkb_{12}+2hlb_{13}+2klb_{23}])$						
Atom	b ₁₁	b ₂₂	b ₃₃	b ₁₂	b ₁₃	b ₂₃
Cu	23(.2)	218(2)	48(1)	-19(1)	-0.3(.2)	21(1)
O ₁ A	23(1)	206(14)	50(3)	-14(4)	6(2)	32(6)
O ₂ A	30(1)	335(18)	54(4)	-10(4)	4(2)	44(7)
C ₁ A	22(2)	258(21)	50(5)	10(5)	9(2)	2(9)
C ₂ A	17(1)	259(20)	52(4)	-0.3(5)	8(2)	- 2(8)
N(A)	21(1)	208(17)	55(4)	- 6(4)	11(2)	3(8)
C ₃ A	19(1)	273(25)	101(6)	13(6)	11(2)	12(11)
C ₄ A	20(2)	344(24)	78(5)	21(6)	6(2)	33(10)
C ₅ A	28(2)	349(28)	157(9)	-21(7)	27(4)	-19(14)
C ₆ A	31(2)	417(31)	191(9)	-32(9)	25(3)	- 7(19)
C ₇ A	27(2)	594(42)	166(9)	-19(8)	16(4)	76(17)
C ₈ A	26(2)	776(50)	145(9)	7(9)	31(4)	40(19)
C ₉ A	27(2)	636(46)	95(6)	7(7)	20(3)	-0.2(14)
O ₁ B	22(1)	212(15)	47(3)	-12(3)	2(2)	3(6)
O ₂ B	28(1)	361(19)	57(4)	- 8(4)	- 1(2)	51(7)
C ₁ B	24(2)	183(19)	47(5)	12(5)	11(2)	- 3(8)
C ₂ B	17(1)	176(22)	56(4)	0.7(4)	5(2)	3(8)
N(B)	22(1)	191(17)	48(4)	- 6(4)	9(2)	3(8)
C ₃ B	20(2)	341(24)	64(5)	-16(5)	6(2)	-10(10)
C ₄ B	23(2)	293(23)	65(5)	-19(5)	2(2)	-29(10)
C ₅ B	41(2)	333(33)	165(9)	-24(8)	29(4)	32(15)
C ₆ B	68(4)	601(47)	167(10)	-69(14)	45(5)	44(22)
C ₇ B	37(3)	995(67)	145(10)	-85(12)	35(4)	-68(22)
C ₈ B	26(2)	1080(69)	165(10)	6(11)	22(4)	-65(25)
C ₉ B	28(2)	535(35)	129(8)	11(7)	10(3)	10(14)

TABLE 4c

Hydrogen Parameters of Bis(L-phenylalaninato)copper(II)

Atom	X	Y	Z	Biso*
H(C ₂ A)	0.346	0.012	-0.059	3.17
H ₁ (NA)	0.362	-0.034	0.206	3.14
H ₂ (NA)	0.428	-0.143	0.107	3.14
H ₁ (C ₃ A)	0.303	0.388	0.160	3.86
H ₂ (C ₃ A)	0.267	0.421	-0.025	3.86
H(C ₅ A)	0.230	-0.142	-0.089	5.04
H(C ₆ A)	0.105	-0.390	-0.071	5.80
H(C ₇ A)	0.016	-0.256	0.102	6.04
H(C ₈ A)	0.054	0.106	0.257	6.34
H(C ₉ A)	0.183	0.343	0.247	5.32
H(C ₂ B)	0.666	0.193	0.355	2.90
H ₁ (NB)	0.564	0.603	0.411	3.03
H ₂ (NB)	0.615	0.553	0.276	3.03
H ₁ (C ₃ B)	0.677	0.602	0.577	3.72
H ₂ (C ₃ B)	0.722	0.296	0.624	3.72
H(C ₅ B)	0.718	0.828	0.364	5.55
H(C ₆ B)	0.839	0.947	0.250	7.45
H(C ₇ B)	0.960	0.672	0.289	7.50
H(C ₈ B)	0.964	0.298	0.437	7.74
H(C ₉ B)	0.845	0.178	0.552	5.47

* Biso was calculated by adding 1.0 to the Biso value of the atom to which the hydrogen was attached.

to its relative displacement and independent of neighboring atoms (47). In a real crystal the displacement of one atom must affect the neighboring atoms. It is probable that the inability of the conventional anisotropy expression to compensate for the interdependence of the thermal motion of an atom with its neighbors is reflected in this difference Fourier.

All other peaks in the difference Fourier were below $0.322 e/\text{\AA}^3$.

As a further proof of the "correctness" of the structure all intermolecular distances were calculated less than 4.0\AA . These are listed in Table 5. It can be seen from the table that there are no unusually short distances. The shortest distance in the table is the O_1A to $N(B)$ distance. This distance occurs in the square-plane of the coordination sphere and is equal, within the standard deviation, to the sum of the Van der Waal's radii of oxygen (1.40\AA) and nitrogen (1.50\AA). The normal Van der Waal's radius for overlapping aromatic rings is 3.4 to 3.7\AA . There is only one distance given in Table 5 that falls below 3.4\AA , viz., the C_8A --- C_9B' distance of 3.350\AA . The nearest-neighbor aromatic rings in bis(L-phenylalaninato)copper(II) do not overlap to any great extent. A similar arrangement of aromatic rings occurs in the nicotinamide structure (66) such that the rings do not overlap. In that structure there is an intermolecular carbon-carbon distance of 3.34\AA . There are many instances of intermolecular carbon-carbon distances in aromatic systems being less than 3.4\AA , but usually the charge-transfer mechanism is invoked to explain the shortened distances. It is highly doubtful that such a mechanism is operative for the L-phenylalanine complex for two reasons. First, there is no polarizing field in the

TABLE 5

Van der Waal's Contacts Less Than 4.0 Å *

Atom X	Atom Y	Distance
O ₁ A	O ₁ A' (1-x, y-½, 1-z)	3.227
O ₁ A	O ₂ A' (1-x, y-½, -z)	3.391
O ₁ A	O ₂ A' (1-x, y+½, -z)	3.331
O ₁ A	O ₂ B' (1-x, y+½, 1-z)	3.318
O ₁ A	N(A)''(x, 1+y, z)	3.217
O ₁ A	N(A)'(1-x, y+½, -z)	3.213
O ₁ A	N(B)	2.894
O ₁ A	C ₁ A' (1-x, y+½, -z)	2.962
O ₁ A	C ₁ A' (1-x, y-½, -z)	3.696
O ₁ B	O ₂ A' (1-x, y-½, -z)	3.177
O ₁ B	O ₁ B' (1-x, y-½, 1-z)	3.102
O ₁ B	O ₂ B' (1-x, y-½, 1-z)	3.393
O ₁ B	O ₂ B' (1-x, y+½, 1-z)	3.225
O ₁ B	N(A)	2.952
O ₁ B	N(B)''(x, y-1, z)	3.270
O ₁ B	N(B)'(1-x, y-½, 1-z)	2.981
O ₁ B	C ₂ B' (1-x, y-½, 1-z)	3.341
O ₁ B	C ₃ B' (1-x, y-½, 1-z)	3.788
N(A)	O ₂ A' (1-x, y-½, -z)	3.218
N(A)	O ₂ B' (1-x, y-½, 1-z)	3.413
N(A)	O ₂ B' (1-x, y+½, 1-z)	3.442
N(A)	C ₁ A' (1-x, y-½, -z)	3.459
N(A)	C ₁ A''(x, y-1, z)	3.767
N(A)	C ₁ B' (1-x, y-½, 1-z)	3.924
N(A)	C ₃ B' (1-x, y-½, 1-z)	3.739
N(B)	O ₂ A' (1-x, y-½, -z)	3.364
N(B)	O ₂ A' (1-x, y+½, -z)	3.173
N(B)	O ₂ B' (1-x, y+½, 1-z)	3.189

TABLE 5 - continued

Van der Waal's Contacts Less Than 4.0 Å *

Atom X	Atom Y	Distance
N(B)	C ₁ B' (1-x, y+½, 1-z)	3.367
C ₁ A	O ₂ A' (1-x, y-½, -z)	3.858
C ₁ A	O ₂ B' (1-x, y+½, 1-z)	3.948
C ₁ A	N(A)' (1-x, y+½, -z)	3.459
C ₁ A	N(A)'' (x, 1+y, z)	3.767
C ₁ A	C ₁ A' (1-x, y-½, 1-z)	3.800
C ₂ A	O ₁ A' (1-x, y-½, -z)	3.249
C ₂ A	O ₂ B' (1-x, y+½, 1-z)	3.846
C ₂ A	C ₁ A' (1-x, y-½, -z)	3.984
C ₃ A	O ₂ B' (1-x, y+½, 1-z)	3.511
C ₃ A	C ₅ B' (1-x, y-½, -z)	3.887
C ₄ A	C ₃ B' (1-x, y-½, 1-z)	3.861
C ₄ A	C ₆ B' (1-x, y-½, -z)	3.818
C ₅ A	C ₅ B' (1-x, y+½, -z)	3.972
C ₅ A	C ₆ B' (1-x, y-½, -z)	3.453
C ₅ A	C ₇ B' (1-x, y-½, -z)	3.490
C ₆ A	C ₃ A'' (x, y-1, z)	3.742
C ₆ A	C ₄ A'' (x, y-1, z)	3.801
C ₆ A	C ₇ A' (-x, y-½, -z)	3.918
C ₆ A	C ₈ A' (-x, y-½, -z)	3.925
C ₆ A	C ₉ A'' (x, y-1, z)	3.532
C ₆ A	C ₇ B' (1-x, y-½, -z)	3.656
C ₇ A	C ₇ A' (-x, y-½, -z)	3.817
C ₇ A	C ₈ A' (-x, y-½, -z)	3.853
C ₇ A	C ₉ A'' (x, y-1, z)	3.821
C ₈ A	C ₄ B' (1-x, y-½, 1-z)	3.733
C ₈ A	C ₈ B' (1-x, y-½, 1-z)	3.845
C ₈ A	C ₉ B' (1-x, y-½, 1-z)	3.350

TABLE 5 - continued

Van der Waal's Contacts Less Than 4.0 Å *

Atom X	Atom Y	Distance
C ₉ A	C ₃ B' (1-x, y-½, 1-z)	3.531
C ₉ A	C ₄ B' (1-x, y-½, 1-z)	3.541
C ₉ A	C ₉ B' (1-x, y-½, 1-z)	3.689
C ₁ B	O ₂ A' (1-x, y-½, -z)	3.556
C ₁ B	O ₁ B' (1-x, y-½, 1-z)	3.532
C ₁ B	O ₂ B' (1-x, y+½, 1-z)	3.854
C ₁ B	N(B)''(x, y-1, z)	3.641
C ₁ B	C ₁ B' (1-x, y+½, 1-z)	3.807
C ₂ B	O ₂ A' (1-x, y-½, -z)	3.288
C ₂ B	C ₅ B'' (x, y-1, z)	3.884
C ₃ B	O ₂ B'' (x, y+1, z)	3.623
C ₅ B	O ₂ A' (1-x, y+½, -z)	3.651
C ₅ B	C ₉ B'' (x, y+1, z)	3.614
C ₆ B	C ₈ B'' (x, y+1, z)	3.610
C ₇ B	C ₈ B' (2-x, y+½, 1-z)	3.838

* A primed symbol indicates the two-fold screw operation, whereas a double prime indicates a unit translation of the coordinates listed in Table 4a.

vicinity of the rings, and, secondly, the 3.35 Å distance is not extreme enough. More correctly, what is being observed is efficient packing. It is seen that the Van der Waal's distances do reinforce the structural determination.

An average value for the standard deviations for the light atoms for the x,y, and z coordinates is 0.0003, 0.0014, and 0.0006 respectively.

Further insight into the accuracy of the structure can be gained from a comparison of the observed and calculated structure factors. These are presented in Appendix III.

Discussion of Structure. As mentioned previously one of the primary reasons for doing the structure was to determine the position of the aromatic rings with respect to the copper(II) ion. Contrary to what was observed in the bis(L-tyrosinato)copper(II) complex (4) the rings in the L-phenylalanine complex are extended out and away from the coordination sphere. This is shown clearly in Figure 3 which is a projection onto the ac plane. The coordination sphere can be seen located approximately in the center of the unit cell with the aromatic rings located at the extremes. The copper(II) is coordinated only by oxygen and nitrogen atoms.

Table 6 lists the bond distances and angles involved in the coordination around the copper ion. Figure 4 shows the arrangement of the ligands around the metal. One can see that the coordination to a first approximation is octahedral with tetragonal distortion. The four ligand atoms (O(1A), N(A), O(2A), N(B)) attached to the two ligands,

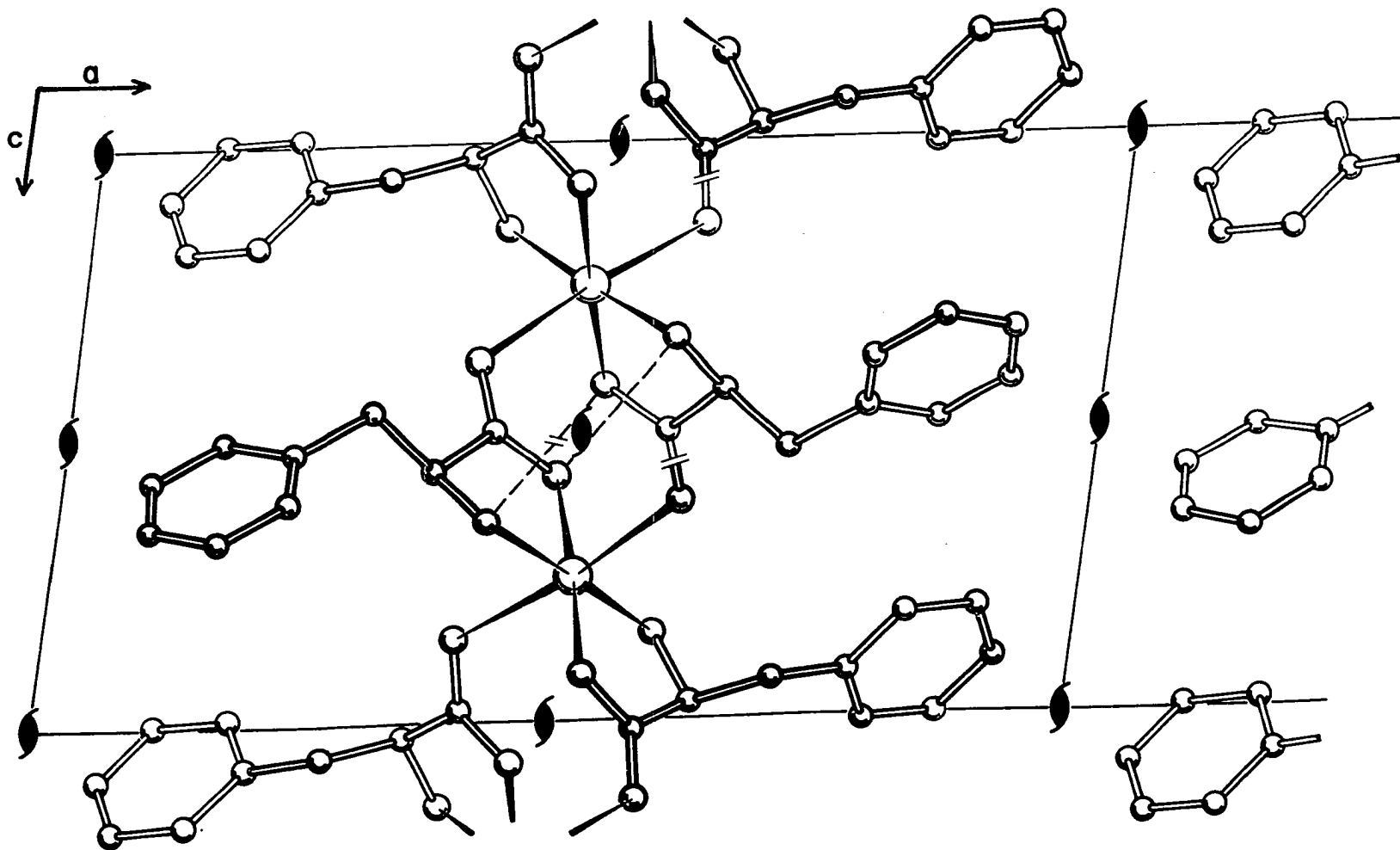


Figure 3. Projection Onto "ac" Plane

TABLE 6

Bond Distances and Angles Around Copper

Bond Distances	
Bond	Distance
Cu - O ₁ A	1.947(0.003)
Cu - N(A)	2.000(0.004)
Cu - O ₂ A'	2.690(0.004)
Cu - O ₁ B	1.959(0.003)
Cu - N(B)	1.990(0.004)
Cu - O ₂ B'	2.579(0.004)

Note: Primes indicate the screw-related positions

Atoms	Angle (deg.)	Atoms	Angle (deg.)
O ₁ A-Cu-N(A)	84.84(0.15)	O ₁ B-Cu-O ₂ A'	84.67(0.13)
O ₁ A-Cu-N(B)	94.63(0.16)	O ₁ B-Cu-O ₂ B'	89.51(0.13)
O ₁ A-Cu-O ₂ A'	92.57(0.13)	N(B)-Cu-O ₂ A'	90.63(0.14)
O ₁ A-Cu-O ₂ B'	93.22(0.14)	N(B)-Cu-O ₂ B'	87.52(0.14)
N(A)-Cu-O ₁ B	96.43(0.16)	O ₁ A-Cu-O ₁ B	176.84(0.15)
N(A)-Cu-O ₂ A'	85.28(0.14)	N(A)-Cu-N(B)	175.84(0.17)
N(A)-Cu-O ₂ B'	96.63(0.14)	O ₂ A'-Cu-O ₂ B'	174.04(0.12)
O ₁ B-Cu-N(B)	83.90(0.15)		

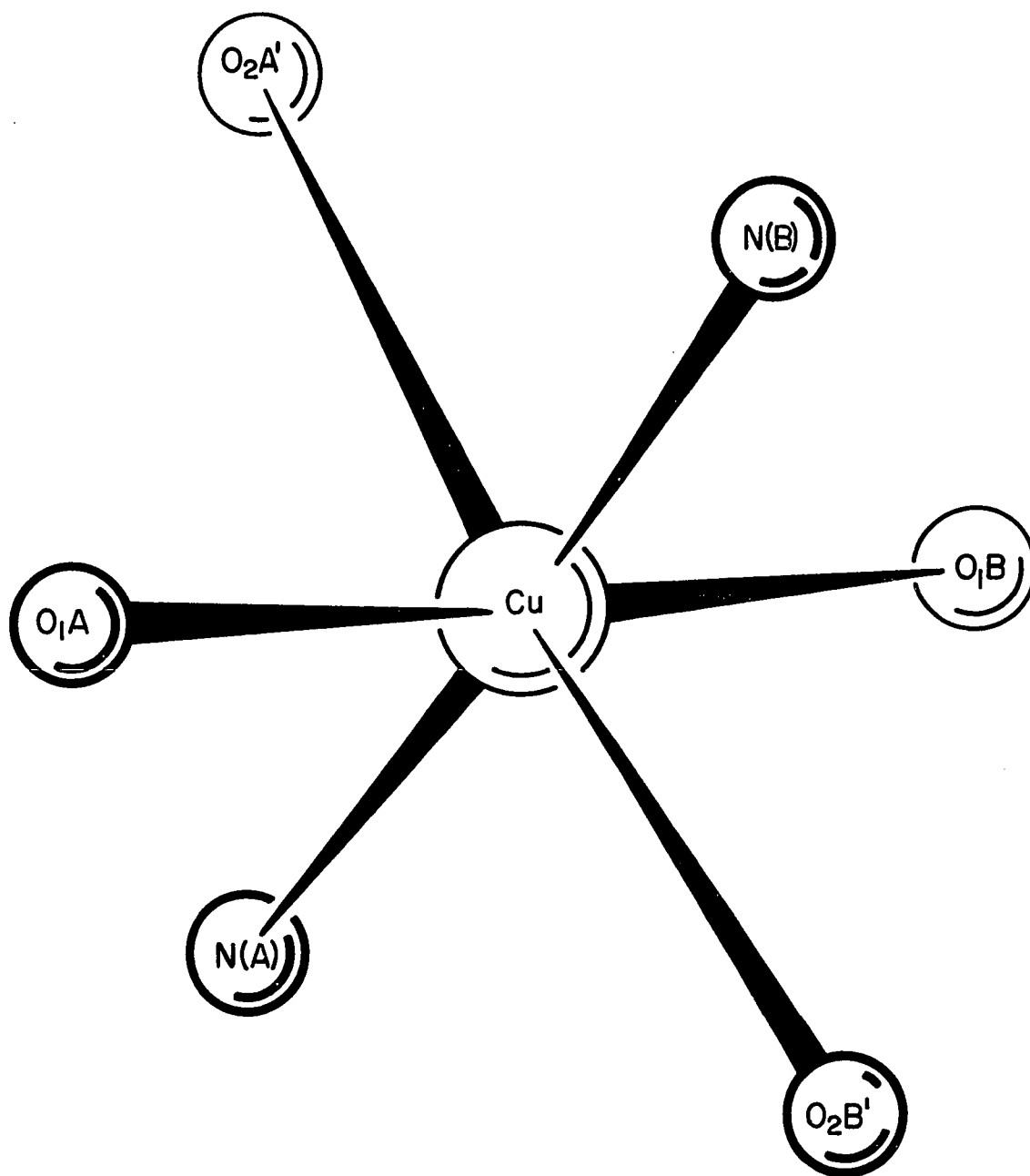


Figure 4. Coordination Sphere of Copper Ion

A and B, form the square-plane in the octahedron. This is demonstrated also in Figure 11. The octahedron is completed by taking the other oxygen atoms (O(2A) and O(2B)) on each of the two carboxyl groups and operating on them with the two-fold screw axis. The four closest ligands are coordinated trans with respect to each other. Although this is the usual configuration involving a five-membered ring with oxygen and nitrogen being the donors, recent evidence indicates that the cis form may be more prevalent than was previously thought. For example, bis(L-alaninato) copper(II) has been crystallized in both forms (48, 49). Another notable example is the bis(L-serinato)copper(II) complex (50) which occurs in the cis configuration. Also, the bis(glycinato)copper(II) monohydrate has been characterized as being in both the cis (51) and trans (52) configuration. The bond lengths from the copper atom to the four closest ligands are in the proper range. Freeman (53) reports average values of 2.000 (0.007) Å for Cu-NH₂ and 1.980 (0.012) Å for Cu-O bonds obtained from several copper complexes of amino acids and peptides. These compare to 1.995 (0.004) Å and 1.953 (0.003) Å for the average of the respective distances in the L-phenylalanine complex. The bond lengths to the two distant atoms completing the octahedron are considerably longer than the square-plane oxygen-copper bonds (2.634 Å av.). It should be pointed out that this distance is quite variable in other copper-amino acid complexes. Freeman reports these axial bond distances ranging from 2.30 Å to 2.74 Å.

To gain some idea of the distortion from octahedral symmetry, one can examine the distances between the ligands lying in the square plane, look at the least-squares planes through various sets of ligands,

and study the ligand-copper-ligand angles. The distance between N(A) and O₁A in one of the chelate rings and the distance between N(B) and O₁B of the other chelate ring are 2.663 Å and 2.640 Å respectively. The other two possible distances are 2.894 Å and 2.952 Å for O₁A-N(B) and O₁B-N(A) respectively. One can see that the square-plane is more correctly a rectangle. This distortion is further demonstrated when the angles in the square-plane are examined. The O₁A-Cu-N(A) and the O₁B-Cu-N(B) angles are both less than 90° (84.84° and 83.90°). The O₁A-Cu-N(B) and O₁B-Cu-N(A) angles are both greater than 90° (94.63° and 96.43°). Other subtleties of distortion are also present. For example, the last three angles listed in Table 6 should be 180° for O_h, D_{4h} or D_{2h} site symmetry. It is seen that they are not.

The various least-squares planes for the coordination sphere are shown in Tables 7a,b,c. The program used to calculate the planes was written by T. Willoughby at the University of Oklahoma. The method of Schomaker, Waser, Marsh, and Bergman (54) was used in the calculation. Table 7a consists of the planes calculated for the square-plane. The average displacement from Plane 1 in Table 7a is 0.02 Å. This indicates that the deviation from planarity is quite small. However, when one looks at Plane 2 in Table 7a, it is noticeable that the Cu atom is slightly out of the plane formed by the four nearest-neighbor atoms. In fact, the copper atom, as can be seen from the table, is displaced toward the nearest apical oxygen atom O₂B'. The displacement of the Cu atom is small but apparently significant since it is seen that the displacement from Plane 2 is approximately five times the average displacement of the four atoms defining the plane. A comparison can be made to the same plane in the

TABLE 7a

Least Squares Planes for Coordination Sphere

Plane 1: O₁A, O₁B, N(A), N(B), Cu
Equation: 12.533x-2.681y-4.959z= 4.287
Plane 2: O₁A, O₁B, N(A), N(B)
Equation: 12.534x-2.681y-4.959z= 4.299

Atom	Distance From Plane 1	Distance From Plane 2
O ₁ A	0.000	-0.012
O ₁ B	0.000	-0.012
N(A)	0.024	0.012
N(B)	0.024	0.012
Cu	-0.048	-0.060
O ₂ A'	2.632	2.620
O ₂ B'	-2.618	-2.631

TABLE 7b

Least Squares Planes for Coordination Sphere

Plane 1: O₁A, O₂'A, O₁B, O₂'B, Cu

Equation: $11.765x+3.228y+2.301z= 7.179$

Plane 2: O₁A, O₂'A, O₁B, O₂'B

Equation: $11.766x+3.227y+2.302z= 7.186$

Atom	Distance From Plane 1	Distance From Plane 2
O ₁ A	0.004	-0.002
O ₂ A	0.007	0.002
O ₁ B	0.003	-0.002
O ₂ B	0.008	0.002
Cu	-0.023	-0.028

TABLE 7c

Least Squares Plane for Coordination Sphere

Plane 1: O₂A', O₂B', N(A), N(B), Cu

Equation: $9.564x+3.151y-7.505z = -1.093$

Plane 2: O₂'A, O₂'B, N(A), N(B)

Equation: $9.107x+3.151y-7.504z = -1.107$

Atom	Distance From Plane 1	Distance From Plane 2
O ₂ A	-0.081	-0.070
O ₂ B	-0.082	-0.069
N(A)	0.056	0.068
N(B)	0.059	0.071
Cu	0.048	0.060

bis(L-serinato)copper(II) complex (50) where the environment is penta-coordinate and the displacement of the copper is more extreme. For the serine complex the average displacement is 0.10 Å for Plane 1. For Plane 2 in the serine complex the copper is displaced toward the apex oxygen by 0.14 Å as opposed to 0.06 Å for the L-phenylalanine complex. It is seen from this comparison that the L-phenylalanine is closer to being a true plane.

Table 7b gives the two planes for the four oxygen atoms and the copper atom. The average displacement for Plane 1 is 0.009 Å. For Plane 2 the average displacement is 0.002 Å. Of the three ways for passing planes through the copper atom presented in Tables 7a, b, c, the way in Table 7b comes closer to containing the atoms defining the plane than the other two ways.

Table 7c contains the data for the planes through the two apical oxygen atoms and the two nitrogen atoms. Plane 1 and Plane 2 both have an average displacement of 0.07 Å. The greatest distortion occurs for these planes. One can see from Table 7c that both oxygen atoms fall on one side of the plane while both nitrogen atoms fall on the other. This indicates a distortion to a tetrahedral configuration when one considers only these five atoms. This can be seen also in Table 6 where the $O_2A'-Cu-O_2B'$ angle is seen to be 174.0° and the $N(A)-Cu-N(B)$ angle is given as 175.8° .

The dihedral angles between the three principal planes defined by the coordination sphere were calculated to gain more insight into the distortion. The dihedral angles are all close to 90° . The largest deviation from 90° occurs between the planes defined by O_1A , O_1B , O_2A' ,

O_2B' and O_2A' , O_2B' , $N(A)$, $N(B)$. The angle is 95.7° . The angles between the planes O_1A , O_1B , O_2A' , O_2B' and O_1A , O_1B , $N(A)$, $N(B)$ and the planes O_1A , O_1B , $N(A)$, $N(B)$ and O_2A' , O_2B' , $N(A)$, $N(B)$ and 93.7° and 91.5° respectively. It is seen the distortion is not severe.

The configuration of the two chelate rings is shown in Fig. 5. The least-squares planes for the two five-membered rings are given in Table 8. For molecule A the average deviation from planarity is 0.09 \AA for Plane 1 and Plane 2. For molecule B the average deviation from planarity is 0.16 \AA and 0.14 \AA for Planes 1 and 2 respectively. There is a greater deviation from planarity for the five-membered ring in molecule B than in molecule A. It is interesting to point out that hydrogen bonding (vide infra) occurs between $N(B)$ and the screw-related O_1B and not between $N(A)$ and the screw-related O_1A . In both molecules the nitrogen atom and the oxygen atom that can act as an acceptor for hydrogen bonding are on the same side of the chelate plane, but $N(B)$ is farther from its plane than $N(A)$ is from the plane defined by molecule A as is seen in Table 8. The actual conformational angles will be discussed later, but it will be seen that more twisting occurs around the C_1-C_2 bond for molecule B than for molecule A.

When one compares the chelate angles in molecules A and B (cf. Table 9) with the mean of several peptide-copper complexes as given by Freeman (53), it is seen that both chelate rings in L-phenylalanine are buckled more than the average. That the rings are buckled to a greater extent is seen from two reasons. First, the sum of the angles is less in both rings than the "average" sum. Secondly, when an angle to angle comparison is made, it is seen that with one small

Figure 5. Configuration of Chelate Rings

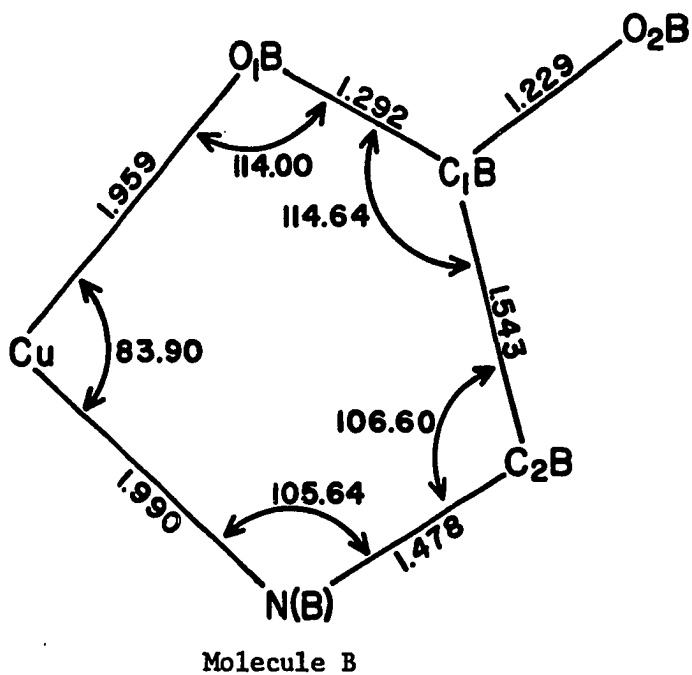
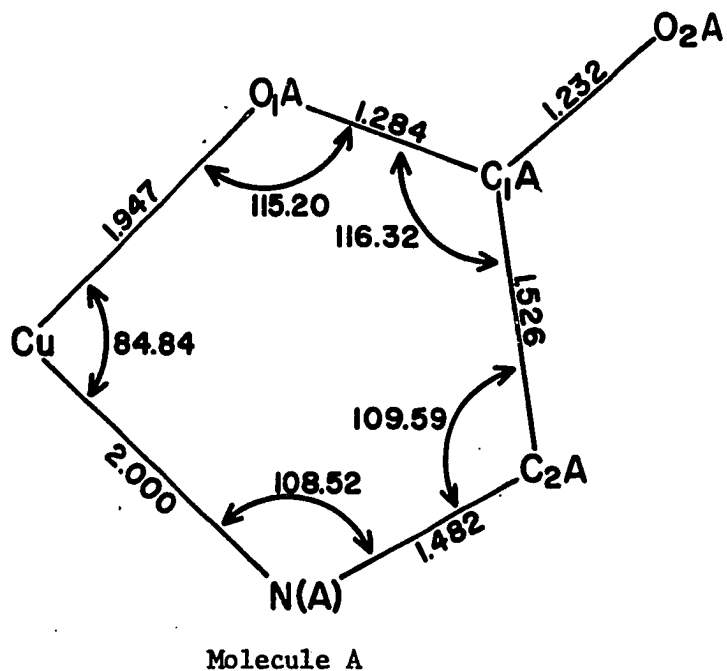


TABLE 8

Least Squares Planes for Chelate Rings

Molecule A	Plane 1: O ₁ A, C ₁ A, C ₂ A, N(A), Cu	
	Equation: 11.917x-2.868y-5.083z= 3.915	
	Plane 2: O ₁ A, C ₁ A, C ₂ A, N(A)	
	Equation: 11.210x-2.855y-5.639z= 3.608	
Atom	Distance From Plane 1 (Å)	Distance From Plane 2
O ₁ A	-0.013	-0.075
C ₁ A	0.098	0.127
C ₂ A	-0.152	-0.113
N(A)	0.124	0.061
Cu	-0.057	-0.232
Molecule B	Plane 1: O ₁ B, C ₁ B, C ₂ B, N(B), Cu	
	Equation: 9.627x-3.017y-6.234z= 2.274	
	Plane 2: O ₁ B, C ₁ B, C ₂ B, N(B)	
	Equation: 7.302x-2.822y-7.312z= 4.713	
Atom	Distance From Plane 1	Distance From Plane 2
O ₁ B	-0.041	0.111
C ₁ B	-0.110	-0.187
C ₂ B	0.260	0.164
N(B)	-0.245	-0.089
Cu	0.135	0.566

exception for molecule A all the angles in molecules A and B are smaller than the average values. Molecule B appears to be more buckled than A, which is congruous with the previous discussion.

TABLE 9
Chelate Angles Compared to Average Values

Angle	Average	Molecule A	Molecule B
Cu-N-CH ₂	110°	108.5	105.6
N-C-CO	111°	109.6	106.6
C-CO-O	118°	116.3	114.6
OC-O-Cu	115°	115.2	114.0
O-Cu-N	<u>87°</u>	<u>84.8</u>	<u>83.9</u>
Sum	541°	534.4	524.7

The buckling of the chelate rings is also reflected in the somewhat short N---O distances. The N(A)---O₁A and N(B)---O₁B distances are 2.663 Å and 2.640 Å respectively. These distances compare to average values of 2.90 Å and 2.87 Å found in bis(β-alaninato)copper(II) hexahydrate and bis(DL-β aminobutyrate)copper(II) dihydrate as given by Freeman (53). Due to the shortened distances, it is a necessary condition that the two chelate rings buckle to a greater extent. The short distances are not anomalous. Similar distances have been reported for bis-L-serinato)copper(II) (50) and the copper chelate of glycyl-L-leucyl-L-tyrosine (3). In the serine complex the average homologous

distances are 2.62 Å. For the glycyl-L-leucyl-L-tyrosine complex the distance is 2.64 Å.

The bond lengths and angles for molecule A and molecule B are given in Table 10 for that part of the molecules involved in chelation and are compared to the same parameters of histidine hydrochloride monohydrate and average values of various copper chelates. The first thing to be noted in the table is that there are no significant deviations of the bond lengths from the reference values. They are, in fact, very close to the average values given by Freeman (53). Another feature to observe is the lengthening of the carbon-oxygen bond involved in chelation. One can see that a hint of shortening in the free carboxyl bond also occurs. This shortening is more noticeable when a comparison is made to the free carboxyl in glycine (1.252 Å) (53) and in DL-serine (1.261 Å) (57).

An even more startling example of the effect of chelation on carboxyl distances is presented in two papers by Gramaccioli and Marsh (58, 59). A convincing argument is given, based upon a comparison of the copper glutamate dihydrate to the zinc glutamate dihydrate structure, that the double bond character is lessened when the metal-oxygen distance becomes smaller. Hence, the carbon-oxygen bond distance increases for the oxygen bonded to the metal. In turn, the "free" oxygen of the carboxyl develops more double bond character with the carbon and a decrease in the bond distance results.

There appears to be a fair amount of distortion in the bond angles around C_2 (cf. Table 10) for both molecules A and B. Distortion from the normal sp^3 hybridization has been noted before (50) for the

Table 10

Comparison of Bond Angles and Lengths of Bis(L-phenylalaninato)Cu(II)
 With Those of Histidine Hydrochloride Monohydrate and
 Other Copper Complexes of Amino Acids and Peptides

Bond Distances				
Bond	histidine hydrochloride monohydrate (55)	complex		Ave. value of Cu Complexes (53,56)
		Molecule A	Molecule B	
C ₁ C ₂	1.530(0.011)	1.526(0.007)	1.543(0.006)	1.520(0.005)
C ₂ C ₃	1.527(0.011)	1.531(0.006)	1.526(0.006)	1.530(0.020)
C ₁ O ₁	1.265(0.011)	1.284(0.006)	1.292(0.005)	1.280(0.007)
C ₁ O ₂	1.240(0.011)	1.232(0.006)	1.229(0.005)	1.230(0.005)
C ₂ N	1.495(0.011)	1.482(0.006)	1.478(0.006)	1.480(0.007)
Bond Angles				
O ₁ C ₁ O ₂	125.8	124.7(0.5)	124.2(0.5)	122.5(1.0)
O ₁ C ₁ C ₂	114.2	116.3(0.4)	114.6(0.4)	117.5(0.9)
O ₂ C ₁ C ₂	120.0	118.8(0.4)	121.0(0.4)	120(1.0)
C ₁ C ₂ N	109.4	109.6(0.4)	106.6(0.3)	110.0(0.6)
C ₁ C ₂ C ₃	113.3	105.5(0.4)	114.4(0.4)	115.0(2.0)
C ₃ C ₂ N	111.1	111.6(0.4)	115.7(0.4)	115.0(1.0)

angles around C_2 in bis(serinato)copper(II). Freeman (53) gives average values for the uncomplexed amino acid around C_2 . The $C_1-C_2-C_3$, C_1-C_2-N , and $N-C_2-C_3$ angles he gives are 111.5° , 110.5° , and 110.5° respectively which are seen to be closer to the normal sp^3 hybridized angles.

More insight about the distortion of the chelate rings can be gained when one examines the least-squares planes through the carboxylic groups of molecule A and molecule B. These data are presented in Table 11. The average deviation from planarity for Plane 1 for molecules A and B is 0.009 \AA and 0.01 \AA respectively. When one looks at the distances of copper and nitrogen from each of the planes, it is seen that chelate rings A and B are in the envelope form. It is also seen from the table that N(B) is farther from its carboxyl plane than N(A). This indicates more twisting has occurred around the C_1B-C_2B bond than around the C_1A-C_2A bond as previously indicated.

The conformational angles for molecules A and B are presented in Table 12. The conventions established at the 1965 Gordon Conference on Proteins (60) are used in describing the angles. The angles were calculated with a program written by H. Nicholas at the University of Oklahoma. Figure 6 relates the labeling used for the atoms in L-phenylalanine. χ_j denotes the angles of rotation around the j th bond, where $j = 1$ is for rotation around the $C^\alpha-C^\beta$ bond, etc.. ψ denotes rotation around the C_1-C^α bond. The angles are positive for a right-handed rotation. When looking along any bond, the far end rotates clockwise relative to the near end to give, from either the cis or trans configuration specified, that configuration which is present. A negative angle denotes counterclockwise rotation.

TABLE 11

Least Square Planes for Carboxylic Groups

Molecule A Plane 1: O₁A, O₂A', C₁A, C₂A
 Equation: 11.583x-3.501y-3.436z= 3.592
 Plane 2: O₁A, O₂A', C₁A
 Equation: 12.017x-3.331y-3.578z= 3.856

Atom	Distance From Plane 1	Distance From Plane 2
O ₁ A	-0.006	-
O ₂ A'	-0.007	-
C ₁ A	0.018	-
C ₂ A	-0.005	0.089
N(A)	0.548	-0.442
Cu	0.357	-0.313

Molecule B Plane 1: O₁B, O₂B', C₁B, C₂B
 Equation: 8.902x-3.934y-4.352z= 2.608
 Plane 2: O₁B, O₂B', C₁B
 Equation: 9.409x-3.766y-4.565z= 2.795

Atom	Distance From Plane 1	Distance From Plane 2
O ₁ B	0.007	-
O ₂ B'	0.008	-
C ₁ B	-0.021	-
C ₂ B	0.006	-0.100
N(B)	-0.787	0.673
Cu	-0.313	0.262

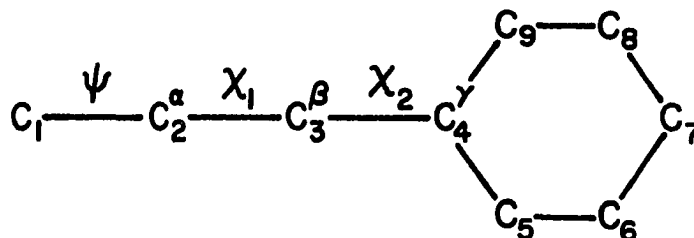


Figure 6. Labeling of Conformational Angles

Table 12

Conformational Angles for L-phenylalanine

Angle	4 Atoms Defining Configuration	Configuration	Molecule A	Molecule B
ψ	O_1, C_1, C_2, N	Cis	-25.3°	36.2°
ψ	O_1, C_1, C_2, C_3	Cis	95.0°	165.4°
ψ	O_2, C_1, C_2, N	Cis	158.2°	-147.8
ψ	O_2, C_1, C_2, C_3	Cis	-81.5	-18.6
χ_1	C_1, C_2, C_3, C_4	Cis	167.2°	151.3°
χ_1	N, C_2, C_3, C_4	Cis	-73.9	-84.2
χ_2	C_2, C_3, C_4, C_5	Cis	-41.2°	77.9°
χ_2	C_2, C_3, C_4, C_9	Cis	146.0°	-100.7°

Table 12 gives a good picture of the differences in the conformation of molecules A and B. Two big differences can be seen. First, there is quite a difference between the rotation around the C_1-C_2 bond. For molecule A the cis configuration involving O_1 , C_1 , C_2 , and N is -25.3° as opposed to 36.2° for molecule B. This shows how N(A) falls on one side of the carboxyl plane for molecule A and N(B) falls on the other side of the carboxyl plane for molecule B. There is a difference of 61.5° between the two angles. The difference between the absolute values of the two angles is 10.9° . This fact once again shows how a great deal more buckling has occurred in ring B than in ring A. Second, there is a big difference in the orientation of the two rings. It has been noted (61) that for planer terminal groups of amino acids, e.g., in arginine, aspartic, and glutamic acids, and the rings in histidine and tyrosine the plane is found to be either coplaner with, or perpendicular to, the plane defined by C_1 , C_2 , and C_3 . This can be seen to be approximately true for molecule B; for example, for the cis configuration defined by C_2 , C_3 , C_4 , and C_5 the angle is 77.9° , and for the cis configuration defined by C_2 , C_3 , C_4 , and C_9 the angle is -100.7° . Both angles are seen to be reasonably close to 90° . One can see that the -41.2° and the 146.0° angles for molecule A are really very close to bisecting the angle formed by vectors parallel and perpendicular to the plane defined by C_2 , C_3 , and C_4 and, therefore, do not follow the generalization cf. Fig. 11). The reason for the deviation can probably be attributed to packing forces. Rotation around the C_3A-C_4A bond in either direction would produce interaction with other aromatic rings. The packing constraints are also reflected in the O_1 , C_1 , C_2 ,

C_3 angles. There is a large difference between the 95.0° and 165.4° angles for molecules A and B.

There is one other conformational angle of vital interest in the L-phenylalanine complex. This is the N, C_2 , C_3 , C_4 angle. There are normally three values which characterize the angle, those being approximately 60° , 180° , or 300° . It has been observed that for tyrosine and phenylalanine side groups, both of which contain benzene rings, the normal angle is 180° . This has been reported for five cases (62). As can be seen from Table 12, the L-phenylalanine molecules are closer to the 300° angle. The rotation around this C_2-C_3 bond is important when one considers the possibility of a Cu^{2+} -aromatic ring interaction. It is seen that the possibility does not exist for L-phenylalanine. The same conformational angle in bis(L-tyrosinato)copper(II) is approximately 60° . There the possibility of a Cu^{2+} -aromatic ring interaction does exist.

Table 13 lists the intramolecular bond distances and angles for the two L-phenylalanine molecules. Figures 7, 8, 9, and 10 show the parameters. There are three distances which need to be discussed in these ligands. The first two distances are the C-O distances of the carboxyl group. These distances have already been mentioned and the variations have been attributed to chelation. The long C-O distances imply that the oxygen is strongly bonded to the copper atom. The third distance to be noted is that between C_3-C_4 . The average distance for the two molecules is $1.512 (0.006) \text{ \AA}$. This compares to the homologous distance of 1.54 \AA in glycyl-L-tyrosine hydrochloride monohydrate (63). At first glance the 1.512 \AA distance looks short; however, it is not

TABLE 13

Intramolecular Bond Angles and Distances

Bond Distances		
Bond	Molecule A	Molecule B
N-C ₂	1.482(0.006)	1.478(0.006)
O ₁ -C ₁	1.284(0.006)	1.292(0.005)
O ₂ -C ₁	1.232(0.006)	1.229(0.005)
C ₁ -C ₂	1.526(0.007)	1.543(0.006)
C ₂ -C ₃	1.531(0.006)	1.526(0.006)
C ₃ -C ₄	1.516(0.007)	1.508(0.006)
C ₄ -C ₅	1.378(0.009)	1.378(0.009)
C ₄ -C ₉	1.381(0.007)	1.382(0.008)
C ₅ -C ₆	1.396(0.008)	1.395(0.009)
C ₆ -C ₇	1.373(0.009)	1.376(0.013)
C ₇ -C ₈	1.366(0.012)	1.356(0.014)
C ₈ -C ₉	1.394(0.009)	1.390(0.009)
*C-H (aromatic)	1.084	1.084
*C-H (parafinic)	1.09	1.09
*N-H (NH ₃)	1.01	1.01

*Assumed distance; Interatomic Distances, The Chemical Society
Burlington House (1958)

Bond Angles		
O ₁ -C ₁ -O ₂	124.7(0.5)	124.2(0.5)
O ₁ -C ₁ -C ₂	116.3(0.4)	114.6(0.4)
O ₂ -C ₁ -C ₂	118.8(0.4)	121.0(0.4)
C ₁ -C ₂ -C ₃	105.5(0.4)	114.4(0.4)
C ₁ -C ₂ -N	109.6(0.4)	106.6(0.3)
C ₃ -C ₂ -N	111.6(0.4)	115.7(0.4)
C ₂ -C ₃ -C ₄	116.9(0.5)	111.9(0.4)

TABLE 13 - continued

Bond Angles		
C ₃ -C ₄ -C ₅	122.9(0.5)	120.8(0.5)
C ₃ -C ₄ -C ₉	119.0(0.6)	120.5(0.5)
C ₄ -C ₅ -C ₆	121.9(0.6)	120.8(0.7)
C ₅ -C ₆ -C ₇	119.5(0.8)	119.1(0.8)
C ₆ -C ₇ -C ₈	119.3(0.6)	120.8(0.6)
C ₇ -C ₈ -C ₉	121.1(0.6)	120.0(0.8)
C ₈ -C ₉ -C ₄	120.4(0.7)	120.6(0.7)
C ₉ -C ₄ -C ₅	117.8(0.5)	118.7(0.5)

Note: For angles involving Hydrogen either sp²(120°) or sp³(110°) hybridization was assumed.

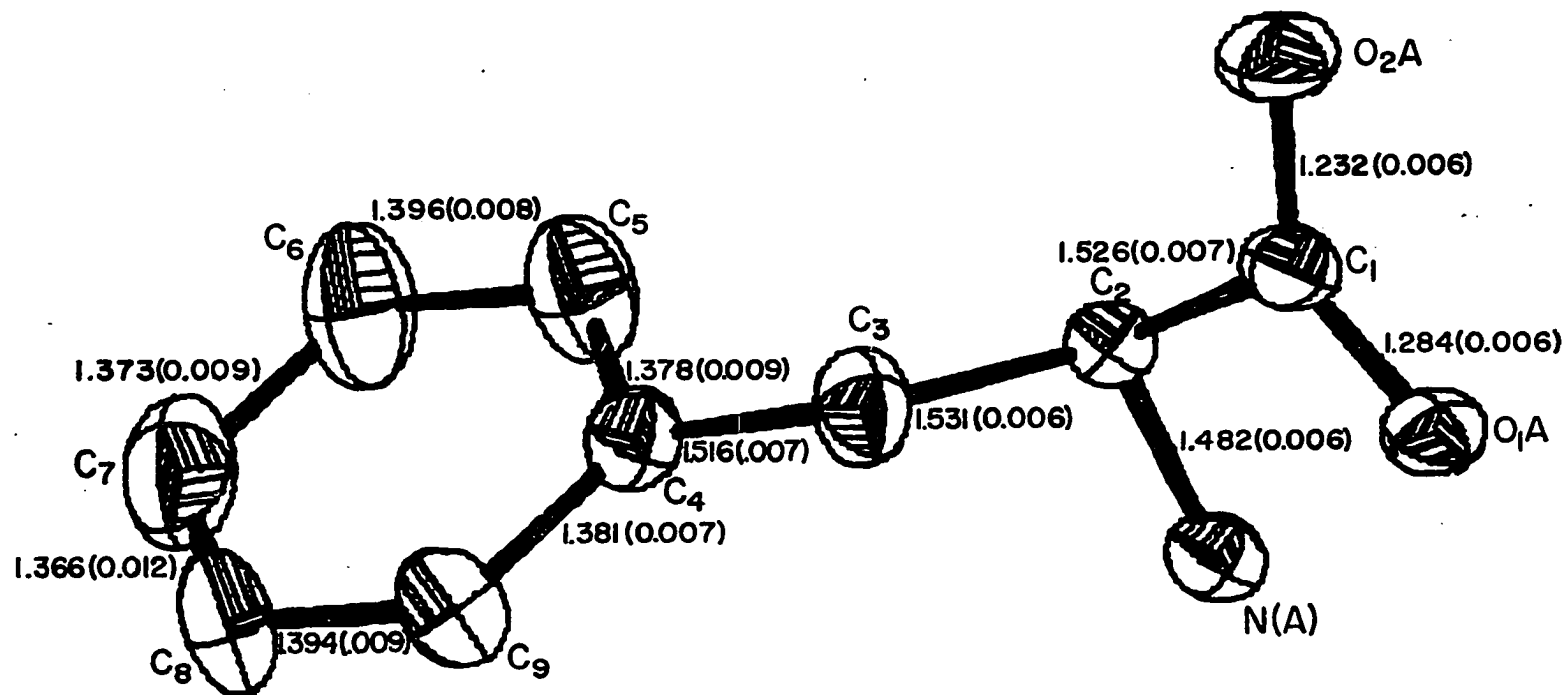


Figure 7. Bond Distances in L-phenylalanine for Molecule A

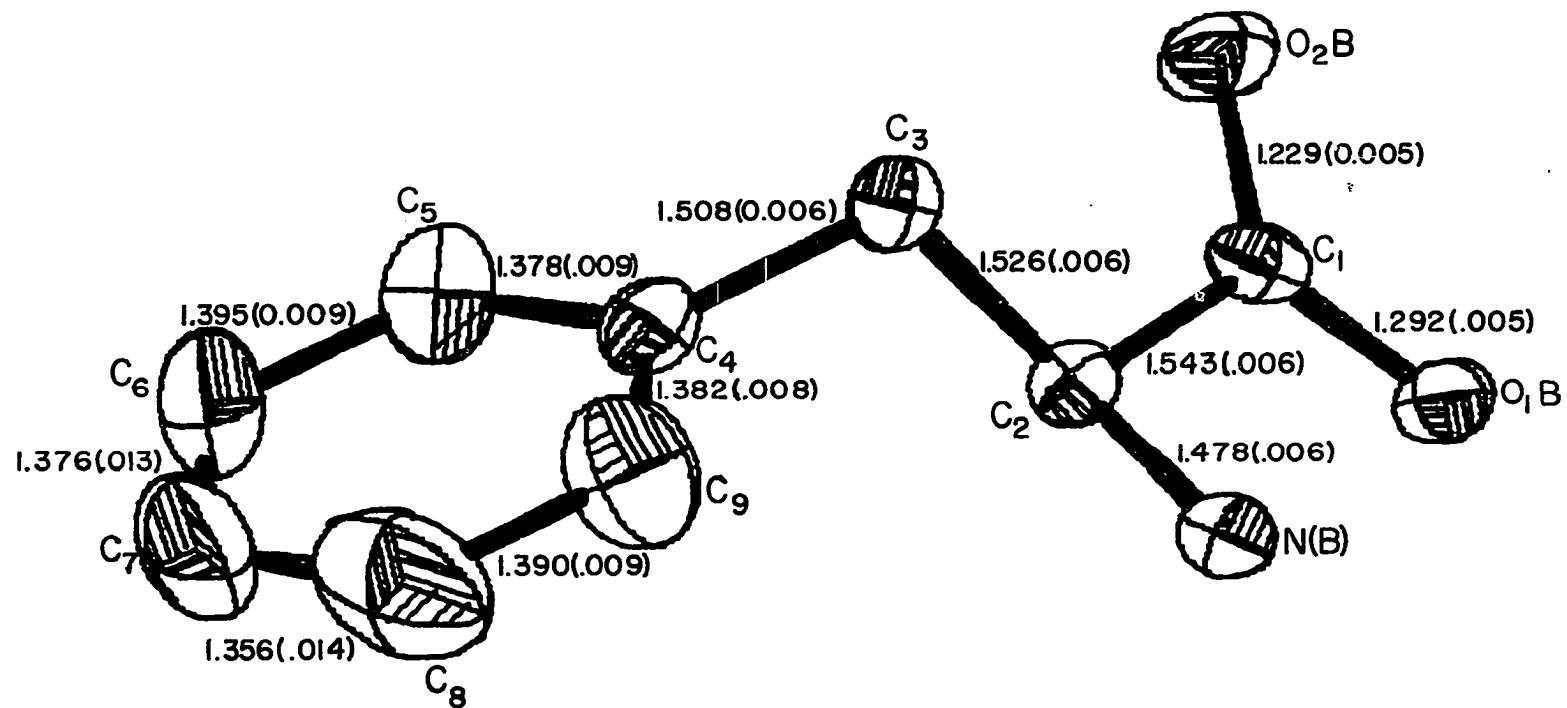


Figure 8. Bond Distances in L-phenylalanine for Molecule B

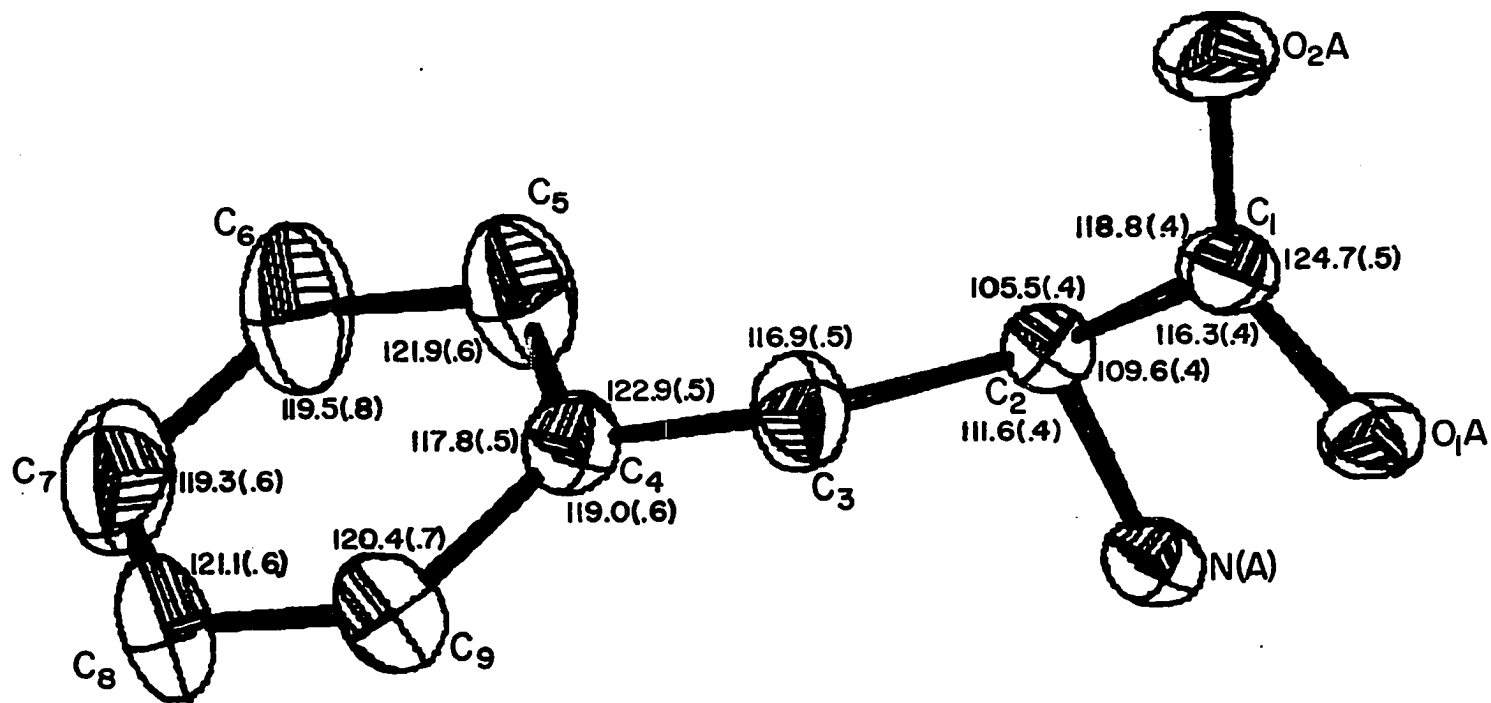


Figure 9. Angles in L-phenylalanine for Molecule A

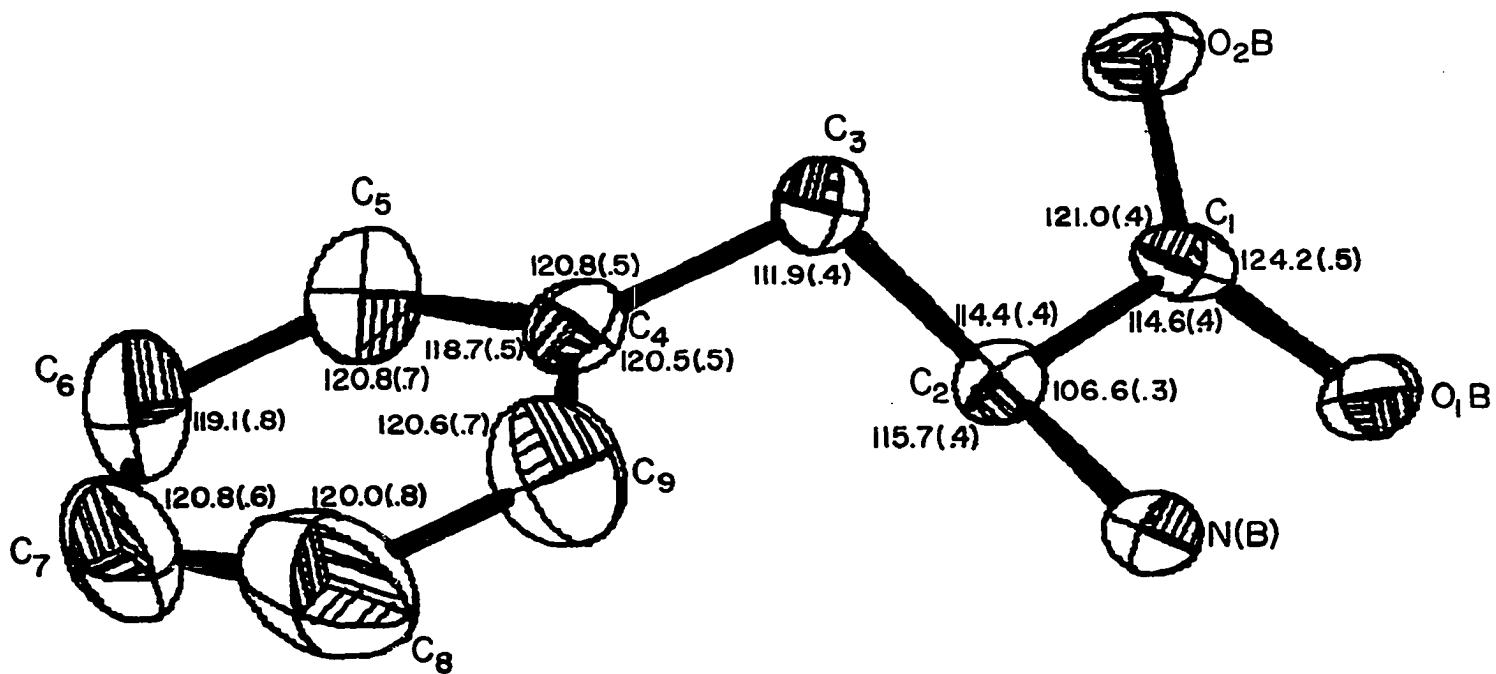


Figure 10. Angles in L-phenylalanine for Molecule B

short when compared to the same distance in toluene (64). For toluene the homologous distance is 1.52 (0.01) Å. The reason for the shortened distance is not difficult to understand. What is present is an sp^3 hybridized carbon bonded to an sp^2 hybridized carbon, hence the shortening of the bond.

An average bond distance for aromatic C-C bonds is 1.395 (0.003) Å (64). One can see that all of the bond distances are within 3σ's of this average value and hence are quite normal.

The rather large deviation of the angles around C_2 has been previously discussed. From the previous discussion it can be concluded that subtle differences do indeed occur between the complexed form of L-phenylalanine and what is probably present in the free amino acid. To reiterate, the primary differences that can be attributed to chelation are changes in the carboxylic acid distances and the angles around C_2 for both molecules. These changes appear in line with previously reported work.

As was mentioned earlier, all of the crystals examined had a large mosaic. The reason for this became apparent once the structure was solved. Upon examination of Figure 3 one sees that the only forces holding the unit cells together in the "a" direction are weak Van der Waal's forces arising from interaction between the aromatic rings. Happily, this is the thin direction of the crystal habit as it should be due to the weak forces in this direction. This means that the aromatic rings are free to a certain extent to flop or waggle in that region of the cell. This freedom of movement is reflected in the thermal parameters for the aromatic ring. Table 14 lists the angles

Table 14

Angles Between Principal Axes of Thermal Ellipsoids and
the Mean Planes of the Rings*

Molecule A			Molecule B		
Atom	B	Angle (deg)	Atom	B	Angle (deg)
C ₄	4.22	-10	C ₄	3.67	8
	2.56	36		2.68	-22
	1.86	52		1.73	74
C ₅	5.96	64	C ₅	6.27	61
	3.85	-26		4.79	-22
	2.30	1		2.58	18
C ₆	6.90	55	C ₆	9.51	5
	5.05	-34		6.98	85
	2.45	0		2.87	1
C ₇	7.76	-7	C ₇	12.19	13
	4.85	81		5.05	76
	2.51	6		2.24	4
C ₈	8.65	-24	C ₈	12.02	23
	5.40	65		5.68	66
	1.96	7		2.52	4
C ₉	6.93	-36	C ₉	5.90	43
	3.83	53		4.55	44
	2.19	1		2.96	13

*The mean planes are defined by all six atoms of the rings.

that the principal axes of thermal vibration make with the plane of the rings. The main features to be gleaned from Table 14 are that there are two axes which show quite large values for atoms five through nine for both molecules, and for both molecules these axes either fall close to being parallel or perpendicular to the plane of the ring. The thermal ellipsoids can be seen to be the resultant of these two principal motions. For example, in molecule A carbon atoms five and six have their principal axes close to the perpendicular of the plane. Atoms seven and eight have their principal axes close to the plane. The same trend can be seen in molecule B. Carbon atom 5B has its principal axis close to the perpendicular of the plane, whereas carbon atoms 6B, 7B, and 8B have their principal axes close to the plane of the aromatic ring. Figure 11 shows a stereoscopic projection of copper coordinated with molecules A and B. The thermal motion of the atoms can be seen from the drawing. It is very interesting to point out that the ring motion can be described in terms of oscillation and rotation around the C_2-C_3 and C_3-C_4 bonds. A very striking comparison can be made between molecules A and B. The rather odd configurational angles of -41.2° and 146.0° in molecule A have been previously discussed and attributed to packing forces. What this means in terms of rotation around the C_2-C_3 and C_3-C_4 bonds is that movement of the ring is more restricted for molecule A than for molecule B. This fact is seen from the B values for the two rings. In all instances the two thermal axes which are commensurate with rotation around these two bonds are larger for molecule B where the restriction is less. One can see this from Fig. 11 and Table 14. The high mosaic encountered in the crystals is undoubtedly a result of this perpendicular

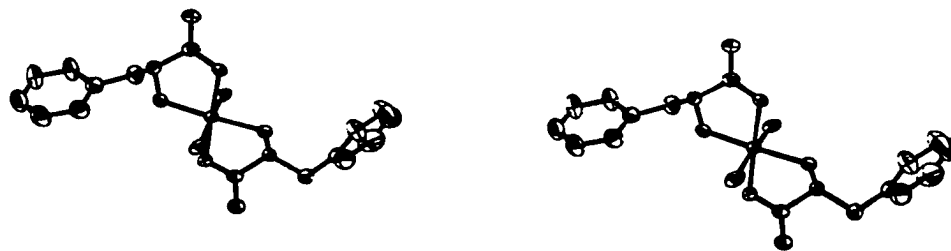


Figure 11. Stereoscopic Drawing (97) of Bis(L-phenylalaninato)Copper(II) (Projection onto "ac" plane followed by a rotation of 20° counterclockwise about the vertical axis, a 10° rotation counterclockwise about perpendicular axis, and a 10° rotation clockwise about horizontal axis.) Molecule A is on the Left. Molecule B is on the Right.

and parallel motion manifest in the ring.

The least-squares planes for the aromatic rings are shown in Table 15. The average deviation for molecule A is 0.0055 Å. For molecule B the average deviation from planarity is 0.0030 Å. These small deviations show that, in fact, the rings are quite planar.

The principal axes of the anisotropic ellipsoids are shown in Table 16 along with the direction cosines with respect to the cell edges. The high values for the rings have already been discussed. The other feature of interest is the difference in the thermal parameters for atoms O₁A and O₁B and for atoms O₂A and O₂B. In both instances the oxygen atom involved in the long copper-oxygen bond has the higher B value: 4.26 for O₂A and 4.57 for O₂B as opposed to 3.06 for O₁A and 2.80 for O₁B. When one calculates the isotropic thermal parameters for all four atoms, the same trend is seen. For example, O₁A and O₁B have B_{iso} values of 2.17 and 2.12 respectively, whereas O₂A and O₂B have B_{iso} values of 2.98 and 3.02 respectively. In the structure refinement the scattering factor curves that were used for O₁ and O₂ were derived by taking the average of the 0° and 0⁻¹ scattering factors for the respective intervals of sin θ/λ. This was considered as a fair approximation to the real situation. In reality there would be a greater than 50% probability of finding the electron on O₁ rather than on O₂ due to the closer distance of approach of O₁ to the positively charged copper atom. Therefore, one would expect the thermal motion of O₁ to be smaller than O₂ as a result of a stronger bond between O₁ and copper.

Apparently hydrogen bonding occurs at only one site in the structure. The donor atom is N(B) and the acceptor is the screw-related

Table 15

Least Squares Planes for Aromatic Rings

Molecule A

Plane 1: C₄A, C₅A, C₆A, C₇A, C₈A, C₉A

Equation: $6.781X - 3.223Y + 5.771Z = 1.531$

Plane 2: C₄A, C₅A, C₆A

Equation: $7.028X - 3.235Y + 5.645Z = 1.572$

Atom	Distance from Plane 1	Distance from Plane 2
C ₄ A	0.000	-----
C ₅ A	-0.008	-----
C ₆ A	0.009	-----
C ₇ A	-0.002	0.036
C ₈ A	-0.007	0.049
C ₉ A	0.008	0.018

Molecule B

Plane 1: C₄B, C₅B, C₆B, C₇B, C₈B, C₉B

Equation: $4.145X + 2.869Y + 7.158Z = 7.977$

Plane 2: C₄B, C₅B, C₆B

Equation: $3.986X + 2.913Y + 7.143Z = 7.875$

Atom	Distance from Plane 1	Distance from Plane 2
C ₄ B	0.006	-----
C ₅ B	-0.005	-----
C ₆ B	0.002	-----
C ₇ B	0.000	0.020
C ₈ B	0.001	0.030
C ₉ B	-0.004	0.028

TABLE 16

Principal Axes and Direction Cosines with Respect to the
Cell Edges of the Anisotropic Ellipsoids

Atom	B	l_1	l_2	l_3
Cu	3.39	0.729	-0.631	-0.369
	1.83	0.676	0.601	0.323
	1.49	-0.109	-0.490	0.871
O ₁ A	3.06	-0.665	0.670	-0.330
	2.26	0.694	0.390	-0.606
	1.18	0.371	0.527	0.764
O ₂ A	4.26	0.466	0.881	-0.081
	3.11	0.826	-0.400	0.397
	1.55	-0.382	0.121	0.916
N(A)	2.59	0.774	0.182	-0.607
	2.24	-0.398	0.885	-0.242
	1.59	0.374	0.398	0.838
C ₁ A	3.03	0.517	0.737	-0.435
	2.28	0.842	-0.530	0.102
	1.62	0.079	0.307	0.948
C ₂ A	2.82	-0.012	0.700	0.714
	2.05	0.999	0.037	-0.019
	1.63	-0.037	0.604	-0.796
C ₃ A	3.72	0.174	0.296	0.939
	3.00	0.383	0.858	-0.341
	1.87	0.872	-0.458	-0.173
C ₄ A	4.22	0.261	-0.408	0.875
	2.56	0.881	-0.270	-0.389
	1.86	0.352	0.922	0.159
C ₅ A	5.96	0.306	-0.268	0.913
	3.85	-0.255	0.901	0.350
	2.30	0.862	0.376	-0.339
C ₆ A	6.90	0.193	-0.429	0.883
	5.05	-0.150	0.876	0.458
	2.45	0.931	0.281	-0.233

TABLE 16 - continued

Atom	B	l_1	l_2	l_3
C ₇ A	7.76	-0.119	0.297	0.947
	4.85	0.784	-0.558	0.273
	2.51	0.621	0.723	-0.303
C ₈ A	8.65	0.068	0.353	0.933
	5.40	0.968	-0.248	0.024
	1.96	0.228	0.841	-0.491
C ₉ A	6.93	0.057	0.531	0.845
	3.83	0.993	-0.039	-0.042
	2.19	0.002	0.759	-0.651
O ₁ B	2.80	0.748	0.635	0.191
	1.94	-0.653	0.756	0.047
	1.64	-0.222	-0.251	0.942
O ₂ B	4.57	0.357	0.928	0.108
	2.95	0.851	-0.371	0.371
	1.57	-0.432	-0.095	0.897
N(B)	2.50	0.871	0.273	-0.409
	2.04	-0.399	0.878	-0.264
	1.54	0.157	0.348	0.924
C ₁ B	2.82	0.859	-0.203	-0.471
	1.92	0.408	0.827	0.386
	1.37	0.182	-0.488	0.853
C ₂ B	2.02	0.225	-0.146	0.963
	1.88	0.533	0.846	0.004
	1.81	0.774	-0.485	-0.406
C ₃ B	3.90	-0.297	-0.144	0.944
	2.24	0.948	0.075	0.309
	2.02	-0.071	0.997	-0.025
C ₄ B	3.67	-0.416	0.752	0.512
	2.68	0.862	0.147	0.485
	1.73	-0.226	-0.746	0.626
C ₅ B	6.27	0.375	0.699	0.608
	4.79	0.084	-0.679	0.729
	2.58	0.858	-0.322	-0.400

TABLE 16 - continued

Atom	B	l ₁	l ₂	l ₃
C ₆ B	9.51	0.769	0.166	0.617
	6.98	-0.577	0.596	0.559
	2.87	0.160	0.753	-0.638
C ₇ B	12.19	-0.332	0.261	0.906
	5.05	0.912	0.333	0.239
	2.24	-0.189	0.858	-0.477
C ₈ B	12.03	0.030	0.185	0.982
	5.68	0.980	0.189	-0.066
	2.52	-0.200	0.927	-0.317
C ₉ B	5.90	0.118	-0.075	0.990
	4.55	0.983	-0.134	-0.128
	2.96	0.124	0.988	-0.088

O_1B . The distance between the two atoms is 2.981 Å which is a strong hydrogen bonding distance. The angle formed by $C_2B-N(B)-O_1B'$ (prime denotes screw operation) is 90.6° which is in the acceptable range for hydrogen bonding to occur. It is noteworthy to add that the angle $C_2B-N(B)-O_2B'$ is 122.0° and the $N(B)-O_2B'$ distance is 3.189 Å. It is not too unlikely that the hydrogen atom is being shared somewhat between these two oxygen atoms. One might compare these distances and angles with those found in the bis(L-serinato)copper(II) complex (50). There the hydrogen bond distances fall in the range of 2.95 Å to 3.01 Å. The homologous angles in the serine complex range from 91° to 129° . It is seen that the L-phenylalanine angles fall in the proper range. The hydrogen bonding is demonstrated in Fig. 3 with dashed lines.

There is one other place in the structure where hydrogen bonding might occur. This is between $N(A)$ and O_1A' . The distance between these atoms is slightly larger (3.213 Å) than for the homologous distance in molecule B. The $C_2A-N(A)-O_1A'$ angle is 78.1° . When one considers the $N(A)-O_2A'$ distance (3.218 Å) and the $C_2A-N(A)-O_2A'$ angle (114.0°), it is seen that the hydrogen atom is quite probably located between the O_1A' and O_2A' atoms. The conditions for hydrogen bonding to occur between the two screw-related L-phenylalanine molecules are seen to be more stringent for the two A molecules than for the two screw-related B molecules.

CHAPTER IV

CRYSTAL AND MOLECULAR STRUCTURE OF BIS(INDAZOLE)COPPER(II)CHLORIDE

Solution and Refinement of Structure. Bis(indazole)copper(II) chloride crystallizes as light-green triclinic crystals. The least squares cell dimensions (36) from 82 reflections (Appendix II) measured at 22° C is commensurate with there being one copper atom per unit cell complexed with two chloride atoms and two indazole molecules. The space group information is presented in Table 17.

It is interesting to note that the estimated standard deviations are less for the bis(indazole)copper(II) complex than for the L-phenylalanine complex. Appendices I and II give the error between the observed and calculated values of 2θ that were used to obtain the cell dimensions. The average deviation in 2θ for the indazole complex and the L-phenylalanine complex is 0.07° and 0.08° respectively. This is not a large difference. The main difference between the two compounds is the number of data points taken for use in the least-squares program. For the indazole complex 82 reflections were used, whereas for the L-phenylalanine complex 43 reflections were taken. It appears that the estimated standard deviations in the cell parameters can be significantly lowered by increasing the number of reflections used for the least-squares cell dimensions.

One further point can be made from Table 17. Since the space

Table 17

Crystal Data of Bis(indazole)copper(II) Chloride

Space Group	$P\bar{1}$
No. of Molecules	1
Molecular Formula	$\text{Cu}(\text{C}_7\text{H}_6\text{N}_2)_2\text{Cl}_2$
Formula Weight	370.72
Cell Dimensions	
a	= 6.583 (0.003)
b	= 14.426 (0.009)
c	= 3.792 (0.001)
α	= 97.88 (0.04)
β	= 91.61 (0.04)
γ	= 97.35 (0.04)
Density	
obs.	= 1.71 g/cc
calc	= 1.74 g/cc
Vol.	= 353.34
F(000)	= 187
a*	= 0.1533(0.00008)
b*	= 0.07061(0.00005)
c*	= 0.2665(0.0001)
α^*	= 81.84°(0.04)
β^*	= 87.34°(0.04)
γ^*	= 82.35°(0.04)
Vol*	= 0.002830

group is $\overline{P1}$, it follows that the molecule must be centrosymmetric with the copper atom being located on a center of symmetry.

The crystal used for data taking was cut to the dimensions 0.67 x 0.28 x 0.02 mm. It had a mosaic of 1° . The crystal was mounted with c^* parallel to the polar axis, and a θ - 2θ scan technique at a take-off angle of 3° was used to measure the intensities. All reflections within a 2θ value of 140° were measured using Cu-K α radiation. Of the 1341 reflections within this limit 1204 were observed. Lorentz, polarization, and absorption corrections ($\mu=56.58 \text{ cm}^{-1}$) were applied to the data just as in the L-phenylalanine complex. The program of Dr. Philip Shapiro (75) was used as before for these corrections.

A sharpened Patterson map was calculated using the same sharpening function as was used for the bis(L-phenylalaninato)copper(II) complex. All unobserved reflections were omitted from the synthesis. Since the equivalent positions in the space group $\overline{P1}$ are x, y, z and $\bar{x}, \bar{y}, \bar{z}$, the heavy-heavy atom vector should appear in the Patterson at $2x, 2y, 2z$. Upon examination of the map there was only one peak that was large enough to be considered as a possible copper-copper vector. However, upon closer examination this peak was not the correct size. It was too large. It was of proper magnitude to be two copper-chlorine vectors superimposed. This would be the case with the copper atom at the origin having two chlorine atoms centrosymmetrically arranged about it. The confirmation of this arrangement came when the chlorine-chlorine vector was found where it should be. The only thing left to find from the Patterson was the position of the indazole ring. The ring could be seen in the Patterson. Since the copper atom was at the origin in

in real space, the coordinates of the ring in the Patterson could be taken as the coordinates in real space. To verify these positions, it was possible to locate all of the carbon-chlorine and nitrogen-chlorine vectors. The Patterson was quite clear, and all vectors in the map could be explained.

An initial structure factor calculation yielded an R value of 55.31%. The atomic scattering factors used were taken from the International Tables for X-ray Crystallography (40). The scattering power curves for Cu^{2+} , N° , and C° were taken directly from the tables. The scattering factors that were used later in the refinement for hydrogen were those of Stewart, et al. (41). The structure was being refined using the structure factor and least-squares program written by F. R. Ahmed (67) when the structure factor and least-squares program using the entire matrix (42) became available. Refinement was completed using the Busing-Martin-Levy program. After two cycles of this least-squares program with all atoms isotropic, the R value fell to 17.1%. Unit weights were being used at this stage of refinement. All atoms were then made anisotropic and the data were corrected for anomalous dispersion due to the copper atom just as before. Upon cycling the program two more times, the R value dropped to 11.7%.

A difference Fourier (43) was then calculated that included all observed and unobserved reflections. A value of two counts had been used for all of the unobserved reflections. It had been estimated that anything above four counts could be seen with the scintillation counter, and the value of 2 counts is the statistical average. The difference map was on the absolute scale. Using the hydrogen positions

program of Tatsch (77), it was possible to locate all six of the hydrogen atoms with ease in the difference Fourier. The average peak height for the hydrogen atoms was $0.64 \text{ e}/\text{\AA}^3$. The peak for the hydrogen attached to the nitrogen atom was smaller than the others, but there was definitely positive electron density ($0.37 \text{ e}/\text{\AA}^3$) where the hydrogen atom was calculated to be. Table 18 gives the peak heights for the hydrogen atoms. Calculated hydrogen positions were included in subsequent refinement with new positions being calculated after every cycle of least-squares. After addition of the hydrogen atoms, the residual index fell to 11.4%.

Two things remained to be done in the refinement. The weighting scheme was not satisfactory, and the manner of treating the unobserved reflections was not good. A virial weighting scheme was incorporated exactly like the one used in the L-phenylalanine refinement. The coefficients were arrived at, as before, by making a plot of F_o vs. $|\Delta F|^2$ using the same programs (45, 46). The coefficients used were:

$$A = 6.361$$

$$B = 0.1008$$

$$C = 0.001090$$

$$D = -0.000003152$$

Just as in the bis(L-phenylalaninato)copper(II) complex this weighting scheme gave a reasonably constant value for $w(\Delta F_o)^2$ as a function of F_o . This weighting scheme did not lower the R value any further, but the quantity being minimized, $w(\Delta F_o)^2$, was significantly lowered. The unobserved reflections were included in refinement if the value calculated

TABLE 18

Peak Heights of Hydrogen Atoms in Difference Fourier

Atom	$e/\text{\AA}^3$
H(N)	0.37
H(C ₂)	0.59
H(C ₃)	0.50
H(C ₄)	0.80
H(C ₅)	0.75
H(C ₇)	0.85

for the unobserved reflection was equal to or greater than twice the value used for the unobserved reflection. Nineteen of the unobserved reflections were included in refinement as a result of this test. Using the above modification the shifts in the parameters divided by the errors in the parameters fell below 1/3 after two more cycles of the least-squares program. Refinement was considered complete. Table 19 lists the various final residual indices. The final atomic positions and thermal parameters are listed in Table 20 and Table 21 respectively. The list of structure factors is presented in Appendix IV.

Something is seen to be amiss when one looks at the high R values listed in the table. A final difference Fourier (76) was calculated in an attempt to locate the problem. All data were used in the Fourier. The difference map showed many unexplained maxima. There are 18 peaks of positive electron density between 1.0 and 2.04 e/Å³. There are seven peaks of negative electron density between 1.0 and 2.04 e/Å³. The copper atom is surrounded by both negative and positive peaks in this range. These can be partially attributed to inadequacies in thermal motion as in the bis(L-phenylalaninato)copper(II) complex. The rest of the peaks are more troublesome to explain. A very prominent peak (2.02 e/Å³) occurs at $x = \frac{1}{2}$, $y = 0$, $z = 0$.

It was decided to re-examine on the diffractometer some of the reflections that had been shown by an error analysis program written by P. W. R. Corfield (68) to be different from the calculated reflections. When this was done, it was discovered that the crystal was quite possibly twinned. This possibility offers an immediate explanation to the high R value and noisy difference Fourier. To check the

possibility of twinning a Weissenberg photograph was taken. A zero-level photograph of the $hk0$ reflections revealed that the crystal was, in fact, twinned.

Table 19

R Values for Bis(indazole)Copper(II) Chloride

R factor including unobserved reflections for which $F(\text{calc}) > 2F(\text{unobs})$	12.0%
R factor omitting unobserved reflections	11.4%
Weighted R factor including unobserved reflections for which $F(\text{calc}) > 2F(\text{unobs})$	15.0%
Weighted R factor omitting unobserved reflections	14.3%

In such a case one has two alternatives. A new data crystal can be found and the data can be retaken, or the orientation of the two different lattices in the crystal can be determined and those reflections which occupy the same position in space can be eliminated from the data. The latter course was decided upon for two reasons. First, it was relatively easy to determine the orientation of the two reciprocal lattices. Second, it is quite difficult to obtain crystals of the complex

Table 20

Final Atomic Positions

Atom	X	Y	Z	B _{iso}
Cu	0.0	0.0	0.0	
Cl	0.2576(4)	0.0565(2)	0.4304(7)	
N ₁	0.7061(14)	0.1368(7)	-0.0415(27)	
N ₂	0.8936(14)	0.1261(6)	0.0726(24)	
C ₁	0.8449(18)	0.2763(8)	0.2153(33)	
C ₂	0.8487(21)	0.3739(9)	0.3399(36)	
C ₃	0.6828(23)	0.4160(9)	0.2797(39)	
C ₄	0.5037(23)	0.3656(9)	0.0989(35)	
C ₅	0.4979(20)	0.2702(9)	-0.0251(36)	
C ₆	0.6658(17)	0.2278(8)	0.0395(30)	
C ₇	0.9801(20)	0.2092(8)	0.2315(31)	
*H(N ₁)	0.607	0.083	-0.172	3.79
H(C ₂)	0.980	0.417	0.483	4.53
H(C ₃)	0.693	0.491	0.377	4.95
H(C ₄)	0.370	0.400	0.055	4.82
H(C ₅)	0.364	0.229	-0.170	4.41
H(C ₇)	1.134	0.220	0.353	4.01

* All hydrogen positions are calculated (77). The N-H distance was taken as 1.01 Å. The C-H distances were taken as 1.08 Å (64). B_{iso} was determined by adding 0.5 to the atom to which the hydrogen was attached.

Table 21

Anisotropic Thermal Parameters X 10⁴ *

* $\exp(-[h^2b_{11}+k^2b_{22}+l^2b_{33}+2hkb_{12}+2hlb_{13}+2klb_{23}])$						
Atom	b ₁₁	b ₂₂	b ₃₃	b ₁₂	b ₁₃	b ₂₃
Cu	179(6)	29(1)	474(17)	13(2)	-49(7)	-45(3)
Cl	171(7)	34(1)	490(20)	12(2)	-72(9)	-47(4)
N ₁	156(23)	36(5)	747(83)	27(9)	-22(35)	-24(16)
N ₂	170(22)	25(4)	566(70)	7(8)	23(31)	-33(14)
C ₁	185(28)	36(6)	647(91)	11(10)	43(41)	-21(19)
C ₂	274(37)	36(6)	734(104)	9(12)	-45(50)	-27(20)
C ₃	322(42)	39(7)	823(115)	37(14)	23(56)	-27(22)
C ₄	320(41)	46(7)	641(100)	47(14)	-23(52)	-54(21)
C ₅	210(32)	49(7)	770(105)	39(12)	-32(46)	2(22)
C ₆	167(26)	36(6)	516(80)	15(10)	17(37)	-23(17)
C ₇	277(35)	36(6)	467(81)	8(12)	49(43)	-24(18)

that are suitable for x-ray intensity data. Before data taking was initiated, it took three months of searching before a crystal was found that looked like a reasonable data crystal. The vast majority of crystals examined had reflections with multiple maxima.

Unfortunately, it may not be possible to complete refinement using the method of elimination if too many reflections are found in common. Initial calculations indicate that 511 reflections are in common. The way that this figure was arrived at was to place certain limits upon the differences in the coordinates 2θ , ϕ , and χ of the two orientations. If the difference between the calculated coordinates for both orientations is less than or equal to 1.0° in 2θ and χ and less than or equal to $1.0 + 0.01(\chi) - 0.3(\Delta 2\theta)$ degrees in χ , then the reflections are considered to be in common. The value of $\Delta 2\theta$ is never established unless it passes the first test of being less than or equal to 1.0° . The two restrictions are placed on ϕ because it becomes less sensitive as one increases the value of χ , and as the difference in 2θ becomes larger for the two orientations, the difference in ϕ must become smaller before the two reflections can be considered overlapped.

The reason for twinning is obvious. The indazole molecule can approach the copper atom in either of two orientations. The indazole molecule has a pseudo-two-fold axis through atoms N_2 and C_4 (cf. Fig. 16). Rotation of 180° around this axis yields the two different orientations. If hydrogen bonding does occur (vide infra) between N_1 and the chlorine atom, it is not prohibited in either orientation.

Figure 12 shows the relative orientation of the two reciprocal lattices.

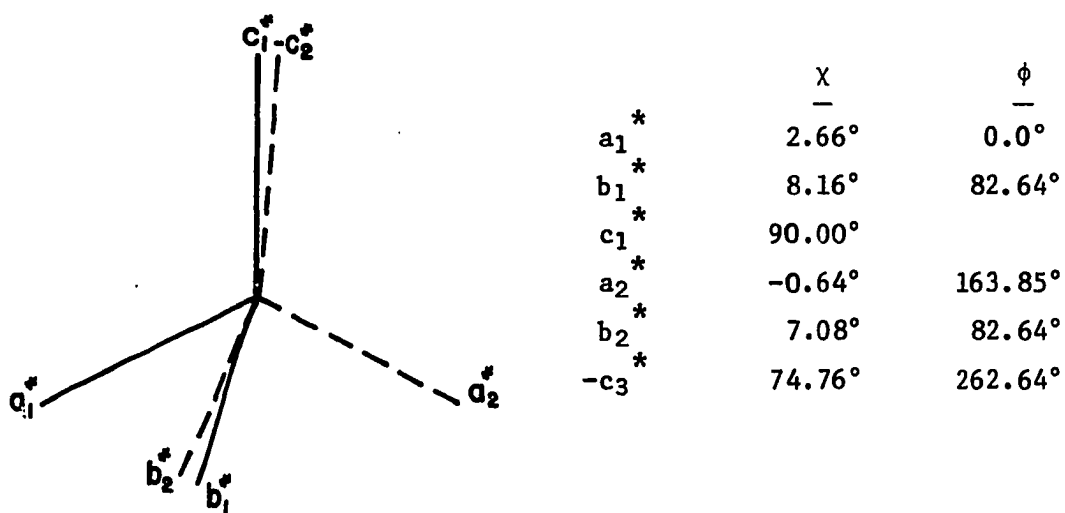


Figure 12. Orientation of Twinned Reciprocal Lattices. (The lattices are oriented such that the set of 0,0,1 and 0,-1,2 planes of the "data" orientation are in common with the 0,1,-1 and 0,1-2 planes respectively of the "twin" orientation.)

TABLE 22

Comparison of "Data" Intensities
With "Twin" Intensities.

<u>h k l</u>	<u>I (data)</u>	<u>h k l</u>	<u>I (twin)</u>
1 1 1	454	-1-1-1	32
-2 3 1	1372	2-3-1	131
1 1 0	7565	-1-1 0	888
3 5 0	539	3 5 0	43
2 3 1	1417	-2-3-1	148

With the following discussion in mind, it must be realized that the following calculations of bond distances and angles will be slightly in error since they are based on data which has been shown to be twinned. However, the essential features of the structure are correct. The bond distances, mean planes, and thermal ellipsoids will all be subject to change when the correct data are used. It is to be noted that even with this twinned data there are no really abnormal features about the structure as will be seen in the following discussion. The reason for this is that the "twin" has much weaker intensities than those belonging to the lattice oriented the way the data was taken. Table 22 gives a comparison of the intensities of the same reflection for the two different orientations.

One way of checking a structure is to calculate the intermolecular distances. Table 23 gives the Van der Waal's intermolecular distances less than 4.0 Å. A normal chlorine-chlorine contact is 3.6 Å. The two chlorine atoms related by the center of symmetry at $(0, 0, \frac{1}{2})$ come to within 3.655 Å of each other which is seen to be quite normal. The shortest distance in the table is the nitrogen-chlorine distance of 3.013 Å. The nitrogen atom position is generated by operating upon the coordinates for N_1 given in Table 20 with the inversion center at $(\frac{1}{2}, 0, \frac{1}{2})$. The normal Van der Waal's distance for nitrogen-chlorine is 3.3 Å. The shortened distance is probably the result of hydrogen bonding (vide infra). The only other short distances are those between the nitrogen and chlorine atoms involved in coordination around the copper ion which is as expected. These distances (3.065 and 3.068) compare to a homologous distance of 3.11 Å in the complex of cupric chloride with

TABLE 23

Van der Waal's Contacts Less Than 4.0 Å *

Atom X	Atom Y	Distance
Cl ⁻	Cl ⁻ ' (1-x,-y,1-z)	3.820
Cl ⁻	Cl ⁻ ' (-x,-y,1-z)	3.655
Cl ⁻	N ₁	3.641
Cl ⁻	N ₁ " (x,y,1+z)	3.497
Cl ⁻	N ₁ ' (1-x,-y,1-z)	3.888
Cl ⁻	N ₁ ' (1-x,-y,-z)	3.013
Cl ⁻	N ₂ " (x-1,y,z)	3.065
Cl ⁻	N ₂ " (x-1,y,z+1)	3.599
Cl ⁻	N ₂ ' (1-x,-y,1-z)	3.504
Cl ⁻	N ₂ ' (1-x,-y,-z)	3.068
Cl ⁻	C ₅	3.919
Cl ⁻	C ₅ " (x,y,1+z)	3.619
Cl ⁻	C ₆	3.879
Cl ⁻	C ₆ " (x,y,1+z)	3.879
Cl ⁻	C ₇ " (1-x,y,z)	3.189
N ₁	N ₂ " (x,y,z-1)	3.602
N ₁	C ₁ " (x,y,z-1)	3.748
N ₁	C ₆ " (x,y,z-1)	3.902
N ₁	C ₇ " (x,y,z-1)	3.539
N ₂	C ₇ " (x,y,z-1)	3.593
C ₁	C ₂ " (x,y,z-1)	3.779
C ₁	C ₅ " (x,y,1+z)	3.729
C ₁	C ₆ " (x,y,1+z)	3.499
C ₁	C ₇ " (x,y,z-1)	3.881
C ₂	C ₂ ' (2-x,1-y,1-z)	3.933
C ₂	C ₃ " (x,y,1+z)	3.749
C ₂	C ₄ " (x,y,1+z)	3.721
C ₂	C ₅ " (x,y,1+z)	3.712

TABLE 23 - continued

Van der Waal's Contacts Less Than 4.0 Å *

Atom X	Atom Y	Distance
C ₂	C ₆ '' (x,y,1+z)	3.741
C ₃	C ₃ ' (1-x,1-y,1-z)	3.881
C ₃	C ₄ '' (x,y,1+z)	3.488
C ₃	C ₄ ' (1-x,1-y,-z)	3.953
C ₃	C ₅ '' (x,y,1+z)	3.727
C ₄	C ₅ '' (x,y,1+z)	3.765
C ₄	C ₇ '' (x-1,y,z)	3.955
C ₅	C ₆ '' (x,y,z-1)	3.738
C ₅	C ₇ '' (x-1,y,z)	3.605
C ₆	C ₇ '' (x,y,z-1)	3.743

* A single prime indicates the inversion operation was performed on the coordinates in Table 20. A double prime indicates a translation was performed.

1:2:4-triazole (69). The normal Van der Waal's distance between aromatic rings is 3.4 Å to 3.7 Å. The closest distance between rings separated by a unit translation occurs between C_3 and C_4'' (unit z translation) which is 3.488 Å. It is seen that there are no abnormally short Van der Waal's distances in the structure. This fact reinforces the idea that the essential features of the structure are correct.

Discussion of Structure. The coordination around the copper atom is once again very close to being octahedral with tetragonal distortion. This can be seen in the stereoscopic drawing in Figure 14. Figure 15 shows the angles and distances in the coordination sphere. To gain a better idea of the distortion from D_{4h} symmetry, the bond angles around copper and the distance between ligand atoms can be examined. Cl' will indicate the long (axial) chloride atom in the following discussion. The angles for Cl'-Cu-Cl, Cl'-Cu-N, and Cl-Cu-N are $92.16^\circ(0.09)$, $91.64^\circ(0.27)$, and $89.94^\circ(0.26)$ respectively. From these angles one can see that the distortion from 90° is so small as to be negligible. Figure 13 shows the angles and distances for the square-plane. From the figure one can see that the square-plane is in reality a rhombus within the estimated standard deviations.

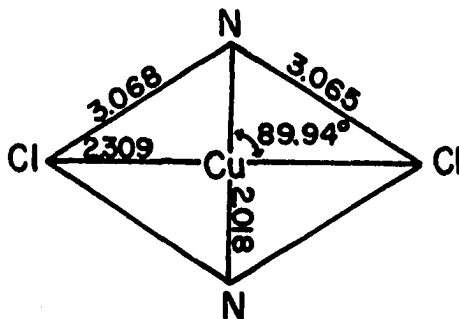


Figure 13. Bond Distances and Angles for Square-Plane in Bis(indazole)copper(II) Chloride

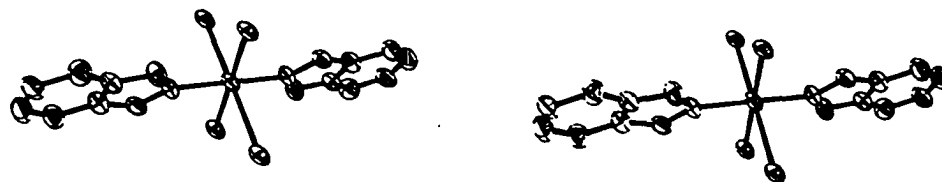


Figure 14. Stereoscopic Drawing (97) of Bis(IndazoleCopper(II) Chloride.
(Projection down the "a" axis.)

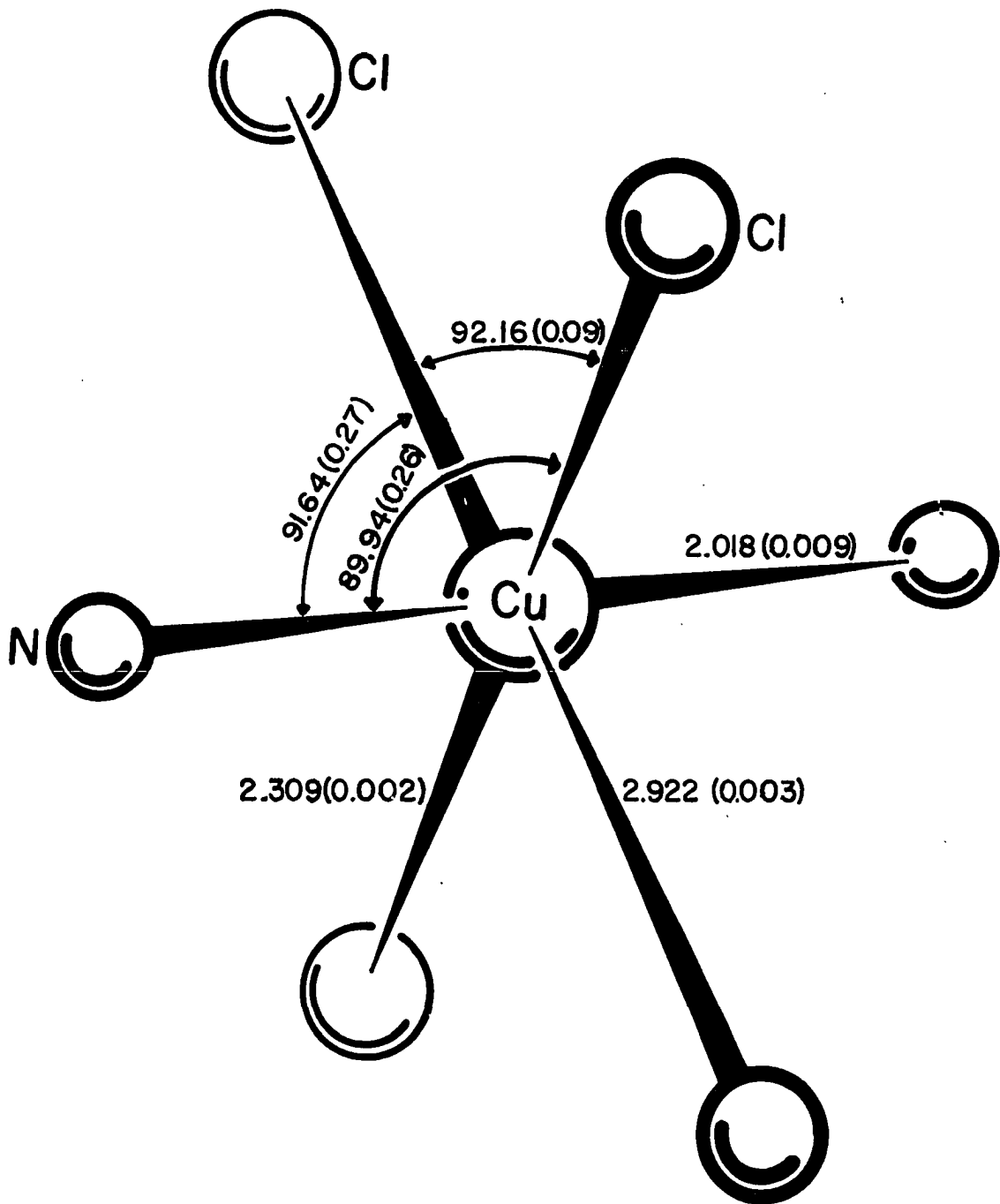


Figure 15. Coordination Around Copper Ion

The Cl-Cu-N angle of 89.94° compares to the homologous angle in the bis(1:2:4-triazole)copper(II) chloride complex (69) quite closely. There the angle is 89.6° . When a comparison is made of the other two angles for the two complexes, it is seen that the triazole complex is more distorted than the indazole complex. In the triazole complex the Cl'-Cu-Cl angle and the Cl'-Cu-N angle are 95.3° and 96.2° respectively. In both structures the copper atom lies on a center of symmetry which means that the three planes through the copper atom describing the coordination are absolute planes. Table 24 gives the dihedral angles between the three planes. The two structures are seen to be similar in the way the copper atom is coordinated. The indazole complex exhibits almost ideal D_{2h} site symmetry, whereas the triazole complex exhibits a small amount of trigonal distortion.

Table 24

Dihedral Angles Between Coordination Planes

Plane 1	Plane 2	Angle
Cl', Cu, N	Cl', Cu, Cl	90.02°
Cl', Cu, N	N, Cu, Cl	92.15°
Cl', Cu, Cl	N, Cu, Cl	91.65°

Table 25 gives a comparison of bond distances for various copper-chloride complexes having octahedral symmetry. Two things can be observed from the table. First, there is a short copper-chloride

TABLE 25

Comparison of Copper-Chlorine Bond Lengths for Various
Structures having Octahedral Coordination (70)

Compound	Distances (Å)
CuCl_2	4Cl at 2.30, 2Cl at 2.95
CsCuCl_3	4Cl at 2.30, 2Cl at 2.65
$\text{CuCl}_2 \cdot 2\text{H}_2\text{O}$	2 O at 2.01, 2Cl at 2.31, 2Cl at 2.98
bis(1:2:4-Triazole) CuCl_2	2 N at 1.98, 2Cl at 2.34, 2Cl at 2.77
bis(Indazole) CuCl_2	2 N at 2.02, 2Cl at 2.31, 2Cl at 2.92

bond distance of approximately 2.30 Å. The bis(indazole)copper(II) chloride structure has a Cu-Cl bond distance that is in close agreement 2.31 Å). Second, there is a long Cu-Cl bond distance that appears to be quite variable. The table lists values from 2.65 Å to 2.95 Å. The indazole complex falls at the long extreme (2.92 Å) in the range.

Table 26 shows a comparison of the bond lengths and angles found in the indazole molecule to certain selected averages. Figures 16 and 17 show the bond lengths and angles for the molecule. The way in which these averages were derived are described in the footnotes. It is difficult to draw conclusions in light of the high estimated standard deviations for the bonds and angles. The average e.s.d. for bond lengths is 0.016 Å. For the angles the average e.s.d. is 1.1°. The main point of interest in the indazole molecule is the bond lengths in the vicinity of the copper atom. When one considers the N₁-N₂ bond of 1.331 (0.013) Å, it is seen that it compares quite well to other N-N bonds in aromatic ring systems. The N₂-C₇ bond, however, appears to be short. The bond length is 1.317(0.014) Å as compared to 1.35 Å when compared to the average given by Interatomic Distances (64). In light of the e.s.d. for the bond, it is seen that it is within 3 σ's of 1.35 Å, but one is still tempted to say that the N₂-C₇ length has changed due to the rings' complexing with copper. This would make chemical sense. The lone pair of electrons on N₂ have been pulled toward the copper atom resulting in a secondary shift of electrons in the ring system such that the double bond character in the N₂-C₇ bond has increased. A similar type of stabilization of C-N double bonds, where the nitrogen atom is chelated to a metal, has been suggested before in the structure of N-salicylidene-glycinatoaquocopper(II) hemihydrate (71). A more definitive answer to

TABLE 26

Intramolecular Bond Angles and Distances for Indazole
Compared to Selected Average Values*

Bond	Indazole		
	Bond Distances	Average* from Four Selected Compounds	Average from <u>Interatomic Distances(64)</u>
N ₁ -N ₂	1.331(0.013)	1.33	_____
N ₁ -C ₆	1.366(0.014)	1.35	1.352(0.005)
N ₂ -C ₇	1.317(0.014)	1.35	1.352(0.005)
C ₇ -C ₁	1.402(0.017)	1.37	1.395(0.003)
C ₁ -C ₂	1.420(0.016)	_____	1.395(0.003)
C ₂ -C ₃	1.344(0.019)	_____	1.395(0.003)
C ₃ -C ₄	1.410(0.020)	_____	1.395(0.003)
C ₄ -C ₅	1.386(0.018)	_____	1.395(0.003)
C ₅ -C ₆	1.362(0.016)	_____	1.395(0.003)
C ₁ -C ₆	1.394(0.016)	1.37	1.395(0.003)

* The distances were obtained by averaging homologous bonds in the 5-membered rings in Xanthazole monohydrate, Adenine hydrochloride hemihydrate, Guanine hydrochloride monohydrate, and the ion in 5-imino-1:3 dimethyltetrazole hydrochloride(64,72,73,74).

TABLE 26 - continued

Intramolecular Bond Angles and Distances For Indazole
Compared to Selected Average Values*

	Bond Angles	Average Values From 3 Spatially Equivalent Molecules*
N ₁ -N ₂ -C ₇	107.0(0.9)	113.
N ₂ -C ₇ -C ₁	110.0(1.1)	106.
C ₇ -C ₁ -C ₂	135.9(1.2)	—
C ₇ -C ₁ -C ₆	106.1(1.0)	108.
C ₆ -C ₁ -C ₂	117.9(1.1)	125.
C ₁ -C ₂ -C ₃	119.3(1.2)	—
C ₂ -C ₃ -C ₄	121.8(1.2)	—
C ₃ -C ₄ -C ₅	119.5(1.2)	—
C ₄ -C ₅ -C ₆	118.4(1.2)	—
C ₅ -C ₆ -C ₁	123.0(1.1)	121.
C ₅ -C ₆ -N ₁	132.4(1.1)	—
N ₁ -C ₆ -C ₁	104.6(1.0)	109.
C ₆ -N ₁ -N ₂	112.4(0.9)	104.

* The values were obtained by averaging the values from Xanthazole monohydrate(64), adenine hydrochloride hemihydrate(72), and guanine hydrochloride monohydrate(73). All three molecules consist of two fused aromatic rings composed of nitrogen and carbon, one of which is 5-membered and the other 6-membered. The averages are found by simply taking the spatially equivalent angles of the polygon formed by the fused 5 and 6-membered rings and averaging the three angles. Unfortunately this means that the angles are not always atomically equivalent, e.g., a N-C-C angle might be averaged with two C-N-C angles.

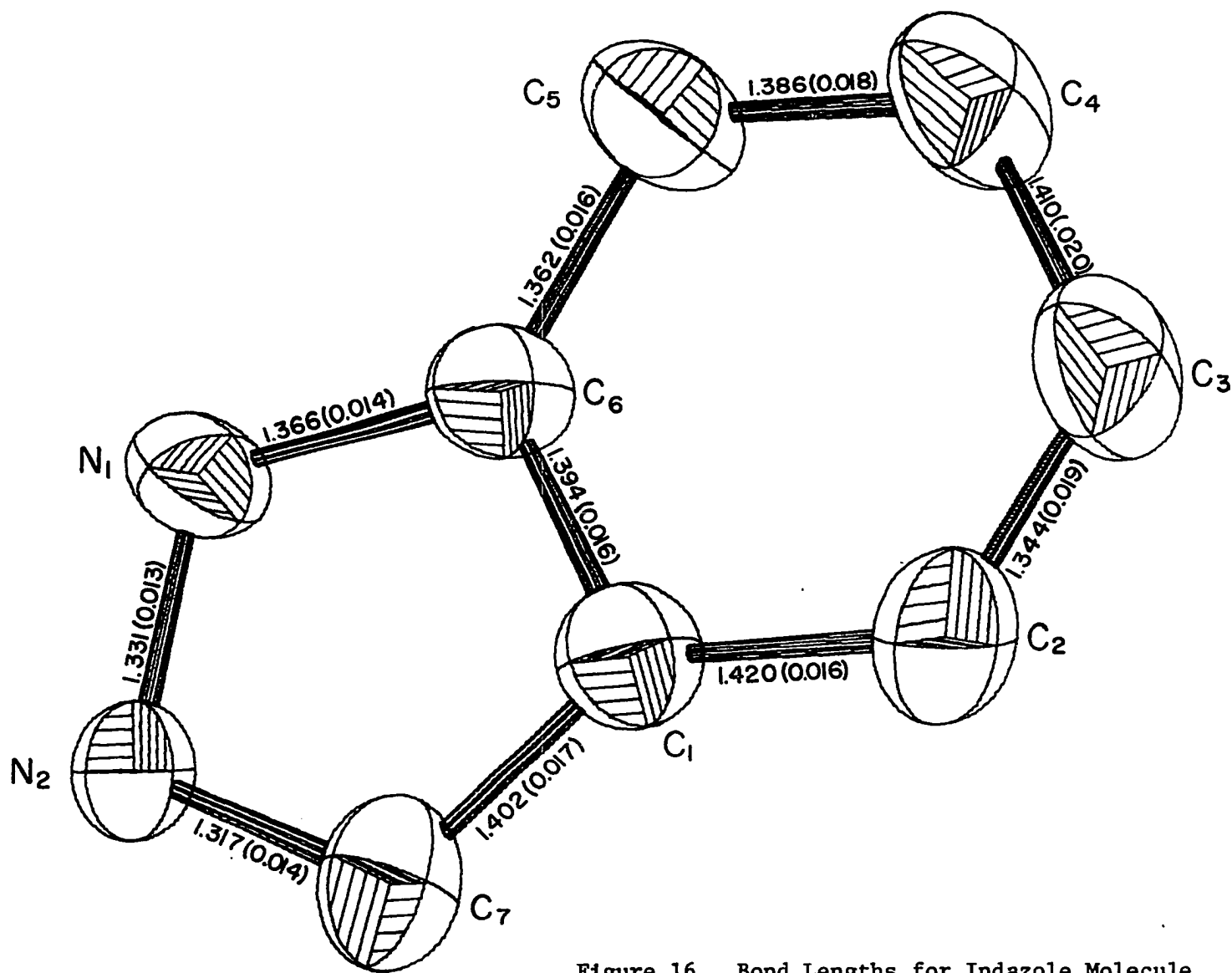
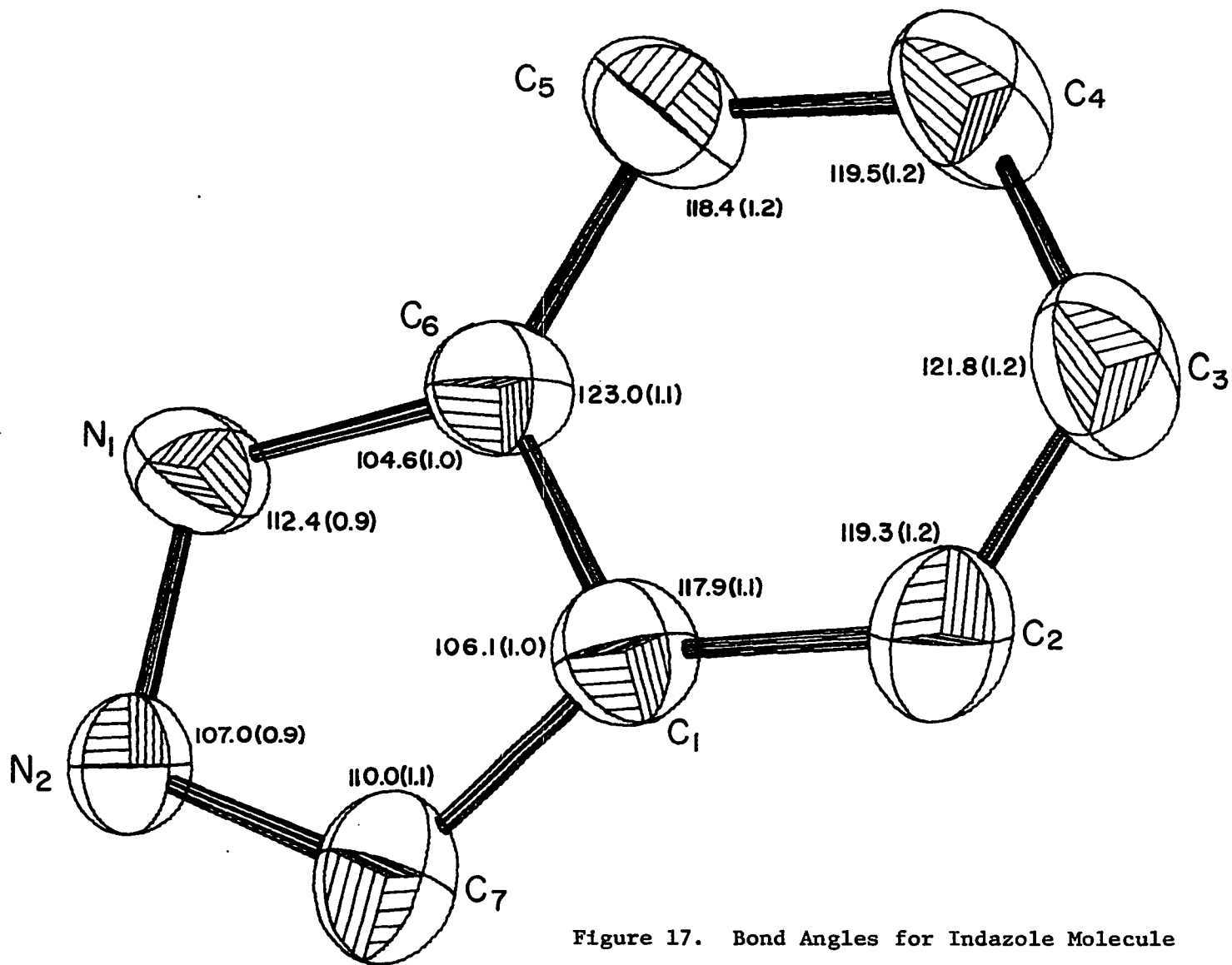


Figure 16. Bond Lengths for Indazole Molecule



this question will have to wait.

There are some rather odd bond lengths in the six-membered ring. The C_2-C_3 distance of 1.344 Å is close to being the length of an isolated double bond. When one looks at the e.s.d. in the length (0.019 Å), it is seen that the bond is within 3 σ 's of the correct length of 1.395 Å. There are two other somewhat strange lengths in this part of the molecule. These bond lengths (1.410 Å and 1.420 Å) occur on either side of the short bond mentioned above. The two long distances are within 3 σ 's of the correct length also. These bond lengths are probably a reflection of the bad data due to the twinning that has been previously discussed.

The bond angles in the five-membered ring of indazole sum to 540° as they should for a planer molecule. The sum of the angles for the six-membered ring is 720° which is also commensurate with a planer ring. The angles in general are in close agreement with those of the other fused five- and six-membered rings cited. The $N_1-N_2-C_7$ angle of 107.0°(0.9) appears quite a bit smaller than the 113° angle which is the average of the three spatially equivalent molecules, but when compared to the N-N-C angle (104°) of the ion in 5-imino-1:3-dimethyl-tetrazole hydrochloride (74) it is seen that the 107° angle is not really abnormal. Similar comparisons can be made for all the other angles in indazole. The essential feature to note is that these angles can be quite variable for fused-ring systems, especially in the five-membered ring.

The least-squares plane for the indazole molecule is given in Table 27. The average deviation from planarity is 0.0056 Å. As men-

Table 27

Least Squares Plane for Indazole

Plane 1: N₁, N₂, C₁, C₂, C₃, C₄, C₅, C₆, C₇

Equation: $2.358X + 4.204Y - 3.484Z = 2.389$

Plane 2: C₂, C₃, C₄

Equation: $2.336X + 4.222Y - 3.488Z = 2.375$

Atom	Distance from Plane 1	Distance from Plane 2
N ₁	-0.004	0.003
N ₂	-0.004	0.009
C ₁	0.015	-0.014
C ₂	0.000	-----
C ₃	-0.004	-----
C ₄	-0.008	-----
C ₅	0.009	-0.016
C ₆	0.001	-0.004
C ₇	-0.004	0.010

tioned previously, the angles around the five- and six-membered rings sum to 540° and 720° respectively. From these three facts it is seen that the ring system is very planer with no evident puckering seen anywhere.

Table 28 gives the angles between the principal axes of the thermal ellipsoids and the indazole plane. The ring as a whole can be seen to move upon examination of the table; for example, when one looks at the angles between the major axis and the plane for C_2 , C_3 , C_4 , C_5 , and C_6 , it is seen that they are all very close. N_1 , N_2 , C_1 , and C_7 do not seem to show this type of movement. It must be remembered that the intensity data are not what they should be and the thermal ellipsoids are actually absorbing some of the error.

Table 29 gives the lengths of the principal axes of the thermal ellipsoids and their direction cosines with respect to the unit cell axes. From the table it is seen that the largest B values occur for C_2 , C_3 , C_4 , and C_5 . This indicates that the molecule is "waving". This is reinforced when the B values of N_2 are examined. N_2 has one of the smallest B values for its major axis which indicates the coordination bond is restricting the motion of the nitrogen atom. As one progresses outwardly along the ring, it is seen that the B's get larger with C_4 having the largest value.

Figure 18 shows a projection down the "a" axis followed by a rotation of 15° around the "b" axis which is horizontal across the page. The drawing shows $2\frac{1}{2}$ unit cells in the "c" direction. The horizontal lines indicate the unit cells. The copper atoms are all contained by the two vertical lines. Three things can be seen from the

TABLE 28

Angles Between Principal Axes of Thermal Ellipsoids and
The Mean Plane of The Indazole Molecule*

Atom	B	Angle (deg)
N ₁	5.10	105
	2.81	-4
	1.99	-14
N ₂	4.03	146
	2.87	30
	1.50	-14
C ₁	4.47	143
	3.11	26
	2.31	-24
C ₂	5.26	70
	4.44	-17
	2.39	-11
C ₃	5.83	56
	5.11	-30
	2.38	-14
C ₄	6.60	52
	4.38	24
	2.01	-27
C ₅	5.32	65
	3.84	-24
	2.62	-5
C ₆	3.96	57
	2.84	10
	2.05	-31
C ₇	4.91	2
	3.69	57
	1.92	-33

* The mean plane was defined using all nine atoms of the ring system.

TABLE 29

Lengths and Direction Cosines With Respect to Unit Cell Axes
of the Principal Axes of The Thermal Ellipsoids.

Atom	B(Å ²)	l ₁	l ₂	l ₃
Cu	4.24	0.388	0.588	-0.755
	2.82	0.919	-0.433	0.248
	1.31	0.061	0.683	0.607
Cl	4.59	0.353	0.625	-0.746
	2.78	-0.903	0.538	-0.083
	1.44	0.243	0.566	0.661
N ₁	5.10	-0.232	-0.516	0.878
	2.81	0.660	0.428	0.448
	1.99	-0.714	0.742	0.168
N ₂	4.03	0.177	-0.564	0.883
	2.87	0.980	0.044	-0.148
	1.50	-0.087	0.825	0.445
C ₁	4.47	0.230	-0.598	0.853
	3.11	0.919	0.273	-0.064
	2.31	-0.320	0.754	0.518
C ₂	5.26	0.634	0.307	-0.733
	4.44	0.766	-0.528	0.509
	2.39	0.104	0.792	0.451
C ₃	5.83	0.721	0.430	-0.541
	5.11	0.624	-0.289	0.757
	2.38	-0.301	0.855	0.368
C ₄	6.60	0.666	0.546	-0.494
	4.38	-0.701	0.442	-0.643
	2.01	-0.256	0.711	0.587
C ₅	5.32	0.473	0.581	-0.697
	3.84	0.334	0.449	0.713
	2.62	-0.815	0.679	-0.077
C ₆	3.96	0.045	0.745	-0.754
	2.84	0.957	0.030	0.194
	2.05	-0.286	0.667	0.628

TABLE 29 - continued

Lengths and Direction Cosines With Respect to Unit Cell Axes
of the Principal Axes of The Thermal Ellipsoids.

Atom	B(Å ²)	l ₁	l ₂	l ₃
C ₇	4.91	0.939	-0.336	0.269
	3.69	0.330	0.741	-0.632
	1.92	-0.099	0.581	0.727

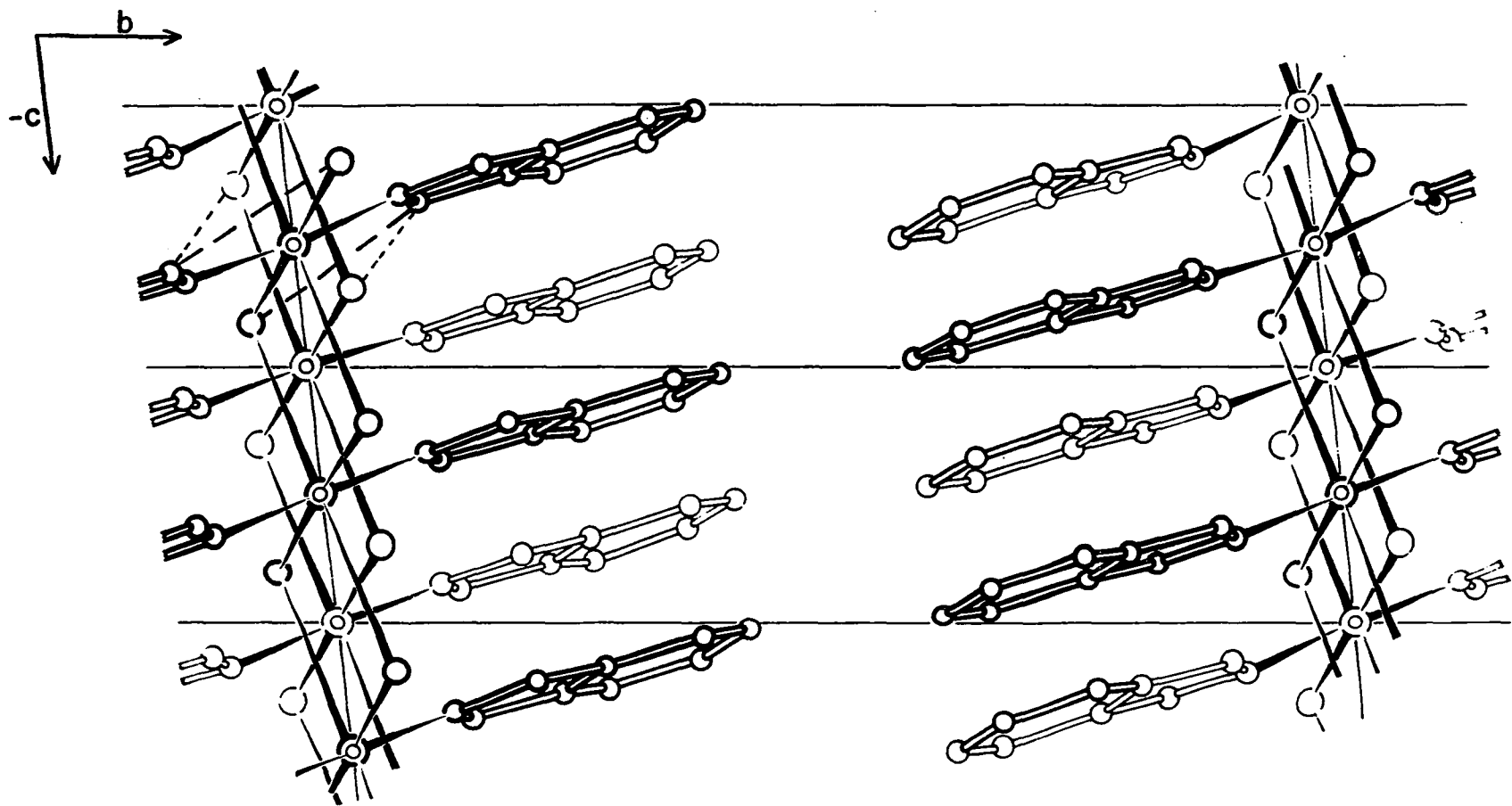


Figure 18. Projection of Bis(indazole)copper(II) Chloride Down "a" Axis Followed by 15° Rotation in Clockwise Direction Around "b" Axis

drawing. First, the packing of the indazole rings can be seen. When one considers all ten of the indazole molecules in drawing, it is seen that they are interleaved similar to when one shuffles a deck of cards. Second, when one considers only five of the molecules in a vertical column, it is seen that upon looking along the plane of the indazole molecules they are also interleaved in that direction. The darker molecules are in one unit cell, whereas the lighter drawn molecules are a unit translation in the negative "a" direction. The third thing to be seen from the figure is how the chlorine atoms fall in the square plane of one copper atom and occupy the apical coordination position of another copper atom. It will aid in this visualization to compare Figure 18 with Figure 13.

Hydrogen bonding occurs at one place in the unit cell. The hydrogen bonding is somewhat unusual in that the hydrogen atom is not really pointed directly at the acceptor atom. Specifically, the N_1-Cl^* (Cl^* generated by operating on the coordinates in Table 20 with the inversion center at $(\frac{1}{2}, 0, \frac{1}{2})$) distance is 3.013 (0.010) Å which is in the proper range for nitrogen to chlorine hydrogen bonding. For example, in the addition complex of $CaCl_2$ with glycyglycylglycine, nitrogen-chlorine hydrogen bonding distances range from 3.1 to 3.3 Å (98). The problem arises when one examines the N_2-N_1-Cl and C_6-N_1-Cl angles. These are 79.7° and 163.0° respectively. These angles are not close to the expected sp^2 hybridized angle of 120° . Also the Cl^*-H-N_1 angles is 118.0° which indicates, as described previously that the hydrogen is not pointed directly at the acceptor. What is probably occurring is the hydrogen atom is being shared by two chlorine atoms. The N_1-Cl (Cl coordinates

are those in Table 20) distance is 3.497 (0.010 Å and the C1-H-N1 angle is 139.0°. Dashed lines in Figure 18 indicate the possible location of hydrogen bonding.

The angle between the planes of the indazole molecule and the square-plane (defined by Cu, Cl, N₁) of the octahedral coordination sphere was calculated to see if the hydrogen bonding has any influence. The octahedral angle is 16.5°, and it is seen that hydrogen bonding along with packing forces result in the planes being almost coincident.

CHAPTER V
THEORY OF CRYSTAL FIELD SPECTRA AND
MAGNETIC SUSCEPTIBILITY

Theory of Spectra. The formalism used in the interpretation of the spectrum of the two complexes is crystal field (78) theory where the ligands are supposed to provide a constant electric potential possessing the symmetry of the ligand nuclei. This potential perturbs the gyrations of the metal electrons from their ordinary excursions in the five "d" orbitals.

The mathematical approach is accomplished using perturbation theory. The Hamiltonian is written as the sum of the various perturbations that are invoked to explain the ordering of the "d" orbitals. For example the spectra of the copper complexes studied herein will be interpreted using two perturbations upon the ordinary free ion. The first perturbation will be the octahedral one where the ligands split the five degenerate orbitals into two levels separated by the spectral parameter $10 Dq$ (Fig. 19). The second perturbation is the tetragonal disturbance where the degeneracy of the orbitals is further removed as shown in Figure 19. Here two new spectral parameters arise and will be referred to as D_s and D_t . Since there are four different energy levels under D_{4h} symmetry it will be necessary to have three parameters

to specify the difference between them. The final perturbation that will be of interest will be spin-orbit coupling where the spin angular momentum interacts with the orbital angular momentum. This part of the Hamiltonian is present in the free ion operator but is ignored in many crystal field treatments. This final perturbation removes all degeneracy and requires a fourth parameter to describe the difference between energy levels. This fourth parameter will be referred to as ξ . The main justification for using these perturbations is, of course, the known structure as determined by x-ray analysis.

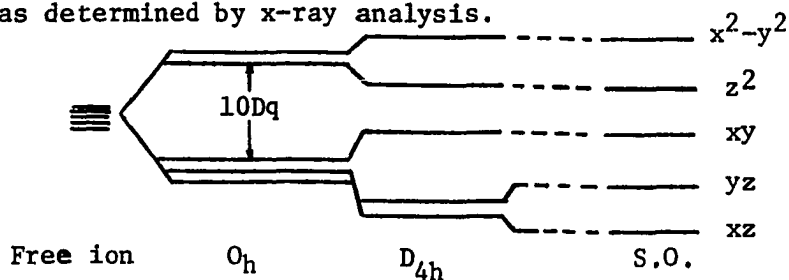


Figure 19. Effect of Various Perturbations on "d" Orbitals

With the previous paragraph in mind one writes the Hamiltonian for the system as follows:

$$\hat{H} = \hat{H}_f + \hat{V} + \hat{V}_t$$

Where \hat{H}_f is the ordinary free ion operator, \hat{V} is the octahedral operator, and \hat{V}_t is the tetragonal operator. Several of the operators take a familiar form. For example the free ion operator has the form:

$$\hat{H}_f = -\frac{\hbar^2}{2m} \sum_i \nabla_i^2 - \sum_i \frac{Ze^2}{r_i} + \frac{1}{2} \sum_{i \neq j} \frac{e^2}{r_{ij}} + \sum_i \xi_i(r) \mathbf{l}_i \cdot \mathbf{s}_i$$

where the first term is the kinetic energy, the second term is the potential energy due to the interaction of electron with nucleus, the third term is the potential energy due to interaction of electron with electron, and the fourth term is the spin-orbit coupling operator. The parameter

ξ is a function of the partial derivative of the potential in which the electron moves and its product with $1/r$ (79). For our purposes it will simply be the fourth parameter with which the spectra will be fitted.

The procedure followed to get the form of the octahedral operator is to expand V in a series of normalized spherical harmonics.

$$\hat{V} = \sum_i \sum_l \sum_m Y_l^m(\theta_i, \phi_i) R_{nl}(r_i)$$

It can be shown that this expansion takes the form (79):

$$\hat{V} = \sum_i \frac{1}{4\pi} R_o(r_i) + Y_4^0 + \sqrt{5/14} (Y_4^4 + Y_4^{-4})$$

The first term gives rise to a uniform shift of the energy levels to a first approximation and may be ignored in the rest of the discussion.

When this operator is applied to the set of "d" orbitals[†], the following table can be compiled.

Table 30

Effect of Octahedral Operator on "d" Orbitals

$$\begin{aligned} \langle d_{\pm 2}^* | \hat{V} | d_{\pm 2} \rangle &= Dq \\ \langle d_{\pm 2}^* | \hat{V} | d_{\mp 2} \rangle &= 5Dq \\ \langle d_{\pm 1}^* | \hat{V} | d_{\pm 1} \rangle &= -4Dq \\ \langle d_o^* | \hat{V} | d_o \rangle &= 6Dq \end{aligned}$$

To see a derivation of these relationships one can consult B. N. Figgis (80).

The tetragonal operator takes the form (79).

[†]The d orbitals will have different labels, and various linear combinations of the spherical harmonics will be used throughout. For the various definitions consult Appendix V.

$$\hat{V}_t = A R_2(r) Y_2^0 + B R_4'(r) Y_4^0$$

The spherical harmonics Y_4^4 & Y_4^{-4} are not included in this expansion because they are a function of x & y and the tetragonal perturbation does not disturb the potential in the xy plane.

The tetragonal operator may be put in different form to see where the previously mentioned parameters D_s and D_t arise. Using the operator equivalent method (81) where \hat{l}_z is substituted for z into equation (2), one arrives at the following:

$$\hat{V}_t = D_s(\hat{l}_z^2 - 2) + D_t\left(\frac{35}{12} \hat{l}_z^4 - \frac{155}{12} \hat{l}_z^2 + 6\right)$$

where D_s and D_t are each composed of a constant times the radial part of the spherical harmonics. The values of the parameters will of course be taken from the assignments of the spectral transitions. The choice of sign for the two parameters determines the stability of the orbitals (cf. Appendix VI). For example, if one chooses D_t to be negative this results in a stabilization of the axial orbital (d_z^2).

The effect of the tetragonal operator can be seen in Table 31 where the ordinary "d" orbitals have been operated upon.

Table 31

Effect of Tetragonal Operator on "d" Orbitals

$$\begin{aligned} \langle d_{\pm 2}^* | \hat{V}_t | d_{\pm 2} \rangle &= 2D_s + D_t \\ \langle d_{\pm 1}^* | \hat{V}_t | d_{\pm 1} \rangle &= -D_s - 4D_t \\ \langle d_o^* | \hat{V}_t | d_o \rangle &= -2D_s + 6D_t \end{aligned}$$

The last operator of interest for the systems under investigation is the spin-orbit operator. This operator has the form:

$$\hat{H}_\xi = \xi \hat{l} \cdot \hat{s}$$

It is easily shown (80) that this operator takes the following appearance:

$$\xi \hat{l} \cdot \hat{s} = \xi (\hat{l}_z \hat{s}_z + \frac{1}{2} \hat{l}_+ \hat{s}_- + \frac{1}{2} \hat{l}_- \hat{s}_+)$$

The operators \hat{l}_\pm & \hat{s}_\pm are the raising and lowering operators, i.e.,
 $\hat{l}_\pm \equiv \hat{l}_x \pm i \hat{l}_y$ & $\hat{s}_\pm \equiv \hat{s}_x \pm i \hat{s}_y$.

Now that the operators have been developed it is necessary to decide upon a set of wave functions to use. The ones chosen will be those given by Ballhausen (79) and reproduced in Table 32.

Table 32*

Wave Functions Used for Perturbation Calculations

$$\begin{aligned} \Gamma_8^a(e_g) &\equiv \Gamma_7^a(b_{1g}) = e_g^b \beta \\ \Gamma_8^b(e_g) &\equiv \Gamma_7^b(b_{1g}) = -e_g^b \alpha \\ \Gamma_8^c(e_g) &\equiv \Gamma_6^a(a_{1g}) = e_g^a \beta \\ \Gamma_8^d(e_g) &\equiv \Gamma_6^b(a_{1g}) = -e_g^a \alpha \\ \Gamma_7^a(t_{2g}) &\equiv \Gamma_7^a(b_{2g}) = \sqrt{1/3}(t_{2g}^0 \beta + \sqrt{2} t_{2g}^+ \alpha) \\ \Gamma_7^b(t_{2g}) &\equiv \Gamma_7^b(b_{2g}) = \sqrt{1/3}(-t_{2g}^0 \alpha + \sqrt{2} t_{2g}^- \beta) \\ \Gamma_8^a(t_{2g}) &\equiv \Gamma_7^a(e_g) = \sqrt{1/3}(-\sqrt{2} t_{2g}^0 \beta + t_{2g}^0 \alpha) \\ \Gamma_8^b(t_{2g}) &\equiv \Gamma_7^b(e_g) = \sqrt{1/3}(-\sqrt{2} t_{2g}^0 \alpha - t_{2g}^- \beta) \\ \Gamma_8^c(t_{2g}) &\equiv \Gamma_6^a(e_g) = t_{2g}^- \alpha \\ \Gamma_8^d(t_{2g}) &\equiv \Gamma_6^b(e_g) = -t_{2g}^+ \beta \end{aligned}$$

It will be seen later that the set that is chosen is not important as long as we have an orthonormal set to use as the basis functions.

* Cf. Appendix V for definitions of t_{2g} and e_g orbitals.

The effect of operating upon this set of wave functions with the spin-orbit operator is shown in Table 33.

Table 33

Results of Applying Spin-Orbit Operator

$$\begin{aligned} \hat{H}_\xi \Gamma_7^{a,b}(b_{1g}) &= \xi \sqrt{3/2} \Gamma_7^{a,b}(e_g) \\ \hat{H}_\xi \Gamma_6^{a,b}(a_{1g}) &= \xi \sqrt{3/2} \Gamma_6^{a,b}(e_g) \\ \hat{H}_\xi \Gamma_7^{a,b}(b_{2g}) &= \xi \Gamma_7^{a,b}(b_{2g}) \\ \hat{H}_\xi \Gamma_7^{a,b}(e_g) &= -\frac{1}{2}\xi \Gamma_7^{a,b}(e_g) + \sqrt{3/2} \xi \Gamma_7^{a,b}(b_{1g}) \\ \hat{H}_\xi \Gamma_6^{a,b}(e_g) &= -\frac{1}{2}\xi \Gamma_6^{a,b}(e_g) + \sqrt{3/2} \xi \Gamma_6^{a,b}(a_{1g}) \end{aligned}$$

Now, following the outlines of perturbation theory one must evaluate the secular determinant as shown in Figure 20.

From Figure 20 it is easily seen that the wave functions are not eigenfunctions of the operators that have been previously described. In the majority of crystal field treatments in the past symmetry arguments have been used to get a set of wave functions that were as close as possible to the eigenfunctions of the major perturbation and then ignore the off diagonal terms on the assumption that they were quite small. It is not necessary to follow that approach any longer. A diagonalization program written by H. Joy (82) was used that will diagonalize the secular determinant and calculate the correct wave functions and eigenstates, provided that one makes the correct assignments of the electron's transitions.

Once the spectral assignments are made there are several ways to check the "correctness" of the assignments. One way of checking

	$\Gamma_7(b_{1g})$	$\Gamma_7(b_{2g})$	$\Gamma_7(e_g)$	$\Gamma_6(a_{1g})$	$\Gamma_6(e_g)$
$\Gamma_7(b_{1g})$	$(6Dq+2D_s+D_t-E_1)$	0	$\sqrt{3/2} \xi$	0	0
$\Gamma_7(b_{2g})$	0	$(-4Dq-7/3D_t+\xi-E_2)$	$(-\sqrt{2}D_s-5/3\sqrt{2}D_t)$	0	0
$\Gamma_7(e_g)$	$\sqrt{3/2} \xi$	$(-\sqrt{2}D_s-5/3\sqrt{2}D_t)$	$(-4Dq+D_s-2/3D_t-\frac{1}{2}\xi-E_3)$	0	0
$\Gamma_6(a_{1g})$	0	0	0	$(6Dq-2D_s+6D_t-E_4)$	$\sqrt{3/2} \xi$
$\Gamma_6(e_g)$	0	0	0	$\sqrt{3/2} \xi$	$(-4Dq-D_s-4D_t-\frac{1}{2}\xi-E_5)$

Figure 20. Secular Determinant From First Order Perturbation Theory

involves the use of polarized light and certain selection rules to eliminate specific assignments for a selected transition.

The transitions of interest are the electric dipole transitions. It has been concluded that any other type of transition is much less intense, e.g., quadrupole or magnetic dipole transitions are much weaker (83). One must therefore investigate the following type of intensity integral,

$$I \propto \int \psi' \mu \psi d\tau$$

where I is the intensity of the transition, ψ' is the wave function of the excited state, ψ is the wave function of the ground state, and μ is the operator corresponding to the vector sum of the three classical components of an electric dipole (84). To investigate the polarized spectrum one may split the intensity integral into its components.

$$I_x \propto \int \psi' x \psi d\tau$$

$$I_y \propto \int \psi' y \psi d\tau$$

$$I_z \propto \int \psi' z \psi d\tau$$

The model that has been assumed is D_{4h} symmetry (the correctness of the model will be argued later). This means that the "d-d" transitions are occurring in a complex that possesses a center of symmetry. All states arising from such a centrosymmetric complex involving the "d" orbitals will be symmetrical with respect to the inversion center (i.e., they will be "g" states). One can see that this results in the intensity integral being zero.

$$\int \psi' (x, y, z) \psi d\tau = \int g u g d\tau = 0$$

Obviously some other mechanism must be invoked to explain the

weak but observed intensities of the centrosymmetric "d-d" transitions. The effects of vibronic coupling (84) will serve as the requisite rationalization. This mechanism involves the complete wave function being written as the product of a vibrational wave function and an electronic wave function, viz.

$$\psi' = (\psi_v \psi_e)'$$
 and $\psi = (\psi_v \psi_e)$

and it is the following type of integral that must be investigated:

$$\int (\psi_v \psi_e)'(x,y,z) (\psi_v \psi_e) d\tau$$

This means that one must determine the vibration symmetry modes and see if the direct product of any of the vibrational modes with the excited and ground state wave functions contains the totally symmetric representation, i.e., does

$$\Gamma(\psi_v \psi_e)' \cdot \Gamma(x,y,z) \cdot \Gamma(\psi_v \psi_e) \text{ contain } A_{1g}$$

where Γ denotes the representation under the assumed symmetry.

Orienting the cartesian coordinate system as in Figure 21 it is shown in Appendix VIII that under D_{4h} symmetry the following selection rules result.

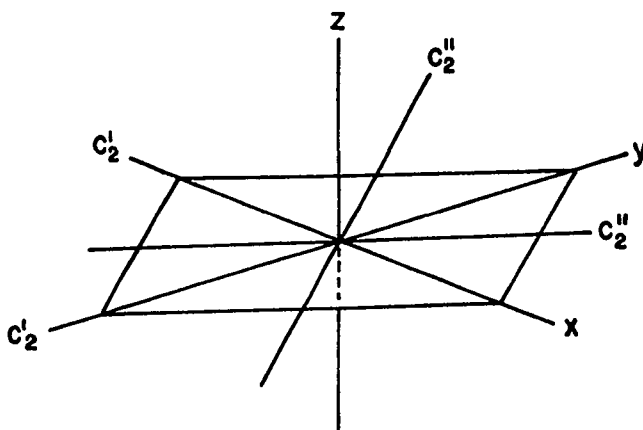


Figure 21. Orientation of Cartesian Coordinates for D_{4h} Symmetry

Table 34

Selection Rules Under D_{4h} Symmetry

z axis polarization	x or y axis polarization
$B_{1g} \rightarrow A_{1g}$ (allowed)	$B_{1g} \rightarrow A_{1g}$ (allowed)
$B_{1g} \rightarrow B_{2g}$ (forbidden)	$B_{1g} \rightarrow B_{2g}$ (allowed)
$B_{1g} \rightarrow E_g$ (allowed)	$B_{1g} \rightarrow E_g$ (allowed)

One can see from the above table that there are selection rules that should aid in the unequivocal assignment of the forbidden transition provided one has run a spectrum with the electric intensity vector of the incident beam parallel to and then perpendicular to the "z" axis.

Unfortunately there are other effects that enter such that the selection rules derived under D_{4h} symmetry do not explain the majority of the copper(II) spectra. There is obviously an anomaly when one considers the fact that under straight D_{4h} symmetry there are only three possible transitions, whereas in many of the reported copper(II) spectra where there is approximate D_{4h} symmetry one sees four transitions.

The way chosen to alleviate the problem is to consider the effects of spin-orbit coupling. This requires that one use "double-groups" to derive the selection rules (79). The double-group for D_{4h} symmetry will be denoted by D_{4h}' . Orienting the cartesian coordinate system as in Figure 22 one gets the selection rules shown in Table 35.

The difference in orientation of the axes in Figure 21 and Figure 22 may appear confusing. The two orientations were chosen because both are encountered in journals and it is instructive to consider

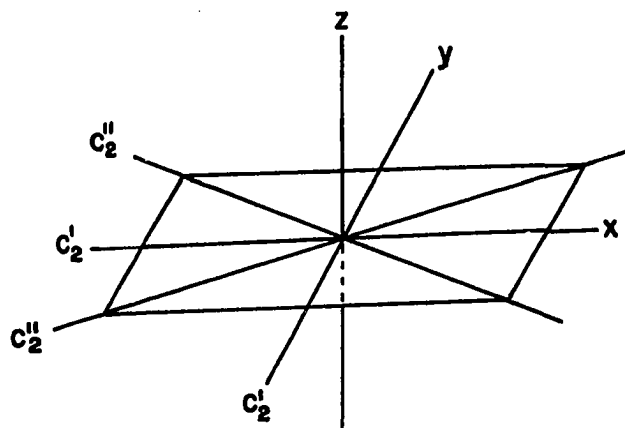


Figure 22. Orientation of Cartesian Coordinates for D'_{4h} Symmetry

Table 35

Selection Rules Under D'_{4h} Symmetry	
z axis polarization	x or y axis polarization
$\Gamma_7(xy) \rightarrow \Gamma_6(z^2)$ (allowed)	$\Gamma_7(xy) \rightarrow \Gamma_6(z^2)$ (allowed)
$\Gamma_7(xy) \rightarrow \Gamma_7(x^2-y^2)$ (allowed)	$\Gamma_7(xy) \rightarrow \Gamma_7(x^2-y^2)$ (allowed)
$\Gamma_7(xy) \rightarrow \Gamma_6(yz)$ (allowed)	$\Gamma_7(xy) \rightarrow \Gamma_6(yz)$ (allowed)
$\Gamma_7(xy) \rightarrow \Gamma_7(xz)$ (allowed)	$\Gamma_7(xy) \rightarrow \Gamma_7(xz)$ (allowed)

the differences between the two. The main difference for the purposes of this development is the symmetry of the ground state. With the axes oriented as in Figure 21 the ground state arises from the d_{xy} (b_{2g}) orbital. This of course makes no difference in the number of forbidden transitions, but appears at first glance to make a difference in the actual orbital jaunt taken by the electron (assuming a particular negative charge). This is of course incorrect since in either of the two orientations the electron is moving between the orbital that has its

lobes directed toward the ligands and some other orbital.

The orientation can make a difference when one is considering the effects of pi bonding, i.e., the molecular orbital formalism. With a d_{xy} ground state, the d_{xz} & d_{yz} orbitals are then available to pi bond because they are in the correct orientation. Such effects have been investigated recently by Billing, et al. (31).

Theory of Magnetic Susceptibility. The susceptibility will be calculated using the following equation (85):

$$(3) \quad \chi_i = N \left[\sum_{n,m} \frac{E_{o,m}^{(1)2}}{j_m kT} - 2 \sum_{n,m} \frac{E_{o,m}^{(2)}}{j_m} \right]$$

where

$$E_{o,m}^{(1)} = \langle \psi_{o,m} | \mu_i | \psi_{o,m} \rangle$$

and

$$E_{o,m}^{(2)} = \frac{\sum_{n,m} |\langle \psi_{o,m} | \mu_i | \psi_{n,m} \rangle|^2}{E_o - E_n}$$

with

$$\mu_i = \beta (\hat{L}_i + 2\hat{S}_i)$$

where j_m is the multiplicity of the ground state, β is the Bohr magneton, \hat{L}_i is the operator for the orbital angular momentum, and \hat{S}_i is the operator for the spin angular momentum.

The two assumptions that are made on the derivation of this equation are that the atom or molecule has a permanent moment and the perturbation matrix for the moment operator involves terms that are only "low or high" with respect to kT . The first assumption needs no amplification. At 300° K the value of kT is 210 cm^{-1} . The separation of the excited states from the ground state is $> 5000 \text{ cm}^{-1}$, so surely the second assumption is valid.

Using the equation for χ_i , a component parallel (χ_{\parallel}) and a

component perpendicular (χ_{\perp}) to the z axis can be calculated. Under D_{4h} symmetry the x and y components are equal and one can see the average susceptibility is given by:

$$(4) \quad \chi_{av} = \frac{\chi_{\parallel} + 2\chi_{\perp}}{3}$$

This "average" susceptibility should correspond to the susceptibility of a powdered sample.

Equation (3) applies in the following manner: For the L-phenylalanine and indazole complexes the original five-fold degeneracy of the "d" orbitals has been completely removed under the crystal field and spin-orbit coupling perturbations. However, the truth is that each of the five orbitals is a doublet due to the quantum number m_s . This final degeneracy can be removed by the presence of a magnetic field (Zeeman Effect). The summation over m in equation (3) is the summation over this spin degeneracy. The second summation is over the five levels present in the absence of a magnetic field. The assumption will be made that the off-diagonal terms in the secular determinant for the Zeeman perturbation will be negligible. This means effectively that only the three levels of Γ_7 symmetry will be considered in the over n, i.e., any element of the form $\langle \Gamma_7 | \mu_z | \Gamma_6 \rangle \approx 0$.

The resulting equation for the parallel component of susceptibility is:

$$(5) \quad \chi_{\parallel} = \frac{N\beta^2}{9kT} [6\sqrt{2} ab - 4\sqrt{6} ac + 3b^2 + 4\sqrt{3} bc - 3c^2]^2 + \frac{2N\beta^2}{9} \frac{[3\sqrt{2}(ba_1 + ab_1) - 2\sqrt{6}(ca_1 + c_1a) + 3bb_1 + 2\sqrt{3}(b_1c + bc_1) - 3cc_1]^2}{E_1 - E_0}$$

$$+ \frac{2N\beta^2}{9} \frac{[3\sqrt{2} (ba_2 + ab_2) - 2\sqrt{6} (ca_2 + c_2a) + 3bb_2 + 2\sqrt{3} (b_2c + bc_2) - 3cc_2]^2}{E_2 - E_0}$$

where the ground state wave functions are:

$$\psi_{g.s.}^I = a\Gamma_7^a(e_g) + b\Gamma_7^a(b_{2g}) + c\Gamma_7^a(b_{1g})$$

$$\psi_{g.s.}^{II} = a\Gamma_7^b(e_g) - b\Gamma_7^b(b_{2g}) + c\Gamma_7^b(b_{1g})$$

and the excited state wave functions are of the same form except differing of course in the coefficients. The excited state coefficients have been subscripted in equation (5).

The perpendicular component is given by:

$$(6) \quad \chi_1 = \frac{N\beta^2}{9kT} [3\sqrt{2}ab - 3b^2 + \sqrt{6}ac + 2\sqrt{3}bc + 3c^2]^2$$

$$+ 2N \frac{\frac{\beta}{12} [-4aa_1 - 4\sqrt{2}(ab_1 + ba_1) + 10bb_1 - 4\sqrt{3}(bc_1 + cb_1) - 2\sqrt{6}(ac_1 + ca_1) - 6cc_1]}{E_1 - E_0}^2$$

$$+ 2N \frac{\frac{\beta}{12} [-4aa_2 - 4\sqrt{2}(ab_2 + ba_2) + 10bb_2 - 4\sqrt{3}(bc_2 + cb_2) - 2\sqrt{6}(ac_2 + ca_2) - 6cc_2]}{E_2 - E_0}^2$$

where the ground state wave functions are taken as a linear combination of the Γ_7^a 's and Γ_7^b 's, viz.:

$$\psi_{g.s.}^I = \frac{1}{\sqrt{2}} \{a\Gamma_7^a(e_g) + b\Gamma_7^a(b_{2g}) + c\Gamma_7^a(b_{1g}) + a\Gamma_7^b(e_g) - b\Gamma_7^b(b_{2g}) + c\Gamma_7^b(b_{1g})\}$$

$$\psi_{g.s.}^{II} = \frac{1}{\sqrt{2}} \{a\Gamma_7^a(e_g) + b\Gamma_7^a(b_{2g}) + c\Gamma_7^a(b_{1g}) - [a\Gamma_7^b(e_g) - b\Gamma_7^b(b_{2g}) + c\Gamma_7^b(b_{1g})]\}$$

The excited state wave functions take the same form once again with appropriate subscripts on the coefficients indicating the excited states.

For a discussion of the development of equation (5) and (6) consult Appendix X.

One should remember that the coefficients a , b , c , a_1 , etc. come from the diagonalization program of Dr. Joy (82), and are a result of the way in which the spectral assignment are made.

CHAPTER VI

CRYSTAL FIELD SPECTRA AND MAGNETIC SUSCEPTIBILITY OF FIVE COPPER(II) COMPLEXES

Spectra of Three Tetraammine Copper(II) Complexes. In order to examine the problems that might be encountered in the assignment of spectral transitions it was decided to investigate some of the published spectra. The ideal spectra would be polarized spectra of copper(II) where the copper is in a true D_{4h} environment and one could observe all four possible transitions under the assumed perturbations. This ideal is approached in several tetra-amminecopper(II) complexes described by Tomlinson, et al. (27). Three of their complexes were chosen for study on the criteria that the site symmetry is true D_{4h} as given by x-ray crystallographic determination, and the magnetic moments for the three complexes are given. In all three complexes the square planer tetra-amminecopper(II) unit is present. The three differ only in that the axial ligand is different, and the tetragonal distortion is different.

Table 36 lists the pertinent data for the complexes.

When one examines the polarized spectra of the three complexes it is seen that there is some question as to the position and number of transitions occurring around the $17,000 \text{ cm}^{-1}$ region. For example the authors make the comment that analysis of the xy polarized

Table 36

Ligand Distances and Magnetic Moments for Three

D_{4h} Copper(II) Complexes

Complex	Cu-N bond distances (Å)	Cu-axial bond distances	magnetic moment
$\text{Cu}(\text{NH}_3)_4(\text{NO}_2)_2$	1.99	N 2.65	1.84
$\text{Cu}(\text{NH}_3)_4(\text{SCN})_2$	2.08	S 3.00	1.81
$\text{Na}_4\text{Cu}(\text{NH}_3)_4\text{Cu}(\text{S}_2\text{O}_3)_2$	1.994	Cu 5.76	1.90

spectrum of the thiosulfate complex resulted in either a fit with a single band at $17,800 \text{ cm}^{-1}$ in the low-temperature spectrum or two bands at $17,400$ and $18,800 \text{ cm}^{-1}$. It was decided to apply the latter analysis and extend the idea to the NO_2 and SCN complexes, i.e., to assume that the transition in the $17,000 \text{ cm}^{-1}$ region could be resolved into two. When this is done one arrives at the correct number of transitions for the three complexes, viz., (four with some reservation about there being a transition in the $16,000 \text{ cm}^{-1}$ region for the S_2O_3 complex).

Two procedures were used to locate these transitions for the three complexes. The first procedure is as follows: The highest energy transition was taken as the maximum of the low-temperature, z polarized curve. The next transition was taken as the maximum of the high-temperature, xy polarized curve. The third most energetic transition was estimated as being at $16,000 \text{ cm}^{-1}$. The lowest energy transition was taken as the maximum of the high-temperature, z polarized curve. The second procedure is as follows: The two high energy transitions were

estimated by taking the value of the maximum for the high-temperature, xy polarized curve and adding 1000 cm^{-1} to it to obtain the most energetic transition, and then subtracting 400 cm^{-1} from the maximum to obtain the second most energetic transition. (This was done as a result of the previously discussed suggestion that the analysis of the xy polarized spectrum of the thiosulfate complex which has a maximum at $17,000 \text{ cm}^{-1}$ can be fit with two bands located at $17,400$ and $18,800 \text{ cm}^{-1}$.) The third most energetic transition was estimated as being at $16,000 \text{ cm}^{-1}$. The lowest energy transition was taken as the maximum of the high-temperature, z polarized curve. The reason for fixing a transition at $16,000 \text{ cm}^{-1}$ is that there appears to be a transition in this region for the three complexes, the exact position of which is difficult to locate, and several trial assignments were made which indicated that the transition always came out as being the $\text{dx}^2\text{-y}^2 \rightarrow \text{dxy}$ transition. The xy orbital should be little affected by axial elongation, and therefore the energy difference between the $\text{x}^2\text{-y}^2$ orbitals should remain essentially constant for the three complexes. This value was therefore assigned to all three complexes.

One can argue against placing four transitions in the visible region for these complexes. To refute this argument one might look at the bis(diethylenetriamine)copper(II) bromide monohydrate complex (30) where the copper atom is surrounded by six nitrogens having approximately $\text{D}_{4\text{h}}$ symmetry. Four transitions are observed ($8.8, 9.9, 15.2, 15.9 \text{ kK}^*$). The $\text{D}_{4\text{h}}$ pseudosymmetry yields an in-plane average distance of 2.07 \AA and

* $\text{kK} = \text{cm}^{-1} \times 10^{-3}$

an average axial distance of 2.40 Å. It is logical that in the tetrammine complexes where the axial distance increases (e.g., to 2.65 Å as in the NO₂ complex) the splitting of the dz² and d_{x²-y²} orbitals will be more pronounced.

At this point in the spectral analysis all twenty-four ways of assigning the spectra were attempted for each of the three complexes using the diagonalization program of Joy. From this analysis there emerged only two feasible ways of ordering the orbitals. Explicitly this means that the calculated transitions agreed closely with the observed. The two ways of ordering the orbitals are presented in Table 37 along with the two ways of estimating the "observed" transitions and the calculated transitions.

Several things can be seen from Table 37. First, it is encouraging that the calculated magnetic susceptibility is in the proper range for all three complexes. The negative side of the situation is that the magnetic moment calculates in the proper range for both ways of assigning the transitions, and therefore cannot be used to eliminate either way.

Secondly, it is seen that both ways of assigning yield calculated energies that agree well with the "observed". The situation is more satisfying in the case where the ordering is xz>yz since upon examination of the spectra, peaks are actually observed, and no assumption is made about resolving a single transition into two transitions using the Dupont Curve resolver as Tomlinson, et al., did for Na₄Cu(NH₃)₄[Cu(S₂O₃)₂]₂.

Finally, one might examine the splitting parameters. The spin-

Table 37

Energy Level Ordering for Selected Copper(II) Complexes Having D_{4h} Symmetry

complex	energy level order	$Dq(\text{cm}^{-1})$	$Ds(\text{cm}^{-1})$	$Dt(\text{cm}^{-1})$	S.O. (cm^{-1})	obs. energies (kK)*	obs. μ (B.M.)
						calc. energies	calc. μ
$\text{Cu}(\text{NH}_3)_4(\text{NO}_2)_2$	$x^2-y^2 > z^2 > xy > xz > yz$	1625	2062	-1061	742	$\frac{17.8, 17.1, 16.0, 13.4}{17.7, 17.2, 16.0, 13.4}$	$\frac{1.84}{1.88}$
$\text{Cu}(\text{NH}_3)_4(\text{SCN})_2$	$x^2-y^2 > z^2 > xy > xz > yz$	1606	2282	-1056	585	$\frac{18.1, 17.5, 16.0, 14.3}{18.1, 17.5, 16.0, 14.3}$	$\frac{1.81}{1.85}$
$\text{Na}_4\text{Cu}(\text{NH}_3)_4$ $[\text{Cu}(\text{S}_2\text{O}_3)_2]_2$	$x^2-y^2 > z^2 > xy > xz > yz$	1610	2147	-1016	512	$\frac{17.8, 17.4, 16.0, 13.6}{17.8, 17.4, 16.0, 13.6}$	$\frac{1.90}{1.84}$
$\text{Cu}(\text{NH}_3)_4(\text{NO}_2)_2$	$x^2-y^2 > z^2 > xy > yz > xz$	1800	1685	-1352	513	$\frac{18.1, 16.7, 16.0, 13.4}{18.1, 16.7, 16.0, 13.4}$	$\frac{1.84}{1.83}$
$\text{Cu}(\text{NH}_3)_4(\text{SCN})_2$	$x^2-y^2 > z^2 > xy > yz > xz$	1834	1803	-1468	702	$\frac{18.5, 17.1, 16.0, 14.3}{18.5, 17.1, 16.0, 14.3}$	$\frac{1.81}{1.86}$
$\text{Na}_4\text{Cu}(\text{NH}_3)_4$ $[\text{Cu}(\text{S}_2\text{O}_3)_2]_2$	$x^2-y^2 > z^2 > xy > yz > xz$	1823	1707	-1390	683	$\frac{18.4, 17.0, 16.0, 13.6}{18.4, 17.0, 16.0, 13.6}$	$\frac{1.90}{1.86}$

* kK = $\text{cm}^{-1} \times 10^{-3}$

orbit coupling parameter is in the correct range for both orderings. The tetragonal parameters show the type of pattern that is suggested by Tomlinson, et al., in their publication, viz., as the tetragonality increases, Ds and Dt increase. (The anomalous complex, $\text{Na}_4\text{Cu}(\text{NH}_3)_4[\text{Cu}(\text{S}_2\text{O}_3)_2]_2$ is discussed in their article and rationalized on the basis of 35% of the negative charge in the d_{z^2} orbital being in the xy plane thereby allowing more interaction when there is actually no axial "bond".) The octahedral parameter is larger in both cases than ordinarily encountered. This last point makes one lean to the assignment with the smallest value for Dq. The increase of this parameter can be partially explained by the fact that the complete secular determinant is being used in the diagonalization program and off-diagonal terms will now be included in the parameter.

It should also be pointed out that the ordering with $d_{xz} > d_{yz}$ is the same as that given in the paper by Tomlinson, et al. They arrive at the ordering by using arguments about which vibrational mode activates the transitions for the different polarizations. For example, the statement is made that the appearance of only one band in the xy-polarization of high intensity and at high energy suggests its assignment as the $x^2 - y^2 \rightarrow xz, yz$ transition presumably activated by the A_{2u} or B_{2u} mode of vibration. If the E_u mode of vibration were the more active, two equally intense bands at different energies would be expected in this polarization. Such arguments are quite logical, and the ordering obtained by them should agree fairly closely with those obtained by the method of diagonalizing the perturbation matrix as used in this analysis. It is comforting that the agreement is present.

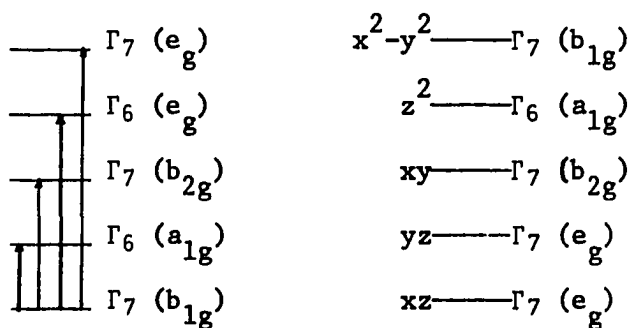
Spectrum of Bis(indazole)Copper(II) Chloride. The spectrum of bis(indazole)copper(II) chloride is shown in Figure 23. Upon close examination one can find four transitions. These are presented in Table 38 with calculated transitions from Dr. Joy's diagonalization program that were considered the most satisfactory.

Table 38

Calculated and Observed Transitions for
Bis(Indazole)Copper(II) Chloride

<u>Assignments</u>	<u>Observed (cm⁻¹)</u>	<u>Calculated (cm⁻¹)</u>
$\Gamma_7(b_{1g}) \rightarrow \Gamma_6(a_{1g})$	9,710	9,710
$\Gamma_7(b_{1g}) \rightarrow \Gamma_7(b_{2g})$	11,400	11,400
$\Gamma_7(b_{1g}) \rightarrow \Gamma_6(e_g)$	12,400	12,400
$\Gamma_7(b_{1g}) \rightarrow \Gamma_7(e_g)$	14,300	14,300

In order to obtain these calculated values the orbitals must be arranged as follows:



Energy Level Diagram Orbital Diagram

and it is seen that the lowest transition is the promotion of a positron from the $\Gamma_7(b_{1g})$ orbital to the $\Gamma_6(a_{1g})$ orbital, etc..

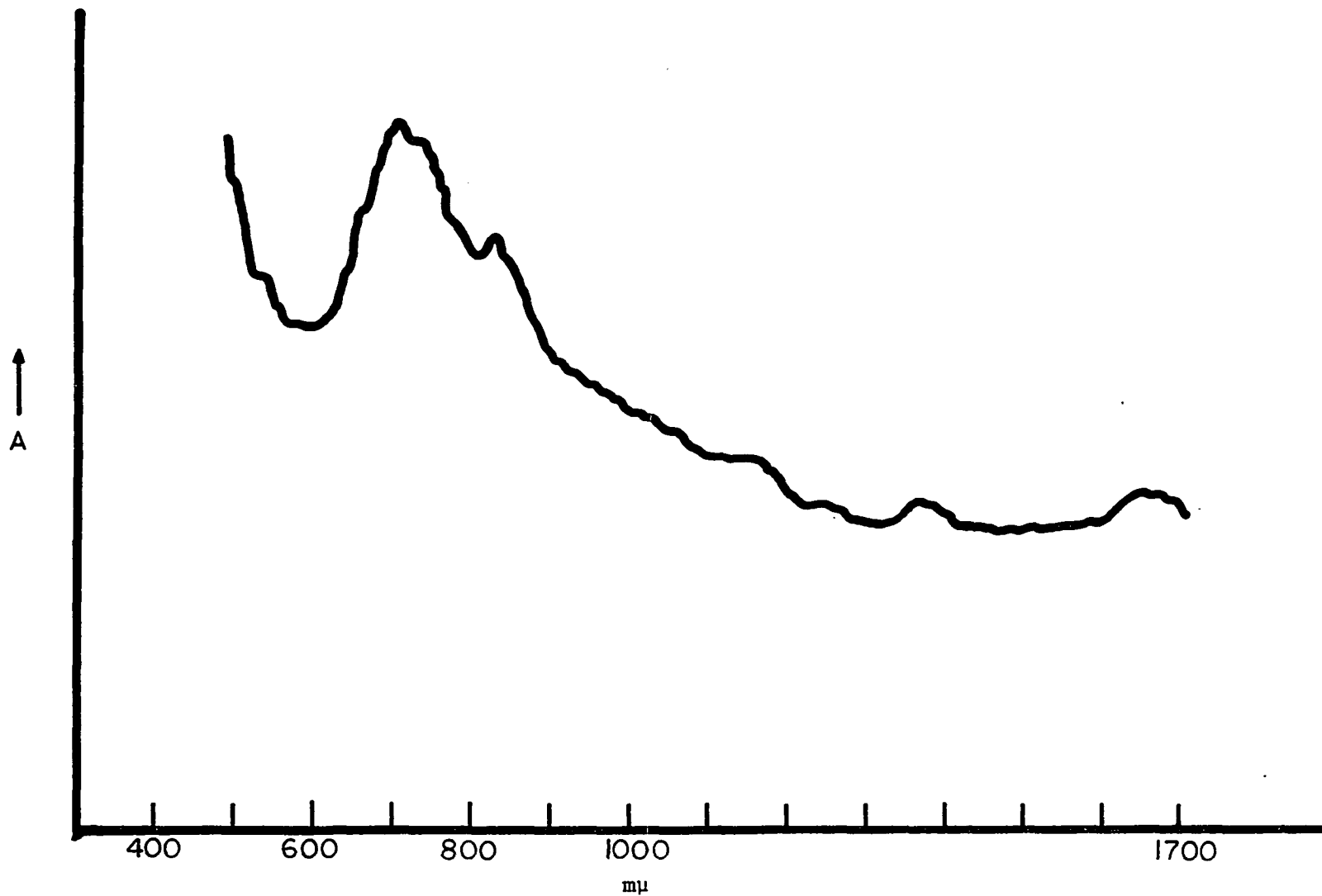


Figure 23. Spectrum of Bis(indazole)Copper(II) Chloride

There were twenty-four ways to order the energy levels. When this was done it was seen that there were only six ways that gave calculated transitions approximately equal to the observed transition. These are presented in Table 39.

One can eliminate the last three ways of assigning the spectrum on the basis of the magnetic moment calculations. One might quibble with the elimination of the fifth way of assigning due to the excellent spectral fit, but the elimination is reinforced by the high value for the spin-orbit coupling parameter and the low value of Dq . The free-ion value for the spin-orbit coupling parameter is 829 cm^{-1} (86). This is the maximum value that could be found for Cu^{2+} ions, and should be found only when copper is free from perturbation by an external potential. The magnetic moment criterion cannot differentiate between the first three ways of assigning the transition. The most satisfactory spectral fit is obtained by assigning the transitions the third way in Table 39.

This way of assigning the spectrum is considered satisfactory on the basis of five criteria: Most obviously, the calculated energies must agree with the observed transitions. Of the three ways considered having magnetic moments in the proper range the third assignment in Table 39 gives the closest agreement. Secondly, the value of the spin orbit coupling constant has been lowered below the free ion value of 829 cm^{-1} (86). It has been noted that the spin-orbit parameter decreases in complexes (87). This can be explained on the basis of charge transfer from the ligand to the central metal ion or in terms of delocalization of the d_z^2 and $d_{x^2-y^2}$ electrons to the ligands. The value of the coupling constant of the bis(indazole)copper(II) chloride agrees quite well with

Table 39

Comparison of Six Ways of Ordering Orbitals in Bis(indazole)copper(II) Chloride

	Ordering of orbitals	14300 cm ⁻¹	12400	11400	9710	magnetic moment B.M.	Dq	Ds	D _s	S.O.
1.	$x^2-y^2 > xy > z^2 > yz > xz$	14,300	12,500	10,600	10,400	1.86	1421	1234	-1461	508
2.	$x^2-y^2 > xy > xz > z^2 > yz$	14,300	12,000	11,800	9,700	1.88	971	2335	-962	462
3.	$x^2-y^2 > z^2 > xy > yz > xz$	14,300	12,400	11,400	9,710	1.89	1413	1079	-1124	663
4.	$x^2-y^2 > xy > yz > z^2 > xz$	14,300	11,000	11,600	10,900	1.77	1429	1175	-1363	150
5.	$x^2-y^2 > xy > z^2 > xz > yz$	14,300	12,400	11,400	9,710	2.08	975	2142	-757	1176
6.	$x^2-y^2 > z^2 > xy > xz > yz$	13,900	13,000	11,200	9,760	2.02	1147	1629	-715	1085

that reported for $[\text{Cu}(\text{H}_2\text{O})_6]^{2+}$ which is -695 cm^{-1} (88). The stereochemistry of the hexahydrate complex is very similar to the indazole complex, viz., a tetragonally distorted octahedron. An even more striking comparison can be made with the work of Gerritsen and Starr (15) where the spin-orbit parameter takes a value of -660 cm^{-1} . They studied Cu(II) in a TiO matrix where the copper was surrounded by six oxygen atoms in a tetragonally distorted octahedral configuration. The third criterion is to examine the signs attached to the tetragonal splitting parameters (cf. Appendix VI). It is seen with D_s positive and D_t negative there should be an elongation of the "z" axis bonds. This is exactly the case as demonstrated by the x-ray analysis (cf. Fig. 4). One may also compare the value of Dq obtained from the assignments and see if it is commensurate with previously reported work. The Dq value for copper-indazole is somewhat higher. Pappalardo (12) reports a value of 1120 cm^{-1} and McClure (89) cites a value of 1260 cm^{-1} for copper(II) hydrates. Gerritsen and Starr (15) report a value of 1510 cm^{-1} , but this is of little comfort due to the way in which they arrive at this value, viz., they assign the $d_{x^2-y^2} \rightarrow d_{xy}$ transition as the most energetic one. Once again the high value of Dq is partially explained on the basis of inclusion of off-diagonal terms in the perturbation matrix. When this is done one must realize that the Dq parameter is no longer simply an "octahedral" splitting parameter, but now has contained in it off-diagonal energy due to spin-orbit coupling. Finally it is quite satisfying to find that the calculated magnetic moment (1.89 B.M.) based on the wave functions does come within experimental error of the empirical value (1.84 B.M.).

Magnetic Susceptibility of Bis(indazole)Copper(II) Chloride.

The experimental susceptibility for bis(indazole)copper(II) chloride is shown in Table 40.

Table 40

Experimental Susceptibility of Bis(indazole)Copper(II) Chloride

T	$\chi_g^{\text{exp}} \times 10^6$	$(\chi_m^{\text{corr}})_1^{\text{exp}}$	$1/(\chi_m^{\text{corr}})_1^{\text{exp}}$
77.4	15.74	0.005920	168.9
194.2	5.865	0.002260	442.5
273.0	4.041	0.001584	631.3
299.3	3.671	0.001446	691.6

The value that is usually reported is the molar susceptibility (cf. Chapter 2). However this molar susceptibility must be corrected for any diamagnetic susceptibility due to the organic ligand and any temperature independent paramagnetism (TIP) arising from excited states. Once these two corrections are made one should find that a plot of $(1/\chi_m^{\text{corr}})_2$ vs T yields a straight line having a positive slope and a zero intercept.

$$(\chi_m^{\text{corr}})_2 = C/T$$

This is the well known law of Curie. A derivation of this law has been given by van Vleck (85):

$$(\chi_m^{\text{corr}})_2 = \frac{N_0 \mu^2 / 3k}{T}$$

where N_0 , and k have their usual values. μ is the magnetic moment in

Bohr Magnetons.

It is quite simple to correct the molar susceptibility for diamagnetism. One simply sums the diamagnetic contribution from each atom using the values of Pascal (87). The diamagnetic correction that had to be added to the copper-indazole susceptibility was 85.4×10^{-6} cgs units.

The way in which one arrives at a value for the TIP is more subtle. Before this is considered one other anomaly should be mentioned.

It is often found that the plot of $1/(\chi_m^{\text{CORR}})_2$ vs T does not yield a zero intercept. This has been explained on the basis of molecular dipole interaction. In the derivation of equation (8) the assumption was made that each molecular dipole is independent of any interaction with neighboring dipoles in the lattice. If one does not make this assumption then the non-zero intercept can be arrived at in an a priori fashion. The new law which includes this interaction is known as the Curie-Weiss law and has the form:

$$(\chi_m^{\text{CORR}})_2 = \frac{C}{T - \theta}$$

where θ is known as the Weiss constant.

In order to obtain a value for the Weiss constant one can make a plot of $1/(\chi_m^{\text{CORR}})_1$ vs. T (Fig. 24) where $(\chi_m^{\text{CORR}})_1$ is the molar susceptibility corrected only for diamagnetism. The intercept is then taken as the value of θ (90).

Using this θ value one can then find a value of the TIP by making a plot of $(\chi_m^{\text{CORR}})_1$ vs $1/(T-\theta)$ (Fig. 25) and evaluating the intercept.

Figure 24. T vs. $1/(x_m^{\text{corr}})_1$ for Bis(indazole)copper(II) Chloride

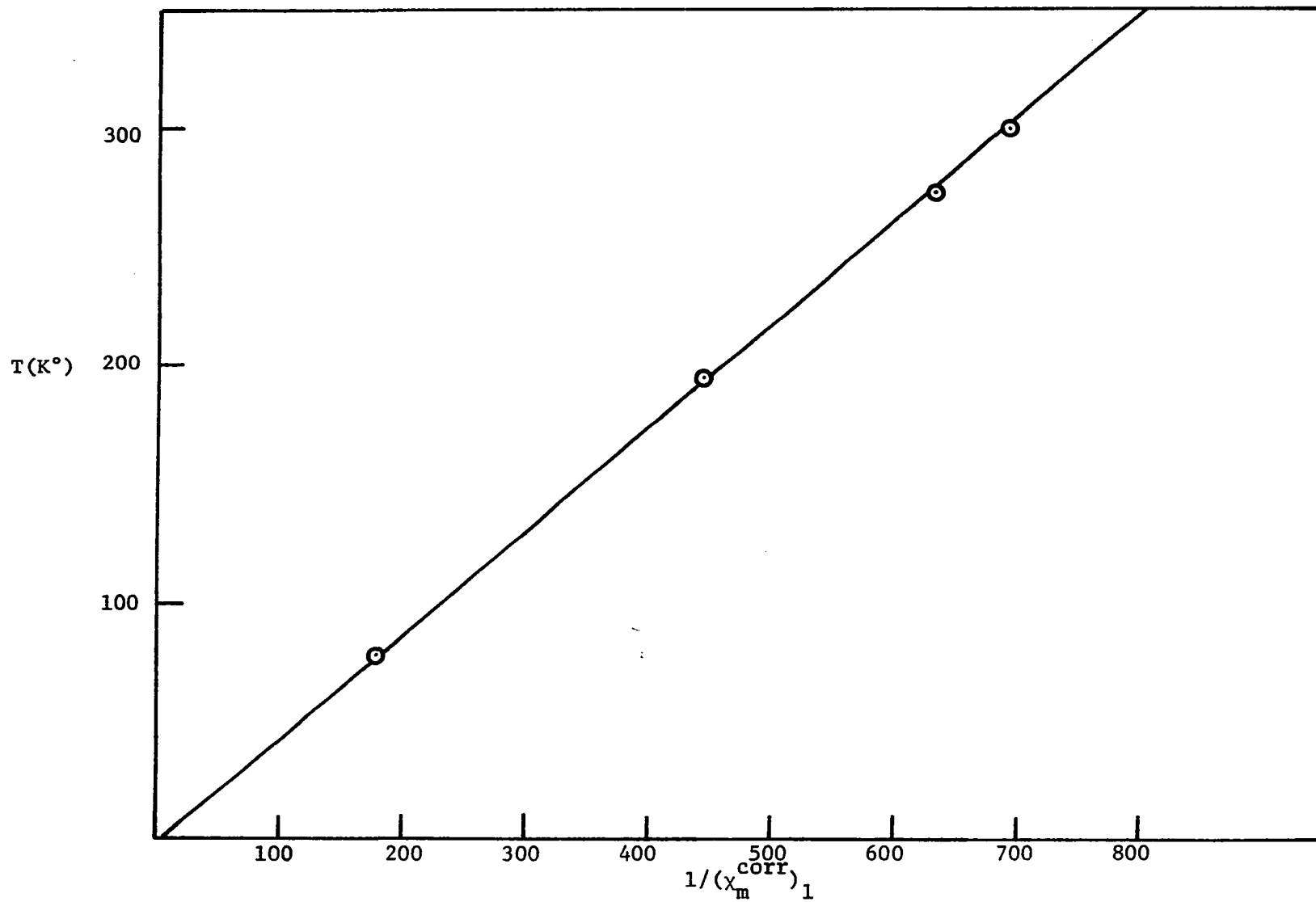
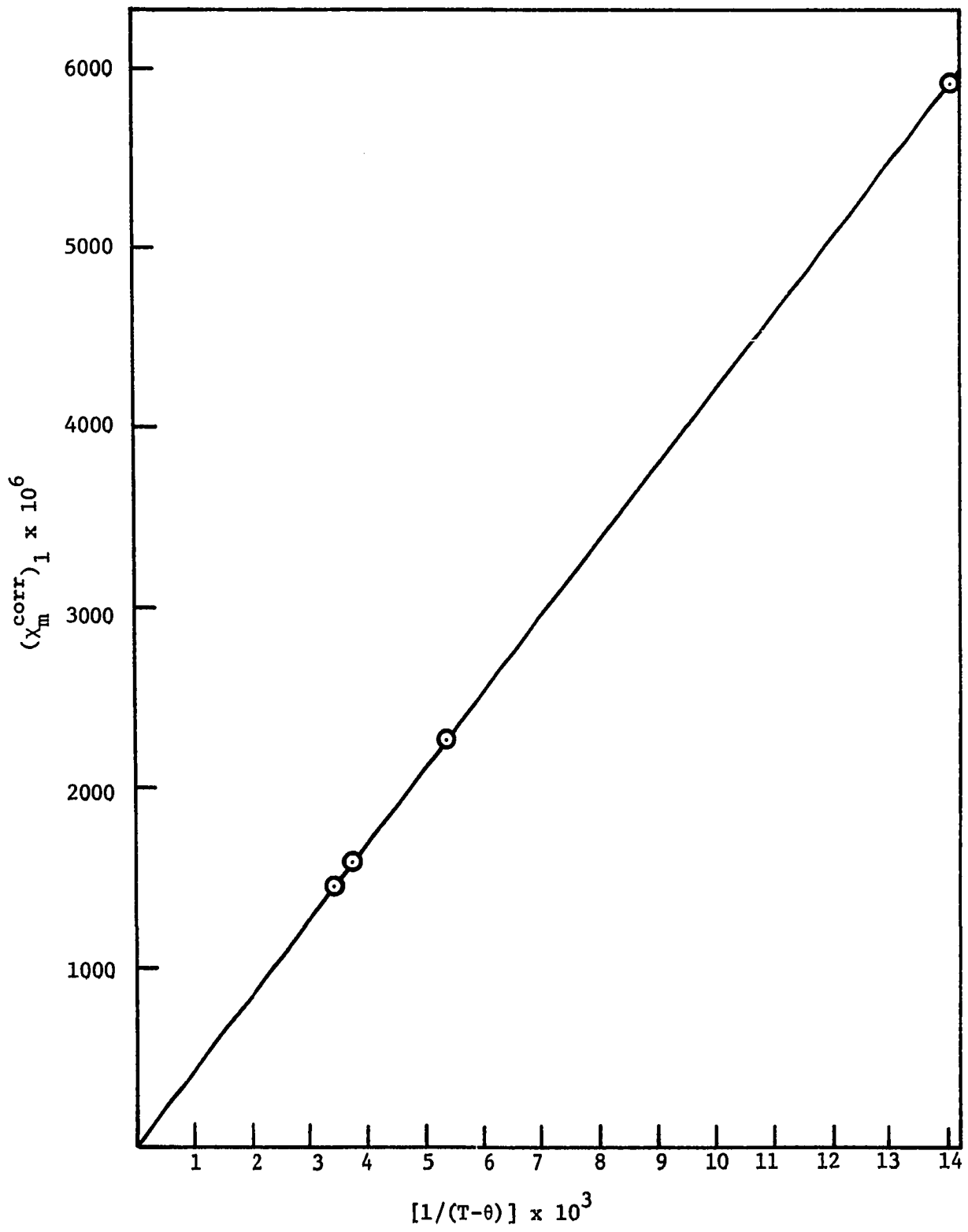


Figure 25. $(x_m^{\text{corr}})_1$ vs $[1/(T-\theta)]$ for Bis(indazole)copper(II) Chloride



The equation describing the experimental susceptibility is:

$$(10) \quad \chi_m = \frac{0.422}{T-\theta} + 9.54 \times 10^{-6}$$

with θ having a value of 6.05. Now using the wave functions given by Joy's diagonalization program:

$$\begin{aligned} \psi_{g.s.}^I &= 0.0592 \Gamma_7^a(e_g) + 0.0055 \Gamma_7^a(b_{2g}) + 0.9982 \Gamma_7^a(b_{1g}) \\ \psi_{e.s.\#1}^I &= 0.4256 \Gamma_7^a(e_g) + 0.9044 \Gamma_7^a(b_{2g}) - 0.0302 \Gamma_7^a(b_{1g}) \\ \psi_{e.s.\#2}^I &= 0.9030 \Gamma_7^a(e_g) - 0.4266 \Gamma_7^a(b_{2g}) - 0.0512 \Gamma_7^a(b_{1g}) \end{aligned}$$

one arrives at the following theoretical susceptibility equation

$$(11) \quad \chi_{av} = \frac{0.449}{T} + 65.9 \times 10^{-6}$$

using equations (4), (5), and (6).

Now comparing equation (8) with equation (9) and evaluating the constants one can write

$$C = \frac{\mu^2}{7.98}$$

and it is seen that once the slope for either equation (10) or equation (11) has been determined one has a way to calculate the magnetic moment of the compound. The theoretical moment is evaluated to be 1.89 B.M. This compares to the empirical moment of 1.84 B.M.

Figure 26 shows a plot of $(\chi_m^{corr})_2$ vs T for the experimental curve and the curve based on the spectral assignments. The agreement between the two curves is quite good (a maximum difference of 6% between the two over the experimental region) which lends credence to the assigned spectral transitions.

The error in the experimental curve has been estimated to be 0.07 B.M. based on the differential technique.

It is interesting to compare the 1:1 complex of cupric chloride

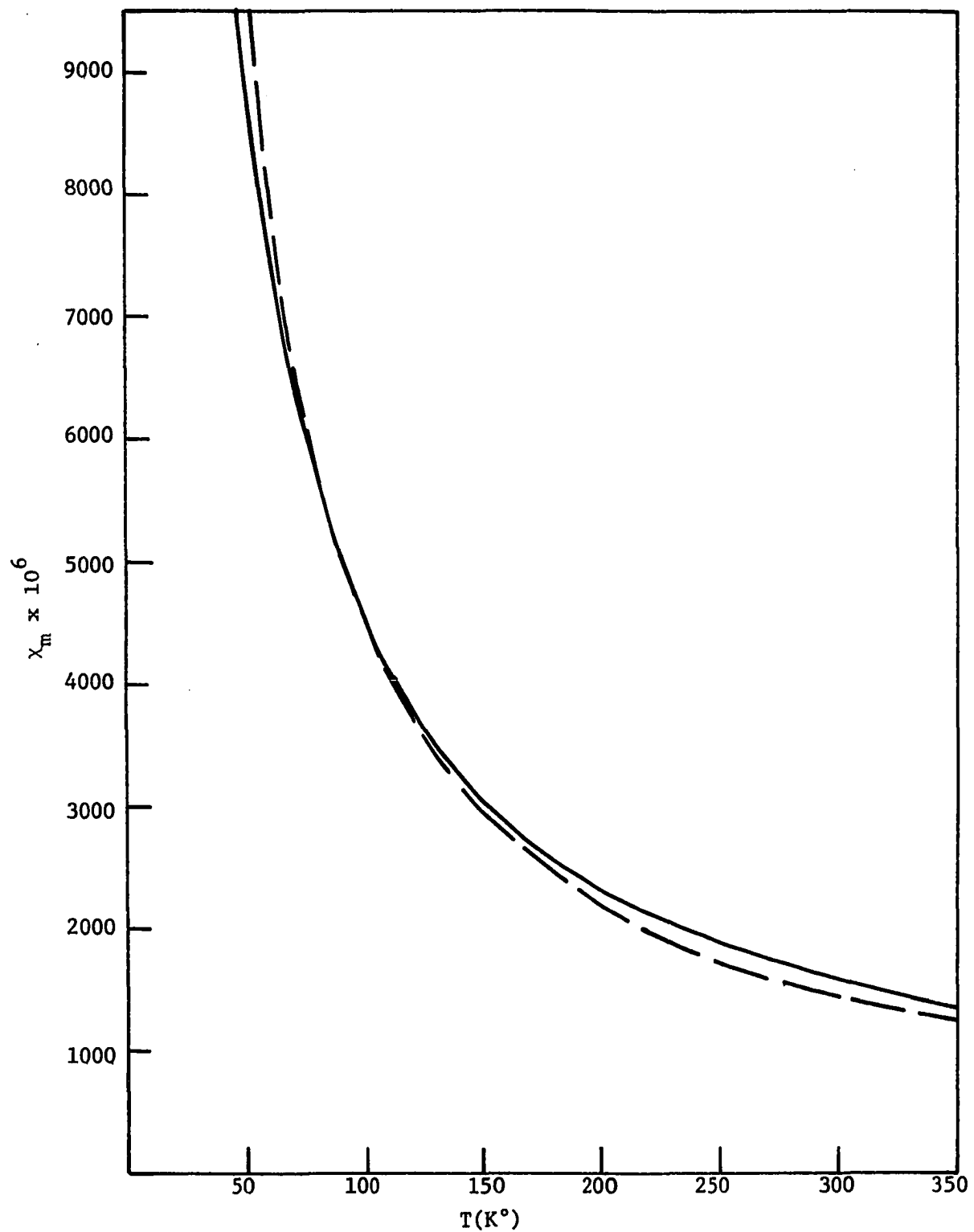


Figure 26. $(x_m^{\text{corr}})^2$ vs T for Bis(indazole)copper(II) Chloride;
Theoretical (—), Experimental (---).

with 1:2:4-triazole (69) and the bis(indazole)copper(II) chloride complex. The copper atom in the triazole complex is in a coordination environment very similar to the one found in the indazole complex as previously described in Chapter 4. The triazole complex is octahedrally coordinated with two nitrogen atoms at 1.98 Å, two Cl atoms at 2.34 Å, and two Cl atoms at 2.77 Å. These distances are comparable to those found in the indazole complex (cf. Fig. 15). Kubo, et al., (92) report the magnetic moment of the triazole complex as 1.81 B.M. The agreement of the two moments is quite satisfying.

The susceptibility determination as a whole compares with the majority of copper(II) susceptibilities (93) where there is no mechanism operating other than the perturbations already considered, i.e., the magnetic moment has been raised slightly above the spin only value of 1.73 B.M. due to spin-orbit coupling.

Spectrum of Bis(L-phenylalaninato)Copper(II). The spectrum of the bis(L-phenylalaninato)copper(II) complex is shown in Figure 27. The maximum is located at ca. 630 m μ , and the curve appears quite symmetrical. One can assume however that there are at least two transitions under this envelope when, for comparison, one examines the polarized spectrum of the bis(L-alaninato)copper(II) complex as given by Dijkgraaf (17). He reports that the absorption spectrum of the L-alanine complex is very similar to the L-phenylalanine complex. This idea of the similarity is reinforced upon examination of the x-ray crystal structure of bis(L-alaninato)copper(II) (48). The two structures are very similar. For example, the orientation of the octahedra in the unit cell is the same in both structures yielding the same type of distorted octahedral

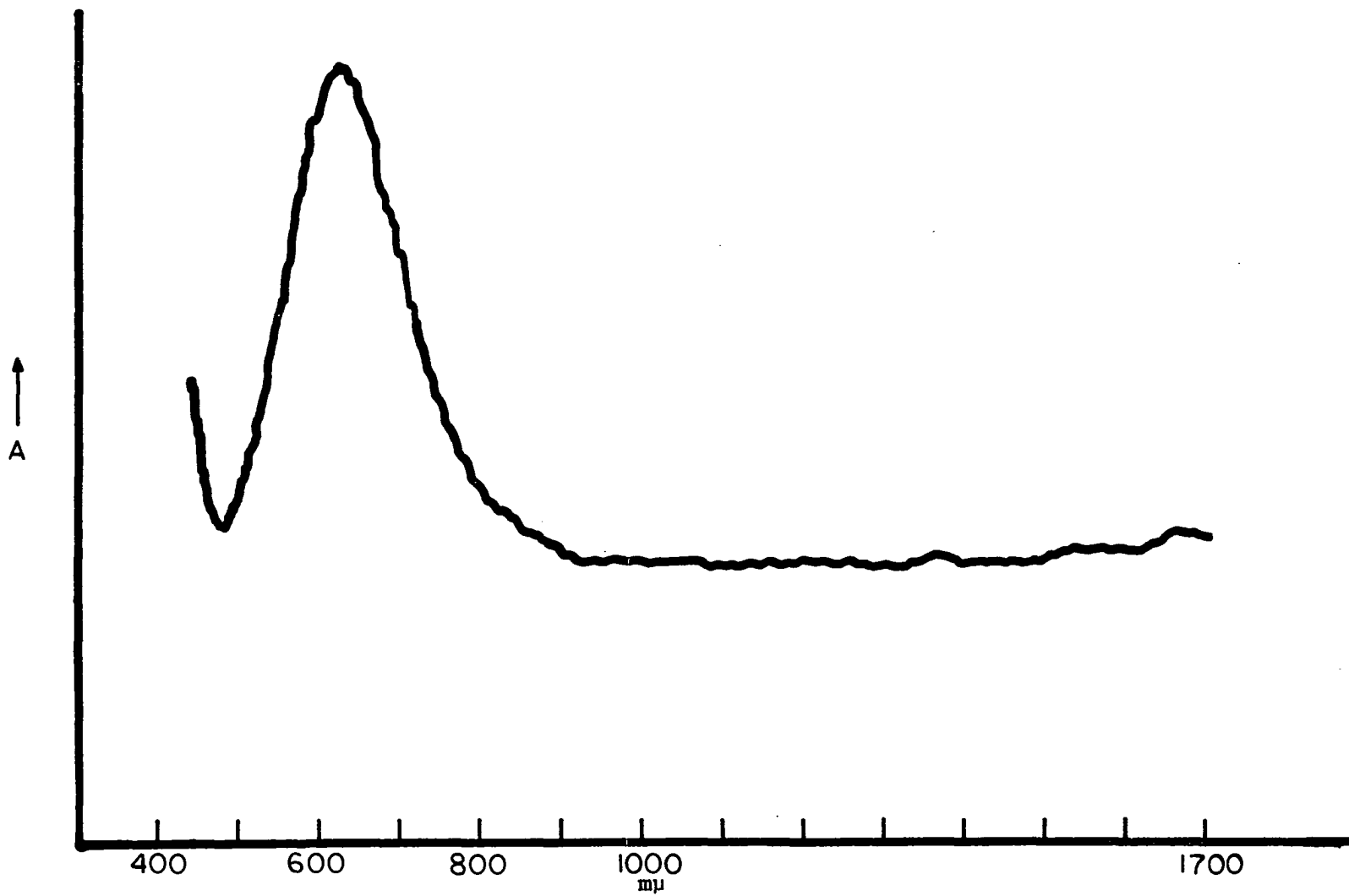


Figure 27. Spectrum of Bis(L-phenylalaninato)Copper(II)

coordination. Also the cell dimensions are almost identical in the "b" and "c" directions. They differ only in the respect that the "a" direction needs to be longer in the L-phenylalanine complex to accommodate the aromatic rings. It should be pointed out that the bond distances of the octahedra are also similar. A comparison of the distances is given in Table 41.

With the above facts one can use as a model for the L-phenylalanine complex the polarized spectrum of the L-alanine complex to study the ordering of the energy levels. In the discussion that follows this is what has been done. The spectrum and magnetic moment calculation are based on the bis(L-alanine)copper(II) complex. With this in mind, one can expect some variation in the calculated and observed magnetic moments. The variation should not be too severe, however, due to the structural similarity.

Table 41

Comparison of the Ligand-Copper Bond Lengths for
Bis(L-alaninato)Copper(II) and
Bis(L-phenylalaninato)Copper(II)

Copper to Ligand Bond Distances (Å)

ligand	N ₁	N ₂	O ₁	O ₂	O ₃	O ₄
bis(L-alaninato)copper(II)	2.01	2.02	1.97	1.96	2.70	2.90
bis(L-phenylalaninato)copper(II)	2.00	1.99	1.96	1.95	2.58	2.69

Before an analysis of the spectrum of the L-alanine complex is made a short digression must be taken.

A parameter describing the tetragonality has been defined by Tomlinson, et al., (27), viz., $T = R_s/R_l$ where R_s represents the four in-plane bond lengths and R_l the axial bond lengths. It is noted that both R_s and R_l increase for various ligands such that T is essentially constant for a large number of compounds investigated.

Calculating the tetragonality for the L-alanine-copper(II) complex by averaging the in-plane bonds and then the axial bonds yields a value of 0.71. This compares to a value of 0.80 for $\text{Cu}(\text{NH}_3)_4(\text{SCN})_2$ and 0.75 for $\text{Cu}(\text{NH}_3)_4(\text{NO}_2)_2$. On this basis one might expect that all four transitions of bis(L-alaninato)copper(II) are under the one envelope observed in the visible region since a successful analysis has been made for the tetramine complexes with this assumption.

One can then postulate transitions occurring at 15.4 kK and 17.7 kK in the polarized spectra given by Dijkgraaf. (This is not unreasonable upon close examination of the spectra.) These two transitions are in addition to the two transitions he demonstrates at 16.1 kK and 17.2 kK.

To further qualify the situation one might assume a value of -1600 cm^{-1} for Dq and -650 cm^{-1} for the spin-orbit coupling parameter analogous to the tetramine copper complexes, and vary D_s and D_t to see if the four transitions can be fit.

The four transitions were assigned all twenty-four different ways. Only two ways of assigning the transitions gave calculated transitions that fit what was assumed as the observed. These are shown in

Table 42 with the calculated magnetic moments based on the two ways of assigning.

It would be senseless to speculate on which of the two ways of ordering the levels is better due to the highly speculative nature by which Table 42 was derived. It is interesting to note however that it does appear possible to place all four transitions under the envelope in the visible region and have reasonable values for the splitting parameters and the calculated magnetic moment. It would be more satisfying had the observed magnetic moment of bis(L-phenylalaninato) copper(II) (2.07 B.M.) been in closer agreement with that calculated for the L-alanine complex using the previously described assumptions. Actually the calculated moment of 1.86 B.M. is commensurate with the vast majority of copper(II) complexes having normal moments. The observed value is at the very high end of acceptable moments for copper(II) complexes and may be suspect.

This interpretation of the bis(L-alaninato)copper(II) spectrum differs from that of Dijkgraaf in two ways. First the formalism used to explain the spectrum is different. Dijkgraaf uses the theory of molecular excitons to interpret the spectra. This consists of deriving selection rules based upon the crystal space group. Second, he insists upon there being only two transitions under the spectral envelope, whereas the analysis just presented requires four. The main point of contention arises in the number of transitions present. Reasonable arguments have been presented that demonstrate that it is quite possible for there to be four transitions in the visible region.

Table 42

Ordering of "d" Orbitals for Bis(L-alaninato)Copper(II)

complex	energy level order	Dq	Ds	Dt	SO	obs energies (kK)	Calc. μ (B.M.)
						calc energies (kK)	
bis(L-alaninato)copper(II)	$x^2 - y^2 > z^2 > xy > x^2 > yz$	1600	-2402	1207	650	<u>15.4, 16.1, 17.2, 17.7</u> 15.4, 15.8, 17.1, 17.8	1.86
"	$x^2 - y^2 > xy > z^2 > xz > yz$	1600	-2498	1299	650	<u>15.4, 16.1, 17.2, 17.7</u> 15.8, 16.0, 17.0, 17.8	1.86

Magnetic Susceptibility of Bis(L-phenylalaninato)Copper(II).

The paramagnetism of bis(L-phenylalaninato)copper(II) was treated the same way as described in the section treating the magnetic susceptibility for bis(indazole)copper(II) chloride. Table 43 contains experimental values for the gram and molar susceptibility for various temperatures.

Table 43

Magnetic Susceptibility of Bis(L-phenylalaninato)copper(II)

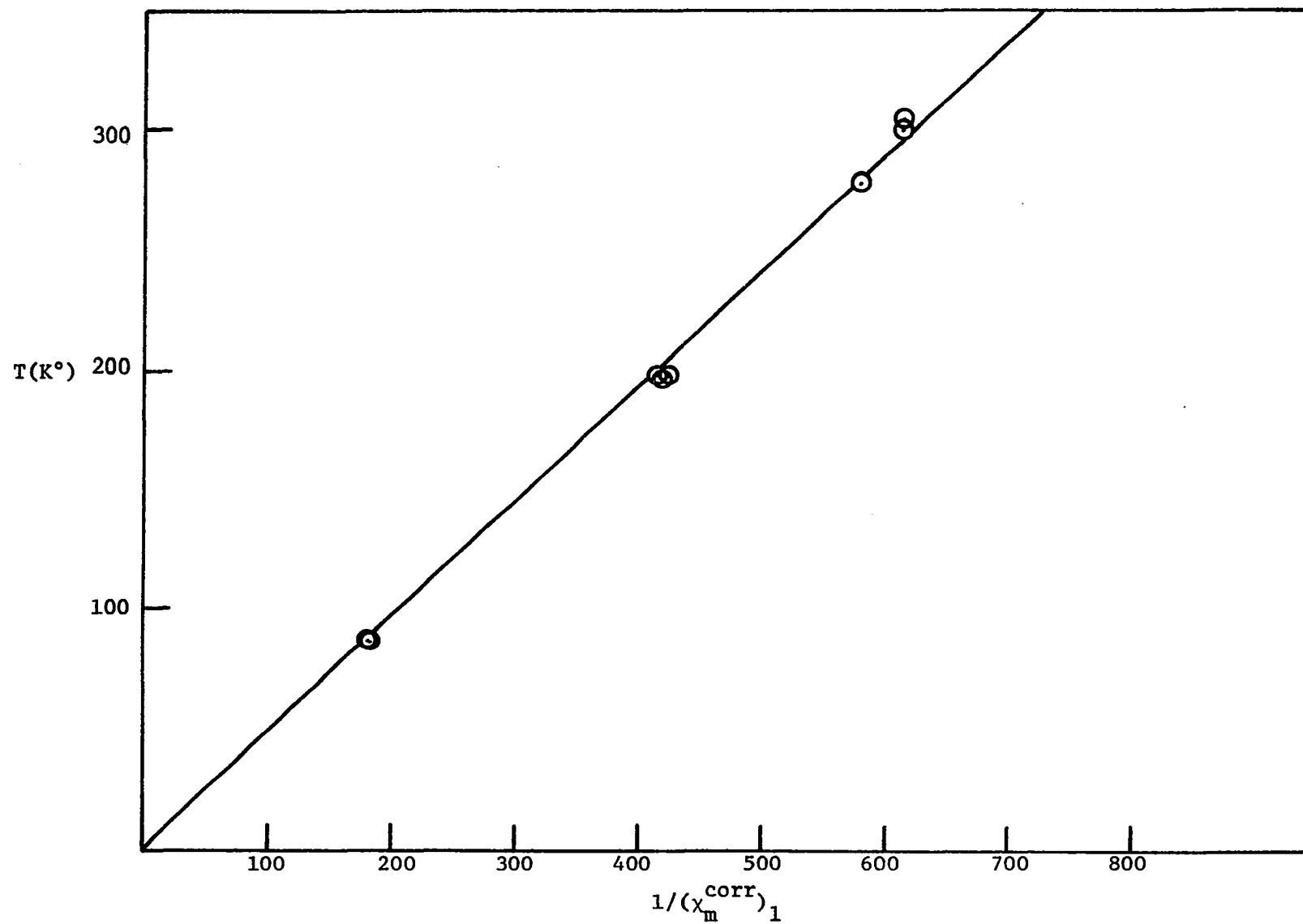
T	$\chi_g^{\text{exp}} \times 10^6$	$(\chi_m^{\text{corr}})_1$	$1/(\chi_m^{\text{corr}})_1$
77.26	13.75	0.005543	180.4
77.30	13.64	0.005500	181.8
194.08	5.737	0.002403	416.1
194.18	5.629	0.002360	423.7
194.21	5.759	0.002411	414.8
276.10	4.030	0.001734	576.7
299.10	3.785	0.001638	610.5
305.19	3.772	0.001633	612.4

Once again the molar susceptibility was corrected for diamagnetism using Pascal's constants. The diamagnetic correction was 155×10^{-6} cgs units.

Figure 28 shows a plot of $1/(\chi_m^{\text{corr}})_1$ vs T that was made to obtain the Weiss constant. Theta has a value of -18.92 for the bis(L-phenylalaninato)copper(II) complex.

Something is apparently wrong with the susceptibility determination. When one makes a plot of $(\chi_m^{\text{corr}})_1$ vs $1/(T-\theta)$ to evaluate the TIP

Figure 28. T vs $1/(\chi_m^{\text{corr}})_1$ for Bis(L-phenylalaninato)copper(II)



a negative value is obtained (Figure 29). The resulting equation for the molar susceptibility is:

$$(12) \quad \chi_m = \frac{0.539}{T-\theta} - 03.6 \times 10^{-6}$$

This essentially means I have managed to arrive at a diamagnetic paramagnetism for the TIP!

Utilizing the slope of equation (12) as before to evaluate the magnetic moment yields a value of 2.07 B.M. It is seen that this is at the very high extreme for acceptable values for copper(II) complexes. There may have been some systematic error in the determination of the susceptibility for this complex.

The wave function given by the diagonalization program for the first way of ordering the orbitals given in Table 42 are:

$$\begin{aligned} \psi_{g.s.}^I &= 0.0475 \Gamma_7^a(e_g) - 0.0016 \Gamma_7^a(b_{2g}) + 0.9989 \Gamma_7^a(b_{1g}) \\ \psi_{e.s.\#1}^I &= -0.5040 \Gamma_7^a(e_g) + 0.8633 \Gamma_7^a(b_{2g}) + 0.0254 \Gamma_7^a(b_{1g}) \\ \psi_{e.s.\#2}^I &= 0.8624 \Gamma_7^a(e_g) + 0.5047 \Gamma_7^a(b_{2g}) - 0.0402 \Gamma_7^a(b_{1g}) \end{aligned}$$

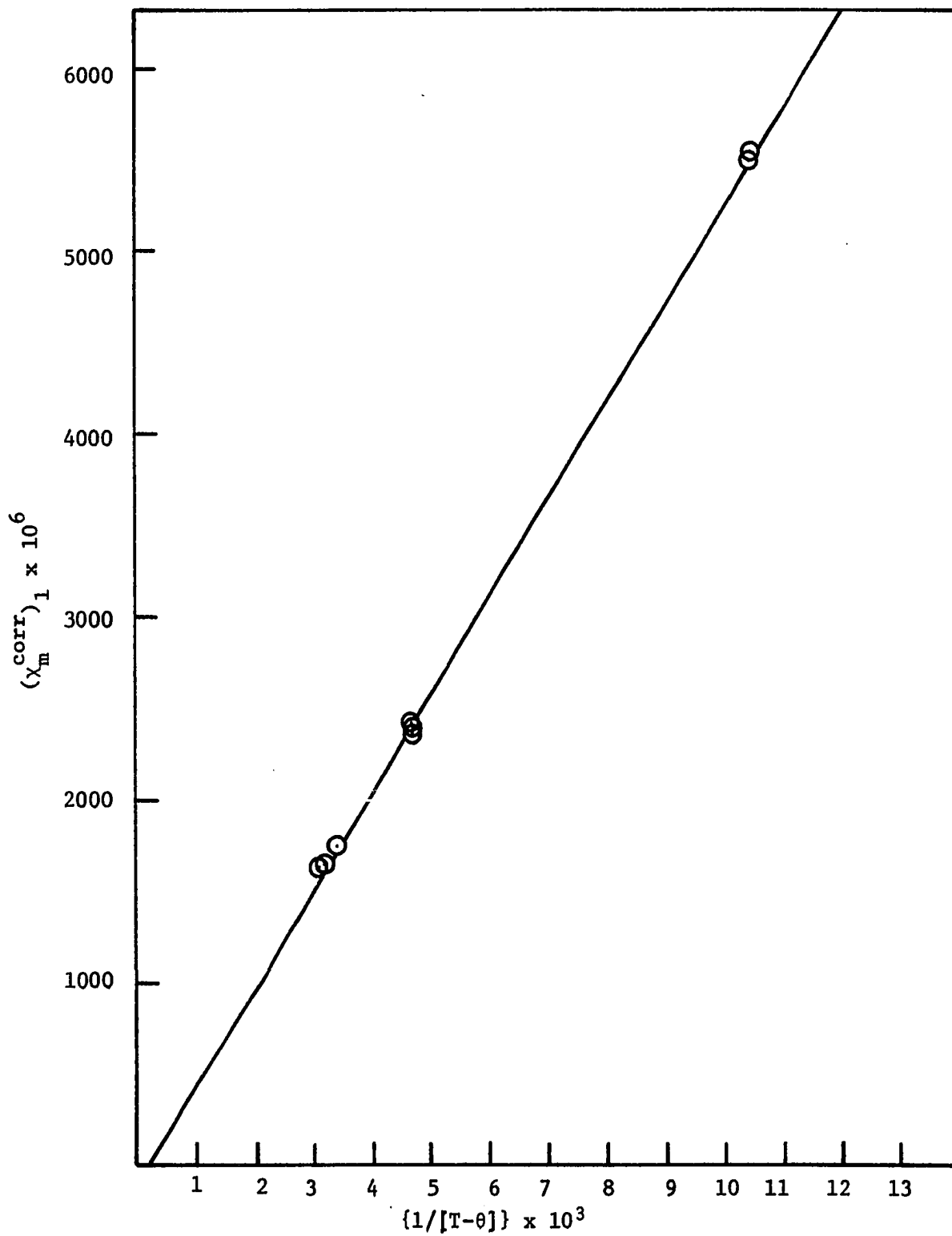
The following theoretical susceptibility equation results:

$$\chi_{av} = 0.435/T + 54.0 \times 10^{-6}$$

The wave functions given by the program for the second way of ordering the orbitals given in Table 42 are:

$$\begin{aligned} \psi_{g.s.}^I &= 0.0477 \Gamma_7^a(e_g) - 0.0014 \Gamma_7^a(b_{2g}) + 0.9989 \Gamma_7^a(b_{1g}) \\ \psi_{e.s.\#1}^I &= -0.4540 \Gamma_7^a(e_g) + 0.8907 \Gamma_7^a(b_{2g}) + 0.0229 \Gamma_7^a(b_{1g}) \\ \psi_{e.s.\#2}^I &= 0.8897 \Gamma_7^a(e_g) + 0.4546 \Gamma_7^a(b_{2g}) - 0.0418 \Gamma_7^a(b_{1g}) \end{aligned}$$

Figure 29. $(\chi_m^{corr})_1$ vs $1/(T-\theta)$ for Bis(L-phenylalaninato)copper(II)



This set of wave functions yields exactly the same equation as the other set of wave functions for the magnetic susceptibility.

Figure 30 shows a plot of $(\chi_m^{\text{corr}})_2$ vs T for the experimental curve and the theoretical curve based on the spectral assignments. The agreement between the two curves is seen to be worse than for the copper-indazole complex. Here a maximum difference of 12% occurs between the two curves over the experimental region.

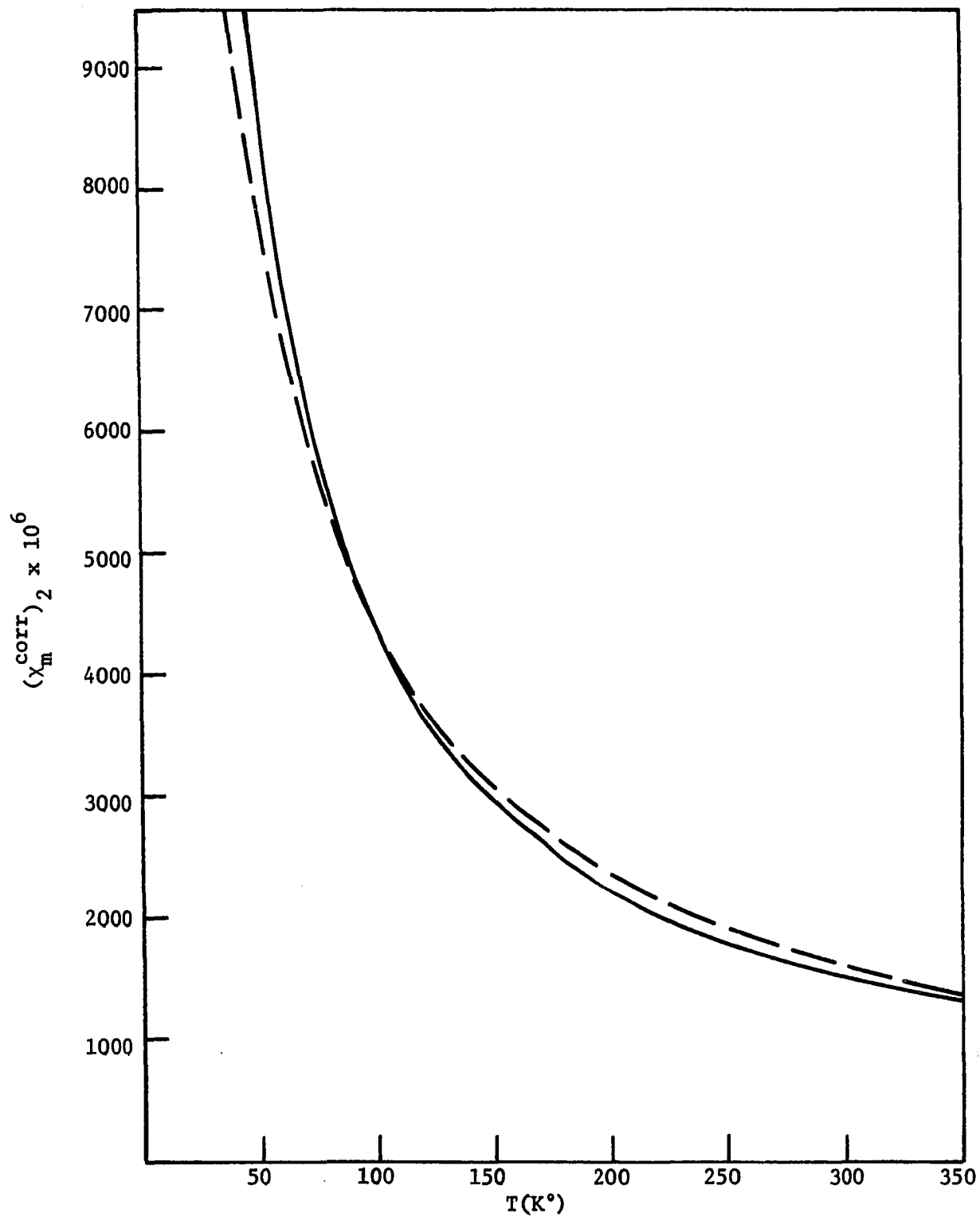


Figure 30. $(X_m^{corr})_2$ vs T for Bis(L-phenylalaninato)copper(II);
Theoretical (—), Experimental (---).

CHAPTER VII

SUMMARY AND CONCLUSIONS

Crystal Field Transitions. The ordering of the "d" orbitals in five copper(II) complexes has been discussed. An ordering has been arrived at on the basis of three criteria, the spectral curves in the visible region, the magnetic moments, and the structure of the complexes as given by x-ray analysis. Using a diagonalization program the off-diagonal terms in the first order perturbation matrix have been utilized to obtain wave functions comprised of a linear combination of the simple "d" orbitals. These wave functions were then used to calculate the magnetic moments from the Langevin-Debye formula.

In four of the five complexes examined there is nice agreement between the structure as given by x-ray analysis, that predicted on the basis of the spectrum, and the magnetic moment calculation. Unfortunately the magnetic moment calculation did not agree for the bis(L-phenylalaninato) copper(II) complex. When an examination of the assumptions that were made in getting the spectral assignments for the L-alanine complex is made, it is easily seen that variation between the calculated and observed moments is expected. However the variation is larger than it should be. One can say immediately that the experimental moment is not what it should be because of the negative value obtained for the

TIP. This value should be redetermined. Due to the relatively large error inherent in the available magnetic balance it was decided to postpone the measurement until better facilities became available.

In all of the spectra examined the salient feature was that the spectral assignments were made with all "d" to "d" orbital transitions appearing in the visible region. As was manifest in the introduction this point has caused controversy. It is concluded on the basis of the spectra examined herein and the spectral interpretations of various other authors (8, 9, 13, 19, 24, 25, 26, 27, 28, 29, 30, 31, 32) that the vast majority of octahedral copper complexes with tetragonal distortion have all four transitions occurring in the visible region. This idea is reinforced when one considers that for a great number of copper complexes the tetragonality as defined by Tomlinson, et al. (27) appears to remain essentially constant and independent of the ligand atom.

One question that arises is how sensitive the magnetic moment calculation is to various spectral assignments. To examine this problem several dummy transitions were assigned based on different values of the four parameters used in the perturbation matrix. Several trends are apparent.

The calculated magnetic moment decreases by approximately 0.02 B.M. for every 1000.0 cm^{-1} increase in Dq . The decrease is expected since the xy orbital is becoming farther removed from the x^2-y^2 and z^2 orbitals. The xy orbital can contribute significantly to the magnetic moment since rotation from the x^2-y^2 to the xy would enhance the orbital contribution.

As the spin-orbit coupling parameter decreases by 100.0 cm^{-1}

the magnetic moment decreases by 0.03 B.M. This is of course expected also since the spin-orbit coupling constant can be considered as a measure of the covalency of the bonds. As the covalency increases the orbital angular momentum would become smaller and hence a lowering of the magnetic moment would occur.

The program would not allow the variation of D_s and D_t while holding D_q and S.O. constant. What happens is that the relative positions of the xy and x^2-y^2 orbitals change in order to compensate for the changing D_s and D_t . The relative positions should change to a small extent since z axis elongation would produce a small contraction in the in-plane bond lengths, but there should be only a very small change. The program calculates a fairly large change in the opposite direction expected.

One can speculate about tetragonal distortion and its effect on the magnetic moment. As a result of the contraction above both the x^2-y^2 orbitals will be raised in energy, but the xy orbital will not be raised as much. Consequently the distance between these orbitals will increase, and the magnetic moment will decrease. This effect should be quite small, however, and will be only secondary in nature. Also as one increases the tetragonal distortion the xz orbital will become stabilized. This means a greater energy difference between the x^2-y^2 orbital and the xz orbital, and hence a lowering of the magnetic moment. It should be remembered that the xy , xz , and x^2-y^2 (Γ_7) orbitals are the ones that can mix according to the symmetry rules derived in the chapter treating the theory of magnetic susceptibility. The overall result of the two effects would be the lowering of the magnetic moment

for elongation.

The magnetic susceptibility equation yields a minimum magnetic moment calculation of 1.84 B.M. and a maximum moment of 2.2 B.M.. These figures were based on maximum and minimum reasonable values for the four parameters ($Dq = 1000$ to 17000 , $Ds = 0.0$ to 1750 , $Dt = 0.0$ to 1750 , and $SO = 850$ to 550 cm^{-1}).

Unfortunately the magnetic moment criterion is not as sensitive as one might desire. However as demonstrated for the bis(indazole) copper(II) chloride it can be used to eliminate some of the assignments. It is very comforting to have an equation that does take the major perturbations into consideration and does calculate very nearly the moment that was observed for the complexes examined.

Corrosion Inhibition. One of the interesting features mentioned in the introduction about the indazole molecule is its ability to prevent corrosion on copper surfaces. The original article (5) describing the ability examined five different aromatic compounds quite similar in structure. These are the first five compounds in Figure 31. Their tarnish resistance is indicated. The author of that paper suggests that it seems necessary to have the labile hydrogen and two nitrogens present to achieve resistance to corrosion. He further suggests the type of bonding demonstrated in Figure 32.

An alternate explanation of the situation is suggested by the bis(indazole)copper(II) chloride structure. It is possible that the only two conditions necessary for corrosive inhibition are the presence of one nitrogen capable of electron donation, and a planer

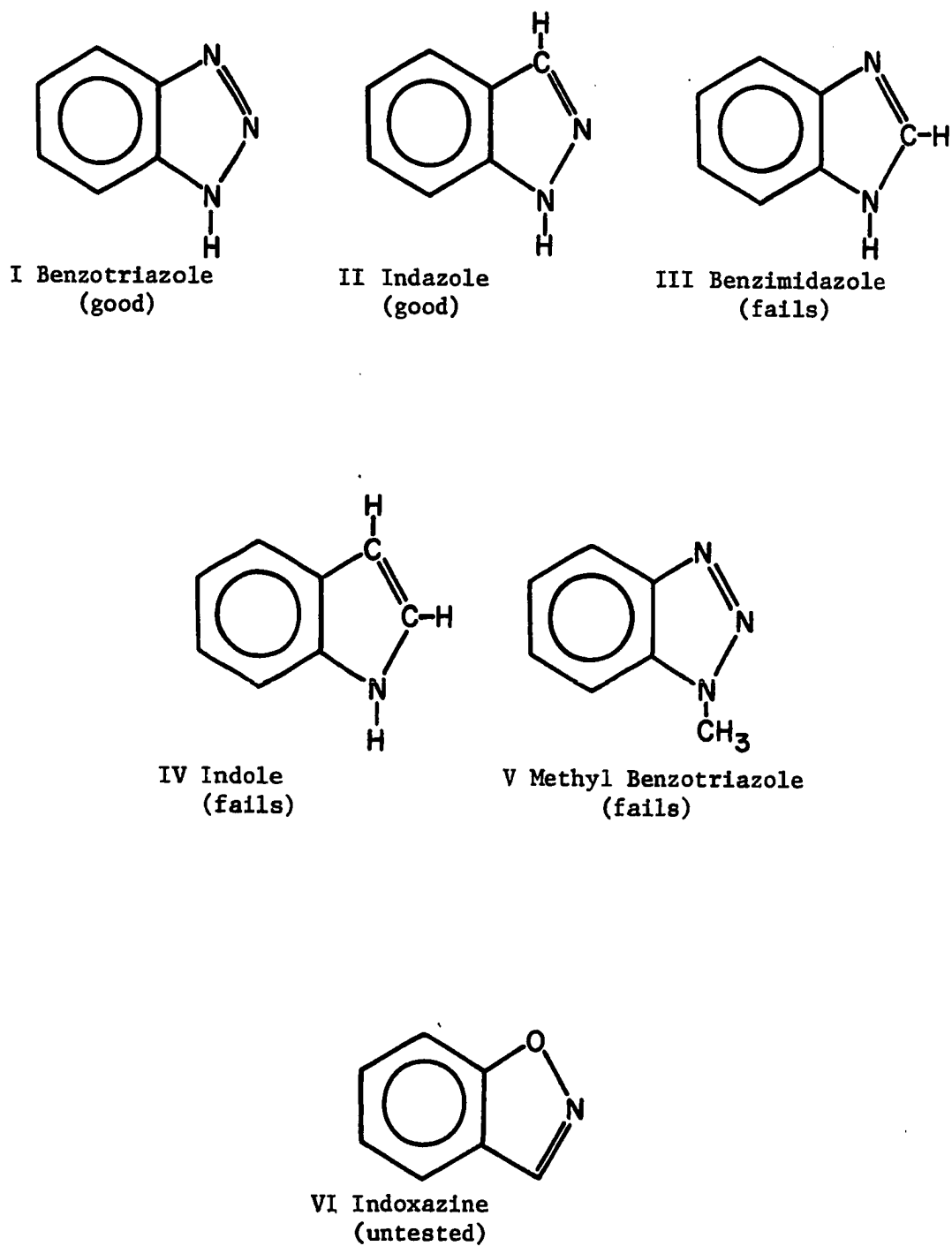


Figure 31. Compounds Conducive to Corrosion Control

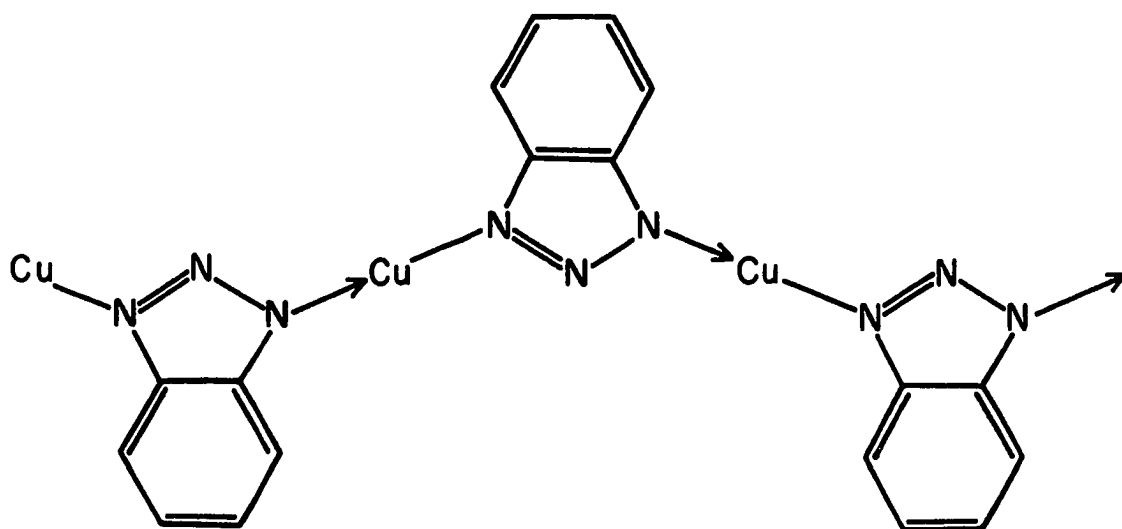


Figure 32. Mode of Bonding Proposed by Cotton (5)

molecule. One can imagine a surface where the indazole molecules are oriented like the bristles of a brush with the nitrogen donating electrons to copper. Such an arrangement allows very nice packing of the aromatic rings that could prevent foreign corrosive agents from approaching the copper surface. One can envision an "invisible protective shield" approximately 7 Å thick at the copper surface.

The inability of molecules like methylbenzotriazole (V) to prevent corrosion could occur because the packing is stereochemically hindered due to the bulky methyl group. Likewise the benzimidazole and indole molecules do not prevent corrosion because of the wrong position of the nitrogen atom. It would be instructive to examine the ability to prevent corrosion of compound VI in Figure 31.

Cu(II) - π Interaction. The aromatic ring in L-phenylalanine shows no interaction with copper(II). Evidently something else is needed for this type of interaction to occur. If the aromatic ring had some type of electron donating substituent attached it is possible that the ring might become electron rich and the interaction could occur. The hydroxyl substituent provides such a moiety when tyrosine is used as the complexing ligand. It is interesting to note that when attempts have been made to grow crystals of dihydroxy-L-phenylalanine complexed with copper(II) a rapid oxidation-reduction of the system occurred which resulted in a black residue in the bottom of the reaction vial (94). This is not inconsistent with the idea that making the aromatic ring electron rich could enhance a copper(II)-aromatic interaction.

APPENDIX I

REFLECTIONS USED IN DETERMINATION OF LEAST SQUARES CELL DIMENSIONS

(bis(L-phenylalaninato)copper(II))

h	k	l	2 θ	2 θ (obs)-2 θ (calc)	h	k	l	2 θ	2 θ (obs)-2 θ (calc)
0	1	-1	19.49	0.03	1	0	4	39.37	-0.10
1	1	-2	25.47	-0.02	1	1	5	52.85	0.09
2	1	-3	33.70	-0.05	3	1	5	56.94	0.17
7	1	-3	47.96	-0.03	5	1	4	53.65	-0.32
7	0	-2	40.20	0.06	9	1	1	55.29	0.08
3	2	-3	46.68	-0.06	3	1	3	39.14	0.06
6	1	-3	43.93	-0.09	0	1	3	33.32	-0.02
6	1	-2	39.34	-0.05	4	2	-1	41.29	-0.03
7	2	-1	52.05	-0.05	4	2	-2	44.10	0.13
9	1	-1	52.41	0.05	5	1	-5	55.32	-0.09
8	1	0	47.38	0.07	0	1	-4	42.19	0.05
0	1	5	51.67	0.03	5	1	-2	35.36	0.06
4	1	2	35.30	-0.09	2	2	-4	52.36	0.01
6	1	2	44.03	0.03	5	1	-3	40.49	-0.03
8	1	2	53.81	-0.13	4	1	-3	37.49	-0.08
7	1	1	44.55	0.13	5	1	-4	47.49	0.13
2	1	4	45.13	0.06	3	1	-4	43.26	0.07
5	1	2	39.39	-0.11	3	1	-5	51.98	-0.07
7	1	2	48.79	-0.04	1	1	-5	51.14	0.00
2	1	3	36.48	0.06	6	0	2	40.11	-0.16
4	1	3	42.44	0.10	8	2	2	62.70	-0.07
8	1	3	59.95	0.19					

APPENDIX II

REFLECTIONS USED IN DETERMINATION OF LEAST SQUARES CELL DIMENSIONS

Bis(indazole)copper(II) Chloride

h	k	l	2θ	2θ(obs)-2θ(calc)	h	k	l	2θ	2θ(obs)-2θ(calc)
-2	-1	1	36.15	-0.11	1	-1	2	50.68	0.12
-2	5	1	48.15	-0.01	-1	-7	1	51.50	-0.02
-1	-5	1	40.67	0.01	-1	-7	2	65.30	0.00
-2	-4	1	43.90	-0.38	-1	-6	1	45.90	0.04
-2	2	1	37.84	0.03	-1	-6	2	60.90	-0.05
-1	3	2	55.89	0.08	-1	-3	1	32.10	0.05
-1	5	1	43.16	-0.01	-2	-6	2	67.10	0.07
0	-4	1	32.28	0.08	-2	-6	1	53.40	0.02
0	5	0	31.69	0.11	-1	-2	1	29.15	0.11
1	-2	1	28.68	0.19	-2	-4	2	60.25	0.05
1	-3	1	30.77	-0.02	-3	-6	3	97.55	-0.02
3	0	0	41.59	0.04	-1	-2	2	50.44	0.08
1	1	1	30.02	0.17	-1	-2	3	76.33	-0.21
1	2	2	55.38	0.06	-3	-6	1	63.85	0.00
1	7	1	58.35	-0.04	-3	-6	2	76.15	-0.02
2	-3	1	38.65	0.00	-4	-8	1	87.20	-0.03
2	5	1	54.50	-0.02	-1	-1	1	27.36	0.12
3	1	1	51.08	-0.04	-1	-1	3	76.37	-0.04
4	-3	0	57.28	0.00	-2	-2	1	38.05	0.06
3	7	0	67.35	0.06	-3	-3	1	52.23	0.00
3	-5	1	54.10	-0.07	-3	-3	2	67.05	0.11
2	3	1	45.40	-0.04	-1	0	1	26.92	0.06

APPENDIX II (continued)

h	k	l	2 θ	2 θ (obs)-2 θ (calc)	h	k	l	2 θ	2 θ (obs)-2 θ (calc)
1	4	1	41.46	-0.03	-2	0	2	55.53	0.16
-1	0	2	50.07	0.09	-4	4	2	80.72	-0.06
-2	0	1	35.70	0.07	-2	2	3	83.81	-0.06
-4	0	2	75.48	0.02	-3	3	1	50.53	0.02
-3	0	2	64.10	0.05	-3	3	2	67.82	-0.03
-5	0	1	76.12	-0.03	-4	4	1	65.17	0.07
-1	1	0	14.30	0.12	1	-8	1	54.34	-0.06
-2	2	0	28.67	0.10	1	-8	2	67.91	-0.07
-3	3	0	43.52	0.07	1	-7	1	48.56	-0.05
-4	4	0	59.16	0.01	1	-7	2	63.35	-0.05
-5	5	0	76.13	-0.06	1	-6	1	43.32	0.08
-1	1	1	28.09	0.12	2	-12	2	95.18	0.23
-2	2	2	57.90	0.10	1	-6	2	59.51	0.08
-3	3	3	92.78	-0.14	1	-6	3	83.12	0.00
-1	1	3	78.19	-0.06	1	-5	1	38.40	0.01
1	-5	3	80.65	-0.01	2	-10	2	82.08	-0.14
1	-4	1	34.16	-0.01	1	-5	2	56.11	0.00
1	-4	2	53.63	0.13	2	-8	2	71.84	-0.13
2	-6	1	48.55	-0.10	2	-6	2	64.09	-0.05

APPENDIX V

SYMBOLISM USED FOR VARIOUS ORBITALS

Using the phase convention of Condon and Shortley (95) and dropping the common factors of $R(r)$ & $\sqrt{5/4\pi}$,

$$\begin{aligned} d_{\pm 2} &= Y_2^{\pm 2} = \sqrt{3/8} (x \pm iy)^2 \\ d_1 &= Y_2^1 = -\sqrt{3/2} (x + iy)z \\ d_0 &= Y_2^0 = \frac{1}{2} (3z^2 - r^2) \\ d_{-1} &= Y_2^{-1} = \sqrt{3/2} (x - iy)z \end{aligned}$$

where the Y_j^i are the angular part of the spherical harmonics. Other orbitals used in the text are:

$$\begin{aligned} t_{2g}^o &= \frac{1}{\sqrt{2}} (d_2 - d_{-2}) & t_{2g}^- &= d_{-1} & t_{2g}^+ &= d_1 \\ e_g^a &= d_0 & e_g^b &= (d_2 + d_{-2}) \end{aligned}$$

The real positive wave functions are sometimes used for convenience:

$$e_g \begin{cases} d_{x^2-y^2} &= \frac{1}{\sqrt{2}} (d_2 + d_{-2}) = \sqrt{\frac{3}{2}} (x^2 - y^2) \\ d_z^2 &= d_0 = \frac{1}{2} (3z^2 - r^2) \end{cases}$$

$$d_{xy} = -i \frac{(d_2 - d_{-2})}{\sqrt{2}} = \sqrt{3} (xy)$$

$$t_{2g} \quad d_{xz} = \frac{d_1 + d_{-1}}{\sqrt{2}} = \sqrt{3} (xz)$$

$$d_{yz} = -i \frac{(d_1 - d_{-1})}{\sqrt{2}} = \sqrt{3} (yz)$$

The notation Γ_7^+ is sometimes used in the text with a parenthetical expression following, e.g., $\Gamma_7^{+(xy)}$ or $\Gamma_7^+(b_{2g})$. The parenthetical quantity simply indicates from which orbital the "Γ" level arose. The superscript indicate the representation of the inversion center is positive.

APPENDIX VI

SIGN CHOICE FOR D_s AND D_t

Application of the Tetragonal Operator Upon the Set of "d" Orbitals

$$\begin{array}{l}
 \hat{l}_z^2 - 2 \\
 (35/12 \hat{l}_z^4 - 155/12 \hat{l}_z^2 + 6)
 \end{array}
 \left|
 \begin{array}{l}
 d_2 = 2d_2 \\
 d_1 = -d_1 \\
 d_0 = -2d_0 \\
 d_{-1} = -d_{-1} \\
 d_{-2} = 2d_{-2} \\
 \\
 d_2 = d_2 \\
 d_1 = -4d_1 \\
 d_0 = 6d_0 \\
 d_{-1} = -4d_{-1} \\
 d_{-2} = d_{-2}
 \end{array}
 \right.$$

One can construct the following type of table where the four possible choices of sign are attached to the tetragonal parameters and examine the effect on the d_z^2 , d_{xz} , d_{yz} , d_{xy} , & $d_{x^2-y^2}$ orbitals.

D_s	D_t	z axis effect	$\langle d_z^2 d_z^2 \rangle$	$\langle d_{xz} d_{xz} \rangle$	$\langle d_{yz} d_{yz} \rangle$	$\langle d_{xy} d_{xy} \rangle$	$\langle d_{x^2-y^2} d_{x^2-y^2} \rangle$
+	+	Elongation	$-2D_s + 6D_t$	$-D_s - 4D_t$	$-D_s - 4D_t$	$2D_s + 2D_t$	$2D_s + D_t$
-	+	Compression	$2D_s + 6D_t$	$D_s - 4D_t$	$D_s - 4D_t$	$-2D_s + D_t$	$-2D_s + D_t$
-	-	Compression	$2D_s - 6D_t$	$D_s + 4D_t$	$D_s + 4D_t$	$-2D_s - D_t$	$-2D_s - D_t$
+	-	Elongation	$-2D_s - 6D_t$	$-D_s + 4D_t$	$-D_s + 4D_t$	$2D_s - D_t$	$2D_s - D_t$

To get an approximate idea of what is going on, one can set D_t approximately equal to D_s (this is approximately true as found from several spectral analyses) and get the following table:

D_s	D_t	d_z^2	d_{xz}	d_{yz}	d_{xy}	$d_{x^2-y^2}$
+	+	$4D_t$	$-5D_t$	$-5D_t$	$3D_t$	$3D_t$
-	+	$8D_t$	$-3D_t$	$-3D_t$	$-D_t$	$-D_t$
-	-	$-4D_t$	$5D_t$	$5D_t$	$-3D_t$	$-3D_t$
+	-	$-8D_t$	$3D_t$	$3D_t$	D_t	D_t

One can see that the net effect on the orbitals containing no "z" component is zero, i.e., regardless of the sign of D_s or D_t the energy difference between the d_{xy} & $d_{x^2-y^2}$ orbitals remains the same. However if one simply scans horizontally the energies for the "+, +" case and the "+, -" case of the d_z^2 , d_{xz} , & d_{yz} orbitals a net negative energy is obtained. This is as it should be for stabilization of the orbitals with a "z" component when elongation occurs.

APPENDIX VII

EVALUATION OF THE a_{22} ELEMENT OF THE SECULAR DETERMINANT

The element a_{22} as given by perturbation theory is:

$$H'_{22} - E_2 = \langle \Gamma_7^*(b_{2g}) | \hat{V} + \hat{V}_t + \hat{H}_\xi | \Gamma_7(b_{2g}) \rangle - E_2$$

Now, considering the operators individually, and starting with the octahedral perturbation,

$$\begin{aligned} \langle \Gamma_7^*(b_{2g}) | \hat{V} | \Gamma_7(b_{2g}) \rangle &\equiv \langle \Gamma_7^*(b_{2g}) | | \Gamma_7(b_{2g}) \rangle = \\ \langle \sqrt{1/3} \{ \frac{1}{\sqrt{2}} (d_2^* - d_{-2}^*) \beta^* + \sqrt{2} d_1^* \alpha^* \} | | \sqrt{1/3} \{ \frac{1}{\sqrt{2}} (d_2 - d_{-2}) \beta + \sqrt{2} d_1 \alpha \} \rangle &= \\ \text{keeping in mind. } \langle \alpha^* | \alpha \rangle \text{ \& } \langle \beta^* | \beta \rangle = 1 \text{ whereas, } \langle \alpha^* | \beta \rangle \text{ \& } \langle \beta^* | \alpha \rangle = 0 & \\ \Rightarrow \quad 1/3 [1/2 \langle (d_2^* - d_{-2}^*) | | d_2 - d_{-2} \rangle + 2 \langle d_1^* | | d_1 \rangle] &= \\ 1/3 [1/2 (\langle d_2^* | | d_2 \rangle - \langle d_2^* | | d_{-2} \rangle - \langle d_{-2}^* | | d_2 \rangle + \langle d_{-2}^* | | d_{-2} \rangle) + 2 \langle d_1^* | | d_1 \rangle] & \end{aligned}$$

From Table 30

$$\begin{aligned} &= 1/3 [1/2 (D_q - 5D_q - 5D_q + D_q) + 2(-4D_q)] \\ &= -4D_q \end{aligned}$$

Now, consider the tetragonal operator:

$$\langle \Gamma_7(b_{2g}) | \hat{V}_t | \Gamma_7(b_{2g}) \rangle \equiv \langle \Gamma_7(b_{2g}) | | \Gamma_7(b_{2g}) \rangle =$$

$$\begin{aligned}
 & \left\langle \sqrt{1/3} \left[\frac{1}{\sqrt{2}} (d_2^* - d_{-2}^*) \beta + \sqrt{2} d_1^* \alpha \right] \middle| \middle| \sqrt{1/3} \left[\frac{1}{\sqrt{2}} (d_2 - d_{-2}) \beta + \sqrt{2} d_1 \alpha \right] \right\rangle = \\
 & 1/3 \left[\left\langle \frac{1}{\sqrt{2}} (d_2^* - d_{-2}^*) \beta^* \middle| \middle| \frac{1}{\sqrt{2}} (d_2 - d_{-2}) \beta \right\rangle + \left\langle \sqrt{2} d_1^* \alpha^* \middle| \middle| \sqrt{2} d_1 \alpha \right\rangle \right] = \\
 & 1/3 \left[1/2 \left\{ \langle d_2^* | | d_2 \rangle - \langle d_2^* | | d_{-2} \rangle - \langle d_{-2}^* | | d_2 \rangle + \langle d_{-2}^* | | d_{-2} \rangle \right\} + 2 \langle d_1^* | | d_1 \rangle \right] = \\
 & 1/3 \left[1/2 (2D_s + D_t + 2D_s + D_t) + 2(-D_s - 4D_t) \right] = -7/3 D_t
 \end{aligned}$$

The final perturbation is from spin-orbit coupling.

$$\begin{aligned}
 & \left\langle \Gamma_7^*(b_{2g}) \middle| H_\xi \middle| \Gamma_7(b_{2g}) \right\rangle = \left\langle \Gamma_7^*(b_{2g}) \middle| \xi \hat{l} \cdot \hat{s} \middle| \Gamma_7(b_{2g}) \right\rangle = \\
 & \left\langle \Gamma_7^*(b_{2g}) \middle| \xi \left(\hat{l}_z \hat{s}_z + 1/2 \hat{l}_+ \hat{s}_- + 1/2 \hat{l}_- \hat{s}_+ \right) \middle| \Gamma_7(b_{2g}) \right\rangle = \\
 & \xi \left[\left\langle \Gamma_7^*(b_{2g}) \middle| \hat{l}_z \hat{s}_z \middle| \Gamma_7(b_{2g}) \right\rangle + \left\langle \Gamma_7^*(b_{2g}) \middle| \frac{1}{2} \hat{l}_+ \hat{s}_- \middle| \Gamma_7(b_{2g}) \right\rangle + \left\langle \Gamma_7^*(b_{2g}) \middle| \frac{1}{2} \hat{l}_- \hat{s}_+ \middle| \Gamma_7(b_{2g}) \right\rangle \right]
 \end{aligned}$$

Now, evaluating each term separately

$$\begin{aligned}
 \left\langle \Gamma_7^*(b_{2g}) \middle| \hat{l}_z \hat{s}_z \middle| \Gamma_7(b_{2g}) \right\rangle &= \left\langle \Gamma_7^*(b_{2g}) \middle| \hat{l}_z \hat{s}_z \middle| \sqrt{1/3} \left(\frac{1}{\sqrt{2}} (d_2 - d_{-2}) \beta + \sqrt{2} d_1 \alpha \right) \right\rangle \\
 &= \left\langle \Gamma_7^*(b_{2g}) \middle| \sqrt{1/3} \left(-\frac{1}{\sqrt{2}} (d_2 \beta + d_{-2} \beta) + \frac{\sqrt{2}}{2} d_1 \alpha \right) \right\rangle
 \end{aligned}$$

also

$$\left\langle \Gamma_7^*(b_{2g}) \middle| 1/2 \hat{l}_+ \hat{s}_- \middle| \Gamma_7(b_{2g}) \right\rangle = \left\langle \Gamma_7^*(b_{2g}) \middle| \sqrt{1/3} (\sqrt{2} d_2 \beta) \right\rangle$$

$$\text{and } \left\langle \Gamma_7^*(b_{2g}) \middle| 1/2 \hat{l}_- \hat{s}_+ \middle| \Gamma_7(b_{2g}) \right\rangle = \left\langle \Gamma_7^*(b_{2g}) \middle| \sqrt{1/3} \frac{1}{\sqrt{2}} d_1 \alpha \right\rangle$$

summing the parts,

$$\xi \left[\left\langle \Gamma_7^*(b_{2g}) \middle| \frac{1}{\sqrt{3}} \left\{ -\frac{1}{\sqrt{2}} d_2 \beta - \frac{1}{\sqrt{2}} d_{-2} \beta + \frac{\sqrt{2}}{2} d_1 \alpha + \sqrt{2} d_2 \beta + \frac{1}{\sqrt{2}} d_1 \alpha \right\} \right\rangle \right]$$

$$\begin{aligned} &= \xi \left[\left\langle \Gamma_7^*(b_{2g}) \left| \frac{1}{\sqrt{3}} \left\{ \frac{1}{\sqrt{2}}(d_2\beta - d_{-2}\beta) + \sqrt{2} d_1\alpha \right\} \right\rangle \right] \\ &\equiv \xi \left\langle \Gamma_7^*(b_{2g}) \left| \Gamma_7(b_{2g}) \right\rangle \right] \\ &= \xi \end{aligned}$$

If all the perturbation energies are now summed it is seen

$$H'_{22} = -4D_q - 7/3 D_t + \xi$$

This completes the derivation for the a_{22} term in the secular determinant.

Similar calculations have to be done for each of the other elements in the secular determinant.

APPENDIX VIII

SELECTION RULES UNDER D_{4h} SYMMETRY

Using the orientation shown in Figure 21, the following intensity integrals result

$$\langle d_{x^2-y^2}^2 | (z) | d_z^2 \rangle = b_{1g} \cdot a_{2u} \cdot a_{1g} = b_{2u}$$

$$\langle d_{x^2-y^2}^2 | (x,y) | d_z^2 \rangle = b_{1g} \cdot e_u \cdot a_{1g} = e_u$$

$$\langle d_{x^2-y^2}^2 | (z) | d_{xy} \rangle = b_{1g} \cdot a_{2u} \cdot b_{2g} = a_{1u}$$

$$\langle d_{x^2-y^2}^2 | (x,y) | d_{xy} \rangle = b_{1g} \cdot e_u \cdot b_{2g} = e_u$$

$$\langle d_{x^2-y^2}^2 | (z) | (d_{xz}, d_{yz}) \rangle = b_{1g} \cdot a_{2u} \cdot e_g = e_u$$

$$\langle d_{x^2-y^2}^2 | (x,y) | (d_{xz}, d_{yz}) \rangle = b_{1g} e_u e_g = a_{1u} + a_{2u} + b_{1u} + b_{2u}$$

where the character table supplied by Cotton (84) has been used.

Now the vibrational symmetry modes are found to be:

$$\Gamma^{\text{vib}} = 2a_{1g} + b_{1g} + b_{2g} + e_g + 2a_{2u} + b_{2u} + 3e_u$$

It is seen that the vibrational representation contains no modes of a_{1u} symmetry. Therefore the transition $b_{1g} \rightarrow b_{2g}$ is not "vibronically" allowed as are the other transitions.

APPENDIX IX

SELECTION RULES UNDER D_{4h}' SYMMETRY

The character table supplied by Koster, et al. (96) was used for these selection rules. The real orbital from which these levels arise is denoted in parentheses, i.e., the " Γ_i^\pm " orbitals are linear combinations of the real orbitals but the probability coefficient in the linear combination is greatest for the parenthetical real orbital. For an explanation of the way of assigning the symmetry representation to a particular orbital see Ballhausen, p. 53 (79). (These orbitals are actually the direct product of the spin representation (Γ_6^+) and the cartesian representation, e.g., the xy orbital belongs to Γ_4^+ . Therefore $\Gamma_i^\pm(xy)$ is given by $\Gamma_6^+ \cdot \Gamma_4^+ = \Gamma_7^+(xy)$).

<u>Orbital</u>	<u>Symmetry</u>
xy	$\Gamma_7^+(xy)$
$x^2 - y^2$	$\Gamma_7^+(x^2 - y^2)$
z^2	$\Gamma_6^+(z^2)$
xz	$\Gamma_7^+(xz)$
yz	$\Gamma_6^+(yz)$

The following intensity integrals result.

$$\begin{aligned} \langle \Gamma_7^+(xy) | z | \Gamma_6^+ \rangle &= \Gamma_7^+ \cdot \Gamma_2^- \cdot \Gamma_6^+ = \Gamma_3^- + \Gamma_4^- + \Gamma_5^- \\ \langle \Gamma_7^+(xy) | x, y | \Gamma_6^+ \rangle &= \Gamma_7^+ \cdot \Gamma_5^- \cdot \Gamma_6^+ = \Gamma_1^- + \Gamma_2^- + \Gamma_3^- + \Gamma_4^- + 2\Gamma_5^- \\ \langle \Gamma_7^+(xy) | z | \Gamma_7^+ \rangle &= \Gamma_7^+ \cdot \Gamma_2^- \cdot \Gamma_7^+ = \Gamma_1^- + \Gamma_2^- + \Gamma_5^- \\ \langle \Gamma_7^+(xy) | x, y | \Gamma_7^+ \rangle &= \Gamma_7^+ \cdot \Gamma_5^- \cdot \Gamma_7^+ = \Gamma_1^- + \Gamma_2^- + \Gamma_3^- + \Gamma_4^- + 2\Gamma_5^- \end{aligned}$$

Keeping Figure 22 in mind³ the vibrational representation is given by:

$$\Gamma^{\text{vib}} = 2\Gamma_1^+ + \Gamma_3^+ + \Gamma_4^+ + \Gamma_5^+ + 2\Gamma_2^- + \Gamma_3^- + 3\Gamma_5^-$$

It is seen that all transitions are vibronically allowed, i.e., there is at least one direct product of each of the intensity integrals and one of the vibrational modes that results in the totally symmetric representation Γ_1^+ .

APPENDIX X

MATHEMATICAL DEVELOPMENT OF MAGNETIC SUSCEPTIBILITY EQUATIONS

$$\begin{aligned}\psi_{g.s.}^I &= a\Gamma_7^a(e_g) + b\Gamma_7^a(b_{2g}) + c\Gamma_7^a(b_{1g}) \\ &= a \left\{ \frac{1}{\sqrt{3}} [-(2-\underline{2})\beta + (1)\alpha] \right\} + b \left\{ \frac{1}{\sqrt{6}} [(2-\underline{2})\beta + 2(1)\alpha] \right\} + c \left\{ \frac{1}{\sqrt{2}} [2+\underline{2}]\beta \right\} \\ \psi_{g.s.}^{II} &= a\Gamma_7^b(e_g) - b\Gamma_7^b(b_{2g}) + c\Gamma_7^b(b_{1g})\end{aligned}$$

where α and β denote $m_s = +\frac{1}{2}$ and $-\frac{1}{2}$ respectively. For a definition of the Γ 's consult Table 32 and Appendix V. The negative sign must be chosen for $\psi_{g.s.}^{II}$ in order to have the proper phase.

These wave functions can be re-written in the following form for easier manipulation:

$$\begin{aligned}\psi_{g.s.}^I &= \frac{1}{\sqrt{3}} [-A(2^-) + B(\underline{2}^-) + C(1^+)] \\ \psi_{g.s.}^{II} &= \frac{1}{\sqrt{3}} [-B(2^+) + A(\underline{2}^+) - C(\underline{1}^-)]\end{aligned}$$

where the superscripts indicate $m_s = +\frac{1}{2}$ & $m_s = -\frac{1}{2}$, and

$$\begin{aligned}A &\equiv a - \frac{b}{\sqrt{2}} - \sqrt{3/2} c \\ B &\equiv a - \frac{b}{\sqrt{2}} + \sqrt{3/2} c \\ C &\equiv a + \sqrt{2} b\end{aligned}$$

The "low-frequency" terms are of the form:

$$(13) \quad \langle \psi_{g.s.}^I | \hat{\mu}_z | \psi_{g.s.}^I \rangle = \frac{\beta}{3} \{A^2 - 3B^2 + 2C^2\}$$

where $\hat{\mu}_z = \beta(\hat{L}_z + 2\hat{S}_z)$ & this β is the Bohr magneton.

Also $\langle \psi_{g.s.}^I | \hat{\mu}_z | \psi_{g.s.}^{II} \rangle = -\frac{\beta}{3} \{A^2 - 3B^2 + 2C^2\}$ and it is seen that the "center of gravity" rule is preserved, i.e., under the Zeeman perturbation the doubly degenerate orbital is split such that conservation of energy is maintained.

When one substitutes the values of A, B, and C back into equation (13) the following results:

$$(14) \quad \langle \psi_{g.s.}^I | \hat{\mu}_z | \psi_{g.s.}^I \rangle = \frac{\beta}{3} [6\sqrt{2} ab - 4\sqrt{6} ac + 3b^2 + 4\sqrt{3} bc - 3c^2]$$

Now the excited state wave functions take the form

$$\psi_{e.s.}^I = a_1 \Gamma_7^a(e_g) + b_1 \Gamma_7^a(b_{2g}) + c_1 \Gamma_7^a(b_{1g})$$

and

$$\psi_{e.s.}^{II} = a_1 \Gamma_7^b(e_g) - b_1 \Gamma_7^b(b_{2g}) + c_1 \Gamma_7^b(b_{2g})$$

Similar substitutions may be made for the coefficients, viz.,

$$A_1 = a_1 - \frac{b_1}{\sqrt{2}} - \sqrt{3/2} c_1$$

etc.,

The "high frequency" term of the expression for χ sums over matrix elements of the form:

$$\langle \psi_{g.s.}^I | \hat{\mu}_z | \psi_{e.s.}^I \rangle = \frac{\beta}{3} \{AA_1 - 3BB_1 + 2CC_1\}$$

when the coefficients are substituted the following results:

$$(15) \langle \psi_{g.s.}^I | \hat{\mu}_z | \psi_{e.s.}^I \rangle = \frac{\beta}{3} \{ 3\sqrt{2}(ba_1 + ab_1 - 2\sqrt{6}(ca_1 + c_1a) + 3bb_1 + 2\sqrt{3}(b_1c + bc_1) - 3cc_1) \}$$

Now when these expressions are substituted into equation 3, Chapter 5, one arrives at the expression for the parallel component of magnetic susceptibility, χ_{\parallel} (equation 5, Chapter 5)

To calculate the perpendicular component of susceptibility the operators μ_x and μ_y must be used. These take the same form as the μ_z operator, viz.,

$$\hat{\mu}_i = \beta(\hat{L}_i + 2\hat{S}_i)$$

It is possible, however, to convert the operators to a more convenient form (80)

$$\begin{aligned} \hat{L}_x &= \frac{1}{2} (\hat{L}_+ + \hat{L}_-) \\ \hat{L}_y &= -\frac{1}{2}i(\hat{L}_+ - \hat{L}_-) \end{aligned}$$

with the spin operators taking analogous forms.

Here the \hat{L}_+ and \hat{L}_- are the familiar raising and lowering operators.

If one examines the matrix element

$$\langle \psi_{g.s.}^I | \hat{\mu}_x | \psi_{g.s.}^I \rangle$$

it is found to equal zero. Therefore a linear combination of $\psi_{g.s.}^I$ and $\psi_{g.s.}^{II}$ must be taken

$$\psi_{g.s.}^{I'} = \frac{1}{\sqrt{2}} \{ \psi_{g.s.}^I + \psi_{g.s.}^{II} \}$$

and

$$\psi_{g.s.}^{II'} = \frac{1}{\sqrt{2}} \{ \psi_{g.s.}^I - \psi_{g.s.}^{II} \}$$

Evaluating the matrix element using these wave functions, it

is seen that

$$(16) \quad \langle \psi_{g.s.}^{I'} | \hat{\mu}_x | \psi_{g.s.}^{I'} \rangle = \frac{\beta}{3} [2AB - 2BC]$$

$$= -\frac{\beta}{3} [3\sqrt{2}ab - 3b^2 + \sqrt{6}ac + 2\sqrt{3}bc + 3c^2]$$

To calculate the "high frequency" term for the $\hat{\mu}_x$ operator one needs the excited states wave function.

As before,

$$\psi_{e.s.}^{I'} = \frac{1}{\sqrt{2}} \{ \psi_{e.s.}^I + \psi_{e.s.}^{II} \}$$

$$\psi_{e.s.}^{II'} = \frac{1}{\sqrt{2}} \{ \psi_{e.s.}^I - \psi_{e.s.}^{II} \}$$

$$\psi_{e.s.}^{I'} = \frac{1}{\sqrt{6}} [-A_1(2^-) + B_1(2^-) + C_1(1^+) - B_1(2^+) + A_1(2^+) - C_1(1^-)]$$

etc.

where the coefficients are those previously defined.

$$\text{Now} \quad \langle \psi_{g.s.}^{I'} | \hat{\mu}_x | \psi_{e.s.}^{I'} \rangle = \frac{\beta}{12} [2A_1B + 2AB_1 - 4BC_1 - 4B_1C]$$

upon re-substitution

$$(17) \quad \langle \psi_{g.s.}^{I'} | \hat{\mu}_x | \psi_{e.s.}^{I'} \rangle = \frac{\beta}{12} [-4aa_1 - 4\sqrt{2}(ab_1 + a_1b) + 10bb_1 - 4\sqrt{3}(bc_1 + b_1c) - 2\sqrt{6}(ac_1 + a_1c) - 6cc_1]$$

When equations (16) and (17) are substituted into equation 3, Chapter 5, one arrives at the expression for the perpendicular component of magnetic susceptibility, χ_{\perp} , as given in equation 6, Chapter 5.

REFERENCES

1. Cotton, F. A. Advanced Inorganic Chemistry. New York: Interscience, 2nd ed., 1966.
2. Levine, W. G. and Peisach, J. Biochim. Biophys. Acta, 63 (1962), 528.
3. Franks, W. A. and van der Helm, D. J. Amer. Chem. Soc., 90 (1968), 5627.
4. Tatsch, C. E. and van der Helm, D. (unpublished structure of bis(L-tyrosinato)copper(II)).
5. Cotton, J. B. Intern. Congr. Metal Corrosion, 2nd, New York City (1963), 590, (pub. 1966).
6. Polder, D. Physica, 9 (1942), 709.
7. Yama, S. and Tsuchida, R. Ann. Rept. Sci. Works Fac. Sci., Osaka Univ. 4 (1956), 79-104.
8. Belford, R. L., Calvin, M., and Belford, G. J. Chem. Phys., 26(5) (1957), 1165.
9. Holmes, O. G. and McClure, D. S. J. Chem. Phys., 26 (1957), 1686.
10. Liehr, A. D. J. Phys. Chem., 64 (1960), 43.
11. Graddon, D. P. J. Inorg. Nucl. Chem., 14 (1960), 161.
12. Pappalardo, R. J. Mol. Spectroscopy, 6 (1961), 554.
13. Ferguson, J. J. Chem. Phys., 34(5) (1961), 1609.
14. Piper, T. S. and Belford, R. L. Mol. Physics, 5 (1962), 169.
15. Gerritsen, H. J. and Starr, A. Arkiv For Fysik, 25(2) (1963), 13.
16. Hatfield, W. E. and Piper, T. S. Inorganic Chem., 3(6) (1964), 841.
17. Dijkgraaf, C. Spectrochimica Acta, 20 (1964), 1227.

18. Dijkgraaf, C. Theoret. Chim. Acta (Berl.), 2 (1964), 422.
19. Dijkgraaf, C. Theoret. Chim. Acta (Berl.), 3 (1964), 38.
20. Davydov, A. S. Theory of Molecular Excitons. New York: McGraw-Hill Book Co. Inc., 1962.
21. Belford, R. L. and Belford, G. Theoret. Chim. Acta (Berl.), 3 (1965), 465.
22. Ferguson, J., Belford, R. L., and Piper, T. S. J. Chem. Phys., 37 (1962) 1569.
23. Ferguson, J. Theoret. Chim. Acta, 3 (1965), 287.
24. Allen, H. C., Jr. J. Chem. Phys., 45 (1966), 553.
25. Cotton, F. A. Rev. Pure and Appl. Chem., 16 (1966), 175.
26. Belford, R. L. and Carmichael, J. W., Jr. J. Chem. Phys., 46(11) (1967), 4515.
27. Tomlinson, A. A. G., Hathaway, B. J., Billing, D. E., and Nicholls, P. J. Chem. Soc., (A) (1969), 65.
28. Billing, D. E., Dudley, R., Hathaway, B. J., Nicholls, P., and Procter, I. M. J. Chem. Soc., (A) (1969), 265.
29. Billing, D. E., Hathaway, B. J., and Nicholls, P. J. Chem. Soc., (A) (1969), 316.
30. Hathaway, B. J., Billing, D. E., Nicholls, P. and Procter, I. M. J. Chem. Soc., (A) (1969), 319.
31. Hathaway, B. J., Bew, M. J., Billing, D. E., Dudley, R. J., and Nicholls, P. J. Chem. Soc., (A) (1969), 2312.
32. Procter, I. M., Hathaway, B. J., Dudley, R., Nicholls, P. J. Chem. Soc., (A) (1969), 1192.
33. Smith, D. W. J. Chem. Soc., 17(A)(1969), 2529.
34. Amateur Scientist, Scientific American, 206 (1962), 155.
35. Adams, D. M. and Raynor, J. B., Advanced Practical Inorganic Chemistry. New York: John Wiley and Sons, 1965.
36. Willoughby, T. V., Least-Squares Cell Parameters Computer Program, Ph.D. Dissertation, University of Oklahoma, 1968.
37. Margenau, H. and Murphy, G. M. The Mathematics of Physics and Chemistry. New Jersey: D. Van Nostrand Co., 2nd ed., 1956.

38. Lipson, H. and Cochran, W. The Determination of Crystal Structures, Vol. III. New York: Cornell University Press, 1966.
39. Stout, G. H. and Jensen, L. H. X-ray Structure Determination. New York: Macmillan, 1968.
40. International Tables for X-ray Crystallography, Vol. III, Kynoch Press, England, 1962.
41. Stewart, R. F., Davidson, E. R., and Simpson, W. T. J. Chem. Phys., 42 (1965), 3175.
42. Busing, W. R., Martin, K. D., and Levy, H. A., USAEC Report ORNL-TM-305, Oak Ridge National Laboratories, Tennessee, 1962.
43. Ahmed, F. R., Fourier Computer Program for Distorted and Undistorted Nets, NRC-8, Ottawa: National Research Council, 1966.
44. Cruickshank, D. W. J. Computing Methods and the Phase Problem in X-ray Crystal Analysis. Edited by Pepinsky, R., et al.. New York: Pergamon Press, 1961.
45. Huber, C. P., Error Analysis and the Agreement Summary Computer Program, NRC-14, Division of Pure Chemistry, National Research Council, Ottawa, 1967.
46. IBM Program (POLRG), Supplied in System/360 Scientific Subroutine Package 1968.
47. Cruickshank, D. W. J. Acta Cryst., 9 (1956), 747.
48. Dijkstra, A. Acta Cryst., 20(4) (1966), 588.
49. Gillard, R. D., Mason, R., Payne, N. C., and Robertson, G. B. Chem. Commun., (1966), 155.
50. Franks, W. A. and van der Helm, D. Acta Cryst., B25 (1969), 451.
51. Tomita, K. Bull. Chem. Soc. Japan, 34 (1961), 280.
52. Yasui, T. and Shimura, Y. Bull. Chem. Soc. Japan, 39 (1966), 604.
53. Freeman, H. C. Advances in Protein Chemistry, Vol. 22, p. 357. New York: Academic Press, 1967.
54. Schomaker, V., Waser, J., Marsh, R. E., and Bergman, G. Acta Cryst., 12 (1959), 600.
55. Donohue, J. and Caron, A. Acta Cryst., 17 (1964), 1178.
56. Freeman, H. C. Biochemistry of Copper. Edited by Pelsach, J., Aisen, P., and Blumberg, W. E.. New York: Academic Press, p. 97. 1966.

57. Shoemaker, D. P., Barieau, R. E., Donohue, J., Lu, C. Acta Cryst., 6 (1953), 241.
58. Gramaccioli, C. M. and Marsh, R. E. Acta Cryst., 21 (1966), 594.
59. Gramaccioli, C. M. Acta Cryst., 21 (1966), 600.
60. Edsall, J. T., Flory, P. J., Kendrew, J. C., Liquori, A. M., Nemethy, G., Ramachandran, G. N., Scheraga, H. A. Biopolymers, 4 (1966), 121.
61. Ramachandran, G. N. and Sasisekharan, V. Advances in Protein Chemistry, Vol. 23, p. 399. New York: Academic Press, 1968.
62. Ramachandran, G. N. and Lakshminarayn, A. V. Biopolymers, 4 (1966), 495.
63. Smits, D. W. and Wiebenga, E. H. Acta Cryst., 6 (1953), 531.
64. Tables of Interatomic Distances and Configuration in Molecules and Ions. Edited by Sutton, L. E., Jenkin, D. G., Mitchell, A. D., and Cross, L. C.. London: The Chemical Society, Burlington House, 1958.
65. Tucker, E., Least-Squares Program to find Best Equation of a Plane Curve, University of Oklahoma (unpublished), 1967.
66. Wright, W. B. and King. G. S. D. Acta Cryst., 7 (1954), 283.
67. Ahmed, F. R., Structure Factor and Least Squares Computer Program, NRC-10, Ottawa: National Research Council, 1966.
68. Corfield, P. W. R., Computer Program for Analysis of R Factors and Weights for Different Classes of Reflections Based on Magnitudes, Sine Theta, and Indices (RANGER), University of British Columbia: 1969.
69. Jarvis, J. A. J. Acta Cryst., 15 (1962), 964.
70. Cotton, F. A. Advanced Inorganic Chemistry. New York: Interscience, 2nd ed., p. 899, 1966.
71. Ueki, T., Ashida, T., Sasada, Y., and Kakudo, M. Acta Cryst., 22 (1967), 870.
72. Broomhead, J. M. Acta Cryst., 1 (1948), 324.
73. Broomhead, J. M. Acta Cryst., 4 (1951), 92.
74. Bryden, J. H. Acta Cryst., 8 (1955), 211.

75. Shapiro, P., Computer Program for Absorption Corrections to Diffracted X-ray Intensities.
76. Zalkin, A. Computer Program (FORDAP) for Fourier Calculation. University of California, Berkeley (Unpublished).
77. Tatsch, C. E. Computer Program for Calculation of Hydrogen Positions. University of Oklahoma (Unpublished), 1969.
78. Bethe, H. A. Ann. Physik, (5)3 (1929), 133: Eng. Trans. Consultants Bureau, N. Y., 1958.
79. Ballhausen, C. J. Introduction to Ligand Field Theory. New York: McGraw-Hill Book Co. Inc., 1962.
80. Figgis, B. N. Introduction to Ligand Fields. New York: Interscience, 1966.
81. Stevens, K. W. H. Proceedings of the Royal Physics Soc., A65 (1952), 209.
82. Joy, H. Computer Program for Diagonalization of Secular Determinant (unpublished), Oak Ridge National Laboratories, 1966.
83. Kauzmann, W. Quantum Chemistry. New York: Academic Press, p. 616, 1957.
84. Cotton, F. A. Chem. Applications of Group Theory. New York: Interscience, p. 230, 1963.
85. Van Vleck, J. H. Electric and Magnetic Susceptibilities. London: Oxford University Press, pp. 187-196, 1952.
86. Jørgensen, C. K., Report to the Xth Solvay Council, Brussels, May 1956.
87. Lewis, J. and Wilkins, R. G. Modern Coordination Chemistry. New York: Interscience, p. 263, 1960.
88. Owen, J. Proc. Roy. Soc., A227 (1955), 183.
89. McClure, D. S. Solid State Physics, 9 (1959)
90. Selwood, P. W. Magnetochemistry. New York: Interscience, p. 85, 1943.
91. Cotton, F. A. and Holm, R. H. J. Chem Phys., 31 (1959), 788.
92. Inoue, M., Kishita, M., and Kubo, M. Inorg. Chem., 4(5) (1965), 626.
93. Kato, M., Jonassen, H. B., and Fanning, J. C. Chem. Review, (1964), 99.

94. Hoover, D., Lab. Assistant at University of Oklahoma (unpublished).
95. Condon, E. V. and Shortley, G. H. The Theory of Atomic Spectra. London: Cambridge, at the University Press, 1964.
96. Koster, G. F., Dimmock, J. O., Wheeler, R. G., and Statz, H. Properties of the Thirty-Two Point Groups. Massachusetts: M.I.T. Press, 1963.
97. Johnson, C. K., ORTEP: A FORTRAN Thermal-Ellipsoid Plot Program for Crystal Structure Illustrations, ORNL-3794, Oak Ridge National Laboratory: Tennessee, 1965.
98. Willoughby, T. V. and van der Helm, D. Acta Cryst., B25 (1969), 2317.